STRUCTURAL MAGNETIC RESONANCE IMAGING IN AMYOTROPHIC LATERAL SCLEROSIS

Cortical morphometry, diffusion properties and lesion detection as potential biomarkers for the state and progression of Amyotrophic Lateral Sclerosis

Inaugural-Dissertation zur Erlangung der Doktorwürde der Fakultät für Psychologie, Pädagogik und Sportwissenschaft der Universität Regensburg vorgelegt von

Anna Maria Wirth aus
Hofdorf
2018

Die Arbeit entstand in gemeinsamer Betreuung durch die Fakultät für Psychologie, Pädagogik und Sportwissenschaft der Universität Regensburg und der Klinik und Poliklinik für Neurologie der Universität Regensburg in der Fakultät für Medizin

Regensburg 2018

Universitätsklinikum Regensburg

Gutachter (Betreuer): Prof. Dr. Mark W. Greenlee

Gutachter: Prof. Dr. Ulrich Bogdahn

PREFACE

The aim of the thesis entitled „Structural Magnetic Resonance Imaging in Amyotrophic Lateral Sclerosis" is to evaluate the potential of cortical morphometry, diffusion properties, and lesion detection as magnetic resonance imaging (MRI) biomarkers for the state and progression of Amyotrophic Lateral Sclerosis (ALS). The thesis is composed of three chapters: introduction, projects, and concluding remarks. The three subprojects of the thesis are listed on page 8 and 9. The references of all three projects are merged in one bibliography at the end of the thesis.

All three projects were submitted to peer-reviewed journals (impact factor > 1.5) and entered their review process. One out of the three projects is successfully published. Chapter 2 includes the pre-print version of the published project with permission from publishers. Yet unpublished projects are represented in their most recently revised versions. The manuscripts of all subprojects are consistently formatted according to the guidelines of American Psychological Association (APA). Numbers of figures and tables are adapted. No other changes have been made to the manuscripts.

The thesis has been conducted on behalf of a multidisciplinary treatment program and within GO-Bio Funding of BMBF. Contributions of co-authors are listed on page 8 and 9.

The past three years of PhD thesis have yielded two other publications of the team and colleagues. These articles are not included in the thesis, as they are not related to ALS biomarker research.

Frank, S. M., Wirth, A. M. & Greenlee, M. W. (2016). Visual-Vestibular Processing In The Human Sylvian Fissure. *J Neurophysiol*, *116*, 263-271

Wirth, A. M., Frank, S. M, Greenlee, M. W. & Beer, A. L. (2018). White Matter Connectivity of the Visual-Vestibular Cortex Examined by Diffusion-weighted imaging. *Brain Connectivity*, *8*, 235-244

EIDESSTATTLICHE VERSICHERUNG

Ich erkläre hiermit an Eides Statt, dass ich die vorliegende Arbeit ohne unzulässige Hilfe Dritter und ohne Benutzung anderer als der angegebenen Hilfsmittel angefertigt habe. Die aus anderen Quellen direkt oder indirekt übernommenen Textpassagen, Daten, Bilder oder Grafiken sind unter Angabe der Quelle gekennzeichnet.

Bei der Auswahl und Auswertung des Materials haben mir die auf der Seite 8 und 9 aufgeführten Personen in der jeweils detaillierten Weise unentgeltlich geholfen; dies ist auch in der Dissertation an den entsprechenden Stellen explizit ausgewiesen. Weitere Personen waren an der inhaltlich-materiellen Erstellung der vorliegenden Arbeit nicht beteiligt. Insbesondere habe ich hierfür nicht die entgeltliche Hilfe von Vermittlungs- beziehungsweise Beratungsdiensten (Promotionsberater oder anderer Personen) in Anspruch genommen. Niemand hat von mir unmittelbar oder mittelbar geldwerte Leistungen für Arbeiten erhalten, die im Zusammenhang mit dem Inhalt der vorgelegten Dissertation stehen.

Die Arbeit wurde bisher weder im In- noch im Ausland in gleicher oder ähnlicher Form einer anderen Prüfungsbehörde vorgelegt.

Ich versichere an Eides Statt, dass ich nach bestem Wissen die reine Wahrheit gesagt und nichts verschwiegen habe.

Vor Aufnahme der obigen Versicherung an Eides Statt wurde ich über die Bedeutung der eidesstattlichen Versicherung und die strafrechtlichen Folgen einer unrichtigen oder unvollständigen eidesstattlichen Versicherung belehrt.

DANKSAGUNG

Oberster Dank gebührt meinem Doktorvater Prof. Dr. Greenlee für die Betreuung und Unterstützung meiner Doktorarbeit. Der Lehrstuhl Prof. Dr. Greenlee bot mir eine anspruchsvolle Forschungsausbildung und intensive Forschungserfahrungen. Zudem möchte ich mich von ganzem Herzen bei Prof. Dr. Bogdahn für die Kooperation mit der Neurologischen Universitätsklinik bedanken. Die Arbeit in der ALS Forschung ermöglichte mir einmalige und intensive Erfahrungen in der klinischen Forschung, Besuche zahlreicher Forschungskonferenzen, und den interdisziplinären Austausch mit so vielen inspirierenden Wissenschaftlern.

Eine besondere Danksagung möchte ich an die vielen Patienten, Angehörigen und gesunden Kontrollprobanden im Rahmen des Heilversuches aussprechen. Dank gebührt neben Prof. Dr. Bogdahn auch Herrn Dr. Bruun, Frau Johannesen, Frau Dr. Hsam, Frau Dr. Meyer, Herrn Dr. Baldaranov, Herrn Dr. Khomenko, Frau Kammermeier und Frau Kobor (M.Sc.) der ALS Ambulanz des Neurologischen Universitätsklinikums Regensburg für die neurologische Untersuchung der Patienten, für deren Rekrutierung für die Magnetresonanztomographie (MRT), und für die große Unterstützung bei den Publikationen. Ich bedanke mich zudem beim Zentrum für Neuroradiologie des UKR und des Bezirksklinikums unter Prof. Dr. Schuierer für die MRT Bildgebung und deren diagnostische Evaluation bei den ALS Patienten. Meinen Kollegen Dr. Khomenko und Dr. Baldaranov danke ich herzlich für die Unterstützung bei der MRT Datenerhebung bei gesunden Kontrollprobanden. Zudem möchte ich mich bei Prof. Dr. Schulte-Mattler, Herrn Dr. Grimm und Frau Kobor (M.Sc.) für die Erhebung und Bereitstellung der neurophysiologischen Daten bedanken. Dank richte ich ebenso an Herrn Dr. Peters, Frau Dr. Küspert, Frau Dr. Iberl, Frau Wirkert, Frau Heydn und Frau Sieboerger des ALS Laborteams. Der interdisziplinäre Austausch und die kollegiale Teamatmosphäre bereicherten die Zeit meiner Promotion. Dank gebührt ebenso der Gründeroffensive Biologie (Go-Bio) für die Finanzierung meiner Doktorarbeit.

Abschließend danke ich meiner Familie, Matthias und meinen Freunden für ihre grenzenlose Unterstützung, ihr Verständnis und ihre Geduld.

CONTENTS

ABSTRACT

Amyotrophic lateral sclerosis (ALS) is a progressive neurodegenerative disease primarily affecting the motor system of the central nervous system. The aim of this thesis is to evaluate the potential of structural magnetic resonance imaging (MRI) biomarkers of the brain grey matter (GM) and white matter (WM) for the state and progression of ALS. The thesis has been conducted on behalf of a treatment program on a named patient basis at the University Hospital of Regensburg. 31 patients with written informed consent are compared to a control sample of 34 age-matched healthy participants. Routine MRI scans have been conducted approximately every 3 months and include T1-weighted imaging, diffusion weighted imaging (DWI), and fluid-attenuated inversion recovery (FLAIR) sequences at 1.5 Tesla. The subprojects of the thesis investigate precentral and postcentral cortical thinning (study 1), spread of alterations of fractional anisotropy (FA) across different WM types (study 2), and FLAIR lesion detection (study 3) in the same ALS cohort. Candidate MRI biomarkers are associated with neurophysiological and clinical biomarkers. Statistical analysis includes both cross-sectional and longitudinal analyses. Special focus is set on the individual patient. Cortical thinning is more pronounced in the precentral cortex than in the postcentral cortex. Combinatory biomarker use reveals evident differences in temporal dynamics of cortical thickness, clinical and neurophysiological biomarkers over time. Reduction of FA is consistently detected in the corticospinal tract (CST) and extra motor WM and most pronounced in the brainstem. Spread of FA alterations resembles both dying-forward and dying-back disease propagation and is not linked to patients' clinical or demographic characteristics. WM lesions as detected by FLAIR hyperintensity are more frequent in ALS patients than in controls, most pronounced in the CST, and associated with an inferior survival. Together, the findings of this thesis suggest that MRI biomarkers may contribute to the diagnosis, prognosis and understanding of ALS disease and disease courses on an individual scope.

CONTRIBUTIONS

Study 1	**Combinatory Biomarker Use of Cortical Thickness, MUNIX, and ALSFRS-R at Baseline and in Longitudinal Courses of Individual Patients with Amyotrophic Lateral Sclerosis**
Authors	Wirth, A. M.[12], Khomenko, A.[1], Baldaranov, D.[1], Kobor, I.[1], Hsam, O.[1], Grimm, T.[1], Johannesen, S.[1], Bruun, T.-H.[1], Schulte-Mattler, W.[1], Greenlee, M. W.[2], Bogdahn, U.[1]
Type	Retrospective cohort study
Study idea	Wirth
Study design	Wirth
Data acquisition	MRI data of ALS patients: Center of Neuroradiology, University Hospital and District Medical Hospital of Regensburg MRI data of controls: Wirth, Khomenko, Baldaranov Clinical data: Johannesen, Hsam, Kobor, Bruun, Bogdahn Neurophysiological data: Schulte-Mattler, Grimm, Kobor
Statistical analysis	Wirth
Manuscript writing	Wirth
Manuscript revision	Khomenko, Baldaranov, Johannesen, Hsam, Schulte-Mattler, Grimm, Kobor, Bruun, Greenlee, Bogdahn
Study supervision	Greenlee, Bogdahn
Publication status	Published in Frontiers in Neurology; July 30th 2018

Study 2	**Dying-forward or dying-back? White matter type-specific alterations of fractional anisotropy in classical Amyotrophic Lateral Sclerosis**
Authors	Wirth, A. M.[12], Khomenko, A.[1], Johannesen, S.[1], Baldaranov, D.[1], Bruun, T.-H.[1], Greenlee, M. W.[2], Bogdahn, U.[1]
Type	Retrospective cohort study
Study idea	Wirth
Study design	Wirth
Data acquisition	MRI data of ALS patients: Center of Neuroradiology, University Hospital and District Medical Hospital of Regensburg MRI data of controls: Wirth, Khomenko, Baldaranov, Bogdahn Clinical data: Johannesen, Bruun
Statistical analysis	Wirth

Manuscript writing	Wirth
Manuscript revision	Khomenko, Johannesen, Baldaranov, Bruun, Greenlee, Bogdahn
Study supervision	Greenlee, Bogdahn
Publication status	Under peer-review in Therapeutic Advances in Neurological Disorders (TAND); October 2018

Study 3	**Value of Fluid-Attenuated Inversion Recovery MRI data analyzed by the Lesion Segmentation Toolbox in Amyotrophic Lateral Sclerosis**
Authors	Wirth, A. M.[12], Johannesen, S.[1], Khomenko, A.[1], Baldaranov, D.[1], Bruun, T.-H.[1], Wendl, C.[3], Schuierer, G.[3], Greenlee, M. W.[2], Bogdahn, U.[1]
Type	Retrospective cohort study
Study idea	Wirth
Study design	Wirth
Data acquisition	MRI data of ALS patients: Center of Neuroradiology, University Hospital and District Medical Hospital of Regensburg MRI data of controls: Wirth, Khomenko, Baldaranov Clinical data: Johannesen, Bruun, Bogdahn Visual evaluation: Schuierer, Wendl
Statistical analysis	Wirth
Manuscript writing	Wirth
Manuscript revision	Khomenko, Baldaranov, Johannesen, Bruun, Greenlee, Bogdahn
Study supervision	Greenlee, Bogdahn
Publication status	Accepted for publication in Journal of Magnetic Resonance Imaging (JMRI); October 30th 2018

[1] Department of Neurology, University Hospital of Regensburg, Germany

[2] Department of Experimental Psychology, University of Regensburg, Germany

[3] Center of Neuroradiology, University Hospital and District Medical Hospital of Regensburg, Germany

ABBREVIATIONS

1.5T	1.5 Tesla
ADM	Abductor digiti minimi
AF	Association fibers
ALS	Amyotrophic lateral sclerosis
ALSFRS-R	ALS-specific functional rating scale revised
BS	Brainstem white matter
X^2	Chi-square
C9orf72	Chromosome 9 open reading frame 72
CC	Corpus callosum
CF	Commissural fibers
CMAP	Compound muscle action potential
CNS	Central nervous system
CSF	Cerebrospinal fluid
CST	Corticospinal tract
DNA	Deoxyribonucleic acid
DWI	Diffusion weighted imaging
DWI6	DWI sequence using 6 orientations
DWI20	DWI sequence using 20 orientations
DTI	Diffusion tensor imaging
ε	Epsilon
ECAS	Edinburgh Cognitive and Behavioral ALS screen
EMG	Electromyography
F	F-value
FA	Fractional anisotropy
FAB	Frontal Assessment Battery
fMRI	Functional magnetic resonance imaging
FLAIR	Fluid-attenuated inversion recovery
FoV	Field of view
FUS	Fused in sarcoma
G-CSF	Granulocyte-colony stimulating factor
GM	Gray matter

κ	kappa
lh	Left hemisphere
LMN	Lower motor neuron
LPA	Lesion Prediction Algorithm
LST	Lesion Segmentation Toolbox
M	Mean
ml	Milliliter
mm	Milimeter
MMSE	Mini Mental State Examination
MN	Motor neuron
MND	Motor neuron disease
MNDA	Motor Neuron Disease Association
MNI	Montreal Neurological Institute
MoCA	Montreal Cognitive Assessment
MPRAGE	Magnetization prepared rapid gradient echo sequence
MRI	Magnetic resonance imaging (Magnetresonanztomographie, MRT)
MRS	Magnetic resonance spectroscopy
ms	Milisecond
MUNE	Motor unit number estimation
MUNIX	Motor unit number index
p	*p*-value
φ	Phi
PF	Projection fibers
PoD	Postcentral dorsal
PoV	Postcentral ventral
PreD	Precentral dorsal
PreV	Precentral ventral
PT	Pyramidal tract
RF	Radiofrequency
r	Bravais-Pearson correlation coefficient
rh	Right hemisphere
RNA	Ribonucleic acid

ROI	Region of interest
s	second
SD	Standard deviation
SIP	Surface interference pattern
SMN	Sensorimotor network
SMUP	Single motor unit potential
SOD1	Superoxide dismutase 1
T	*T*-value
T1	Longitudinal relaxation time
T2	Transverse relaxation time
TARDBP	TAR DNA-binding protein
TE	Time of echo
TLN	Total lesion number
TLV	Total lesion volume
TMS	Transcranial magnetic stimulation
TR	Time of repetition
UMN	Upper motor neuron
WMA	World medical association
yrs	years
z	Standardized deviation from reference

CHAPTER 1: INTRODUCTION

RATIONALE, AIMS AND HYPOTHESES

ALS is a fatal neurodegenerative disease primarily affecting the motor system (Mitchell & Borasio, 2007). Research and clinical treatment are challenged by a broad heterogeneity of clinical phenotypes (Swinnen & Robberecht, 2014), complex and late diagnosis (Al-Chalabi et al., 2016), and lack of understanding of pathogenesis (Morgan & Orrell, 2016). To date, only two medications (Riluzole, Edaravone) are FDA approved (Mitsumoto, Brooks, & Silani, 2014). In Europe, only Riluzole is approved and known for its marginal effect on survival (Miller, Mitchell, & Moore, 2012). Multidisciplinary research has revealed differentiated insights into possible pathogenic processes (Morgan & Orrell, 2016). Still, the vision of the Motor Neuron Disease Association (MNDA) to finally cure ALS (Mitchell & Borasio, 2007) is distant (Schultz, 2018). Biomarkers are biological correlates (Benatar et al., 2016) and may pave the way to ALS treatment by their contributions to timely diagnosis, estimation of individual prognosis and early assessment of treatment effects (Al-Chalabi et al., 2016). Moreover, different biomarkers may be combined in clinical trial designs to reveal benefits of medication for subtypes of ALS (Benatar et al., 2016). Aside from routine clinical and neurophysiological biomarkers, multimodal neuroimaging provides potential biomarkers for the classification of ALS subtypes and for understanding the pathogenesis of ALS (Turner & Verstraete, 2015).

The aim of this thesis is to evaluate the potential of different MRI techniques as diagnostic and prognostic biomarkers for ALS. The focus is set on the combination with other biomarkers and the perspective on the individual patient in the state and course of disease.

Study 1 investigates cortical thinning of the precentral and postcentral cortex in ALS. Brain MRI is combined with neurophysiological and clinical biomarkers. The neurophysiological biomarker is assessed at the hand muscles of patients. The cross-sectional data analysis explores individual states of cortical thinning in addition to group averages. Longitudinal analysis investigates differences in temporal dynamics of multimodal biomarker use.

Study 2 targets the controversy of the dying-forward and dying-back hypotheses, which have gradually lost attention in the past years. Most studies focus on motor-associated WM

only. Here, the approach is to reveal sequential alterations in diffusion properties of different hierarchical types of WM: brainstem WM, projection fibers, association fibers, commissural fibers. Alterations in diffusion properties are associated with clinical and demographic data of patients.

Study 3 aims at the evaluation of conventional FLAIR imaging for the diagnosis and prognosis of ALS. FLAIR imaging is underrepresented in ALS research due to controversial specificity for ALS and lack of objective quantification studies. An automated segmentation toolbox established in multiple sclerosis research enables the fast and objective quantification of FLAIR lesions and may be a promising tool for FLAIR data analysis in ALS.

The following section will provide background information on ALS, biomarkers, and MRI. This information will underline the motivation behind the three studies involved in this thesis.

BACKGROUND

MOTOR NEURONS IN HEALTH AND DISEASE

Motor neurons (MN) are neuronal cells of the central nervous system (CNS) and essential for the transduction of signals from the brain and spinal cord to the muscles enabling movement of the body (Stifani, 2014). For this purpose, MNs need to be involved in both neuronal circuits and innervation of muscles. MNs are characterized by long axons, complex signal processing and connectivity to both CNS and periphery (Parson, 2014). MNs may be differentiated into so-called upper motor neurons (UMN) and lower motor neurons (LMN) (Stifani, 2014). UMNs are located in the motor and premotor cortex and connect to LMN arranged in the brainstem and spinal cord of the motor system. LMNs receive signals from UMNs, sensory neurons and interneurons, and transduce the signal to the muscle targets outside of the CNS. Facing the central role and great size/length of MNs, it is no surprise that MNs require distinct supply of energy and may be especially vulnerable to damage and disease (Parson, 2014). Damage to UMNs leads to muscle weakness (paresis), increased muscle tone (spasticity) and brisk reflexes (Ivanhoe & Reistetter, 2004). In contrast, lesions of LMNs may lead to paresis and muscle atrophy as

no CNS signal can be transferred to muscles (Stifani, 2014). Fineberg et al. (2013) revealed that neuromuscular disorders represent some of the most cost-intense diseases in the United Kingdom. Still, research claims a better understanding of pathogenic processes behind motor neuron diseases (MND) (Parson, 2014). ALS as the most common MND is the focus of this thesis and is described in the following section.

AMYOTROPHIC LATERAL SCLEROSIS

"Let us keep looking, in spite of everything. Let us keep searching. It is indeed the best method of finding, and perhaps thanks to our efforts, the verdict we will give such a patient tomorrow will not be the same we must give this man today."

Charcot (1889)

From Charcot to ice buckets

ALS has first been described and termed by Charcot in 1869 (Charcot, 1869). More than 100 years later, this disease has increasingly attracted scientific and clinical interest (Kiernan et al., 2011). The first clinical trials started in the 1980s and the first standard diagnostic criteria were established and revised in the 1990s (Mitsumoto et al., 2014). Since then, multidisciplinary research has revealed various phenotypes, pathogenic processes, and genetic variants of ALS and has paved the way for therapeutic interventions (Rosenfeld & Strong, 2015). The social media presence of the Ice Bucket Challenge in 2014 has not only increased worldwide attention on this disease, but has also raised more than 140 million dollars of donations for research funding (Hrastel & Robertson, 2016).

What is Amyotrophic lateral sclerosis?

ALS is a rapidly progressive and incurable neurodegenerative disease primarily affecting MNs of the brain and the spinal cord (Calvo et al., 2014). Degeneration of both LMNs and UMNs leads to paresis, muscle wasting, fasciculation, cramps, paralysis, difficulty speaking, swallowing, and shortness of breath (Bozzoni, 2016). The onset of motor symptoms is related to voluntary limb muscles (limb-onset) or the function of speech and swallowing (bulbar-onset), rarely respiratory muscles. Involvement of non-motor areas of the brain may also lead to deficits in behavior and cognition (Goldstein & Abrahams, 2013).

ALS is a rare disease with a prevalence of 7-9/100 000 persons and an incidence rate of 2.6/100 000 persons per year based on European registers (Hardiman et al., 2017). Prevalence of ALS evidently varies across different cultures and geographical origins (Van Es et al., 2017). Comparisons of epidemiological registers of ALS may be challenged by heterogeneous disease onset and differences in diagnostic criteria (Hardiman et al., 2017). Incidence of ALS has been observed to gradually increase. This phenomenon may be linked to enhanced attention to this disease, improved diagnostic criteria and recognition of various phenotypes of ALS. ALS is usually diagnosed at a mean age of 65 years (Turner, Barnwell, Al-Chalabi, & Eisen, 2012). However, ALS may also occur at young age (young-onset ALS). Risk of ALS is considered to be higher for males than females (1.6:1) (Mitchell & Borasio, 2007). The devastating character of ALS is underlined by grave survival prognosis (Paulukonis et al., 2015) and high mortality rates (1.70 per 100 000 population, 2014, USA) (Larson, Kaye, Mehta, & Horton, 2018).

Standardized ALS diagnosis has been enabled by El Escorial Diagnostic Criteria since 1994 (Brooks, 1994). Since then, El Escorial criteria have been revised and adapted to increasing knowledge about ALS and the advancement of clinical methods (Al-Chalabi et al., 2016; Ludolph et al., 2015). Diagnostic criteria are based on the presence and extent of so called UMN and LMN signs. LMN signs are characterized by muscle atrophy, weakness, fasciculation and weak or absent reflexes (Swinnen & Robberecht, 2014). UMN signs are considered positive Babinski sign, positive Hoffman sign, spasticity and brisk reflexes. Special respect is given to the localization (bulbar, spinal regions) and extent (number of regions) of UMN and LMN signs (Al-Chalabi et al., 2016). The most recently revised criteria (Costa, Swash, & Carvalho, 2012; Table 1.1) define definite, probable or possible ALS (Table 1.1). Aside from the presence of both UMN and LMN signs and a progressive character of disease, ALS diagnosis bases upon the exclusion of mimic diseases, especially treatable diseases (Al-Chalabi et al., 2016). Differential diagnosis requires the exclusion of other treatable diseases by detailed anamnesis, diagnostic findings, and monitoring of clinical progress (Swinnen & Robberecht, 2014). Mimic diseases may be differentiated from ALS by neurophysiological, neuroimaging and laboratory findings (Bicchi, Emiliani, Vescovi, & Martino, 2015). The complex process of ALS diagnosis usually lasts one year in average and results in a fatal delay of intervention (Kiernan et al., 2011). The notification of an ALS diagnosis exposes patients and caregivers to an enormous psychological burden and requires adequate and sensible communication (Pizzimenti, Gori, Onesti, John, & Inghilleri, 2015).

Table 1.1

Most recent revised form of El Escorial criteria for ALS diagnosis (Costa et al. 2012).

	Clinical or electrophysiological evidence of UMN and LMN signs
Definite ALS	… in the bulbar region and at least two spinal regions, or UMN and LMN signs in three spinal regions
Probable ALS	… in at least two regions, with some UMN signs rostral to LMN signs
Possible ALS	… in only one region, or UMN signs alone in two or more regions, or LMN signs rostral to UMN signs

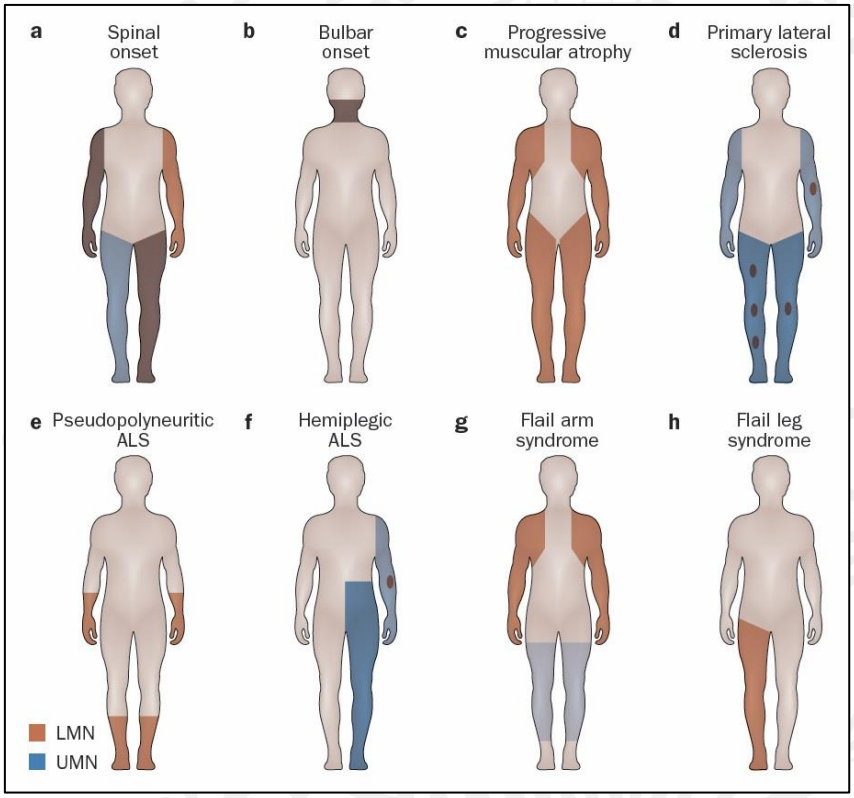

Figure 1.1. Variability of phenotypes of ALS. Figure was adapted from Swinnen & Robberecht (2014). ALS phenotypes include spinal-onset (a), bulbar-onset (b), progressive muscular atrophy (c), primary lateral sclerosis (d), pseudopolyneuritic ALS (e), hemiplegic ALS (f), flail arm (g) and flail leg syndrome (h).

One factor challenging ALS diagnosis is the heterogeneity of ALS phenotypes (Swinnen & Robberecht, 2014) (Figure 1.1). ALS phenotypes substantially vary in extent of MN involvement (UMN, LMN), onset site (bulbar, spinal), locality of symptoms (distal, proximal muscles) and progression. ALS may be differentiated in spinal-onset (Figure 1.1a) and bulbar-onset (Figure 1.1b). Spinal onset is marked by both UMN and LMN signs primarily starting in the limbs of the body. Bulbar onset is less frequent (20% of patients)

and is characterized by muscular weakness of respiratory muscles, deficits in speech (dysarthria) and swallowing (dysphagia). Progressive muscular atrophy (Figure 1.1c) and primary lateral sclerosis (Figure 1.1d) belong to the spectrum of ALS-MND where ALS includes the deterioration of both LMN and UMN at different degrees. ALS symptoms may also be specific to distal limbs (Figure 1.1e), to one body side (Figure 1.1f), to upper limbs (Figure 1.1g), or to lower limbs (Figure 1.1h). Aside from motor symptoms, ALS may include cognitive deficits in speech and executive functions (Beeldman et al., 2016). ALS may even overlap with behavioral variant frontotemporal dementia (Bozzoni, 2016). Moreover, ALS patients may exhibit pathological laughing and crying (pseudobulbar signs) (Mitchell & Borasio, 2007), affective disturbances (depression, anxiety) (Carvalho et al., 2016), sleep disorders (Mitchell & Borasio, 2007) or pain (Chiò & Lauria, 2017).

The ALS patient cohort of this thesis involves spinal-onset and bulbar-onset ALS. The majority of ALS patients are diagnosed spinal-onset ALS. **Study 1 and 2** include only spinal-onset classical ALS patients exhibiting similar UMN and LMN involvement. **Study 3** involves spinal-onset as well as bulbar-onset patients.

Despite the discovery of various pathogenic mechanisms in ALS, the etiology explaining all of these processes remains unclear (Van Es et al., 2017). Multifactorial pathogenesis of ALS may already start early in life and long before ALS is diagnosed in late adulthood (Eisen, Kiernan, Mitsumoto, & Swash, 2014). ALS is associated with a variety of genetic mutations affecting processing of deoxyribonucleic acid (DNA) and ribonucleic acid (RNA) (Morgan & Orrell, 2016). Probably the most important genetic targets in ALS may be chromosome 9 open reading frame 72 (C9orf72), superoxide dismutase 1 (SOD1), TAR DNA-binding protein 43 (TARDBP) and RNA-binding protein FUS (fused in sarcoma). SOD1 mutations are associated with functional and structural cell damage induced by active oxygen species (oxidative stress) (Adly, 2010; Morgan & Orrell, 2016). Mutations in C9orf72, TARDBP and FUS may lead to disturbed transcription of DNA to RNA and deficient translation of RNA to proteins (Morgan & Orrell, 2016). Malformations and dysfunctions of proteins may then result in cytotoxic protein aggregations. Accumulations of misfolded proteins are observed to spread across the whole brain in the course of disease (Brettschneider et al., 2013). Spread of protein aggregations in the CNS is a feature of ALS common with other neurodegenerative diseases like Alzheimer's disease and Parkinson's disease (Lee & Kim, 2015). This observation leads to the controversial theory of ALS being a prion-like disease (Ludolph & Brettschneider, 2015). The involvement of both UMN and LMN in ALS is also the basis for another controversy: Does ALS begin in UMN

or LMN? Two attempts trying to answer this question are the famous dying-forward and dying-back hypotheses (Kiernan et al., 2011). Dying-forward hypothesis postulates the origin of ALS in the motor cortex of the brain. The so-called anterograde degenerative process may be mediated by glutamate excitotoxicity. Dying-back hypothesis proposes the start of ALS in the LMNs or at the neuromuscular junction of the muscles. Based on this theory, lack of neurotrophic hormones may lead to a retrograde degenerative mechanism. Aside from disturbances in DNA/RNA processing and protein aggregations, various other pathogenic mechanisms have been associated with MN degeneration in ALS: mitochondrial dysfunction, disturbances in glial cells and cytoskeleton, defects in vesicle transport, excitotoxicity or immune dysfunction (Van Damme, Robberecht, & van den Bosch, 2017).

Study 1 focuses on the interplay of UMN and LMN by the combinatory use of potential UMN biomarker cortical thickness and a potential LMN neurophysiological biomarker. **Study 2** investigates the Dying-forward and Dying-back hypotheses by examination of diffusion properties of different hierarchical WM types.

Although a variety of genetic mutations have been revealed, hereditary (familial) ALS represents only 5-10% of ALS cases (Kiernan et al., 2011). The majority of ALS patients exhibit no familiar background of ALS, and are therefore considered sporadic.

Only three patients of the ALS patient cohort involved in this thesis are diagnosed with familial ALS. Genetic screening revealed the prominent SOD1, resp. C9Orf mutations.

The interaction of genetic predisposition and environmental risk factors may also play an essential role in ALS (Morgan & Orrell, 2016). Risk factors of ALS have been discussed to involve body mass index, physical activity, traumatic events, smoking, ingestion of heavy metals, pesticides, electric shocks, and cyanotoxins (Ingre, Roos, Piehl, Kamel, & Fang, 2015; Morgan & Orrell, 2016). However, the interplay of trigger factors and genetic predisposition and thus the validity of risk factors remain unclear (Ingre et al., 2015).

Knowing possible pathogenic pathways in ALS has given rise to the development of disease-modifying drugs with various modes of actions (Dorst, Ludolph, & Huebers, 2018). However, as of date, more than 30 drugs tested in clinical trials have failed to prolong survival (Garbuzova-Davis, Thomson, Kurien, Shytle, & Sanberg, 2016). Survival in ALS is 3-5 years from symptom onset (Calvo et al., 2014). In bulbar-onset ALS, patients even suffer from inferior survival of only 2 years (Swinnen & Robberecht, 2014).

The only approved medication worldwide since 1995 is Riluzole, which prolongs survival to an extent of only 3-6 months (Dorst et al., 2018). In 2017, Edaravone has been approved for ALS treatment only in Japan and in the United States of America (Bhandari & Kuhad, 2018). Edaravone targets oxidative stress and slows down disease progression of a homogenous subgroup of early ALS patients – there is no survival benefit so far. The failure of clinical trials may be explained by inadequate animal models, failed crossing of blood-brain-barrier, and challenges of clinical study design (e.g. short trials, low sample sizes) (Garbuzova-Davis et al., 2016). Moreover, heterogeneous phenotypes of ALS, fast progression and late diagnosis may reduce the chance of finding significant benefits of drug treatment in ALS clinical trials (Al-Chalabi et al., 2016; Swinnen & Robberecht, 2014). Aside from disease-modifying intervention, ALS may only be treated symptomatically (Dorst et al., 2018). Nutritional management (e.g. high-caloric diet) aims at the maintenance of body weight. Ventilation devices are relevant for the treatment of respiratory insufficiency. Physiotherapy may help to reduce spasticity or muscle cramps. Additional medication (e.g. antidepressants, opioids, botulinum toxins) may support the symptomatic treatment of depression, emotional lability, insomnia, or excessive salivation (sialorrhoe). Facing the inexorable progression of disease, many ALS patients voluntarily agree to treatment with promising but not yet approved medication (off-label use) (Kiernan et al., 2011). The thesis has been conducted on the behalf of a treatment program, which is introduced in the following section.

Filgrastim treatment on a named ALS patient basis

Granulocyte-colony stimulating factor (G-CSF) is considered a neurotrophic factor for MNs and a potential target for ALS treatment (Pitzer et al., 2008). Receptors of G-CSF are expressed in various brain regions and G-CSF properties allow for passage of the blood brain barrier (Schneider et al., 2005). Potential effects of G-CSF on neurogenesis and plasticity of vasculature have lead to increasing relevance of G-CSF for therapy of stroke (Schäbitz & Schneider, 2007; Wallner et al., 2015), psychiatric and neurodegenerative diseases (Schneider et al., 2005). In SOD1 mouse model of ALS, G-CSF treatment counteracts muscle atrophy, increases survival of MNs, improves motor performance and prolongs survival of mutant mice (Pitzer et al., 2008). In humans, G-CSF is well tolerated and shows a trend of slowing ALS progression (Nefussy et al., 2010). The lack of significant beneficial documented effects of G-CSF so far is believed to result from small

sample sizes, low dosages, short treatment and lack of suitable biomarkers (Duning et al., 2011; Nefussy et al., 2010). Dense dose application and longitudinal G-CSF–treatment up to 3 years are well tolerated and replicate effects on bone marrow function (Grassinger et al., 2014). The treatment program of G-CSF (Filgrastim) with written informed consent involves 36 patients in a treatment observation period since January 2010. All patients have been treated with standard Riluzole and additional G-CSF on a named patient basis. Doses and application modes of G-CSF have been individually adapted. Treatment duration is up to eight years. Safety and monitoring have been ensured by monthly clinical examinations and acquisition of biomarkers in regular intervals. Neuroimaging has been conducted approximately every three months. Neuroimaging data has been acquired in 31 out of 36 patients.

This treatment program includes no control group without G-CSF treatment, as it is not a clinical trial. As the thesis has been conducted on the behalf of the Department of Experimental Psychology, the focus is set on neuroimaging biomarkers rather than medicinal effects of G-CSF.

BIOMARKERS

The demand of valid biomarkers is urgent for the classification of ALS and the evaluation of therapeutic effects (Cheah, Vucic, Krishnan, Boland, & Kiernan, 2011). A biomarker is roughly termed a measurable correlate for biological processes (Benatar et al., 2016). However, biomarkers may have diagnostic, prognostic, predictive and pharmacodynamical functions. Diagnostic biomarkers are essential for the decision, whether patients should be classified as having a disease or not. Prognostic biomarkers enable the estimation of risk or progression of disease. Predictive biomarkers help to evaluate the potential outcome of therapeutic interventions. Pharmacodynamical biomarkers enable the characterization of the biological mode of action of a drug. As of date, multiple candidate biomarkers for ALS have been discovered for different domains: Tissues and fluids, electrophysiological correlates, neuroimaging markers and clinical indicators (Turner et al., 2013, Table 1.2). Saliva, urine, blood and CSF are easily accessible biomarker sources for the analysis of proteins involved in molecular pathological mechanisms like neuroinflammation (Turner et al., 2013; Vu & Bowser, 2017). Tissue analysis of muscles may help to investigate processes of atrophy and denervation (Sorarù et al., 2008). The analysis of post-mortem

tissue is highly relevant, but hindered by lack of disposability or limited conservation of tissue (Corcia et al., 2008; Turner et al., 2013). Neurophysiological biomarkers may include LMN-specific motor number estimation (MUNE), motor unit number index (MUNIX), and UMN-specific transcranial magnetic stimulation (TMS) (Vucic, Ziemann, Eisen, Hallett, & Kiernan, 2012). These biomarkers enable the quantification of functional integrity of LMN and UMN units. Progression of ALS disease is routinely monitored by neurological examination and clinical scores (Rutkove, 2015). The most frequently used clinical score is the ALS-specific functional rating scale revised (ALSFRS-R). The ALSFRS-R includes 12 items concerning functions of speech, salivation, swallowing, handwriting, handling utensils, self-care, turning, walking, climbing, shortness of breath and respiratory insufficiency (Cedarbaum et al., 1999, Appendix 1). Medical doctors rate one score per item from 4 (normal) to 0 (inability) resulting in 48 score points in total. The ALSFRS-R is fast and easy to assess and is considered a reliable correlate to survival (Gordon, Miller, & Moore, 2004). Non-invasive neuroimaging of the brain and spinal cord has given rise to a variety of promising biomarkers relevant to diagnosis and prognosis of ALS (Agosta, Spinelli, & Filippi, 2018).

Table 1.2

Candidate biomarkers for ALS (Turner et al., 2013). MUNE: motor unit number estimation, MUNIX: motor unit number index, TMS: transcranial magnetic stimulation, ALSFRS-R: ALS-specific functional rating scale revised.

Method	**Focus on …**	**Candidate biomarkers**
Body-Fluids	CSF, saliva, blood, urine	E.g. inflammatory biomarkers
Tissues	Muscle, skin, post-mortem tissue	Cell-type analysis
Neurophysiology	Lower motor neuron Upper motor neuron	MUNE, MUNIX TMS
Clinical measures	Disease progression	ALSFRS-R
Neuroimaging	Brain, spinal cord	Various modalities (see below)

Combinatory biomarker use of neuroimaging biomarkers and other biomarker modalities may pave the way to find a signature for ALS (Chen & Shang, 2015). The thesis focuses

on structural MRI biomarkers of the brain and combines these biomarkers with neurophysiological correlates and routine clinical biomarkers.

Study 1 combines MRI cortical thickness with neurophysiological MUNIX and clinical data. **Study 2** and **study 3** use a biomarker combination of MRI with clinical scores, and survival.

In the last twenty years, neuroimaging findings have enormously contributed to the understanding of changes in structure and function of the brain in ALS (Chiò et al., 2014). The following section will enlarge upon the MRI technique and its relevance as a biomarker source for ALS.

MAGNETIC RESONANCE IMAGING

MRI is a non-invasive medical imaging technique enabling the investigation of structure and function of the human body (Vijayalaxmi, Fatahi, & Speck, 2015). MRI is based on the molecular spin of protons in the presence of an external magnetic field (McMahon, Cowin, & Galloway, 2011). The most frequently studied targets of clinical MRI are hydrogen nuclei as the human body is composed of high amounts of water. In the absence of an external magnetic field, the spin of hydrogen protons is random and driven by thermal energy. Based on the positive charge of protons, spin motion generates electrical current. The presence of an external magnetic field induces the protons to align their spin to the magnetic field in either parallel or antiparallel manner (precession, longitudinal magnetization). Parallel state means in the same direction as the magnetic field. The parallel state is the preferred alignment as it provides a low energetic status. In the antiparallel state, spins of protons are opposite to the external magnetic field. The relation of number of spins in parallel to that of antiparallel state is called net magnetization. The application of a temporary radiofrequency (RF) pulse of 90° flip angle perpendicular to the magnetic field leads to a shift of molecular spin of protons from longitudinal to transverse plane and in the same phase. Protons are now in a high energetic status. Protons emit a signal to return to low energetic status in the horizontal plane. This signal is detected as voltage by a receiver coil. The return of spins to the longitudinal plane is called relaxation (Grover et al., 2015). Relaxation may primarily be described by either longitudinal (T1) or transverse (T2) relaxation times (McMahon et al., 2011). Longitudinal relaxation (spin-

lattice) refers to the restoration of longitudinal magnetization. Transverse relaxation describes the loss of transverse magnetization (spin-spin), which is accelerated by spin-spin interactions or inhomogeneity of the magnetic field. The time needed for T1 or T2 relaxation strongly depends on the biological characteristics of tissue. T2 relaxation time is usually much shorter than T1. Therefore, the application of a 180° spin echo pulse is used to restore in-phase spins of protons and delay T2. This procedure prohibits the loss of MRI signal. MRI images also include spatial information aside from chemical characteristics of tissue (Grover et al., 2015). For this purpose, MRI scanners obtain three sets of gradient coils on X, Y and Z axis, which enable the localization of the MR signal. Grey values of voxels (volumetric pixels) of MRI images may be based on T1 and T2 relaxation times, diffusion, perfusion and oxygen levels among others (Plewes & Kucharczyk, 2012).

The thesis focuses on MRI imaging of the brain and different MRI modalities. **Study 1** involves T1-weighted imaging. **Study 2** focuses on DWI. **Study 3** investigates FLAIR imaging.

T1-weighted imaging is based on relaxation times of spins dependent on characteristics of tissue (Grover et al., 2015). The dense structure of bone exhibits short T1 and is visualized in bright stain. Fluids like cerebrospinal fluid (CSF) show long T1 resulting in dark stain on T1-weighted images. T1 contrast enables the evaluation of disease-associated alterations (Maniam & Szklaruk, 2010) as well as the investigation of morphometry (volume, area, cortical thickness) of regions of interest (ROI). DWI aims at the quantification of movement of water molecules (Grover et al., 2015). Similar to classic MRI theory, a RF impulse induces the precession of protons from longitudinal to transverse magnetization in-phase. The precession of the dephasing gradient is followed by a rephasing gradient in opposite tune. The purpose of the rephasing gradient is to return effects of the dephasing gradient. In case of static water molecules, rephasing procedure is expected to be complete. If water molecules move between the set of dephasing and rephasing gradients, rephasing effects will be incomplete resulting in a reduced MRI signal. Based on Brown's law, water molecules move randomly in all directions (isotropic), if the surrounding environment is free of obstacles. Biological structures restrict the movement of water molecules. In this case, diffusion is described anisotropic, as it is rather directed than free and random. Diffusion of water molecules can be described by a 3D ellipsoid called a diffusion tensor. The tensor estimates diffusion by three eigenvalues and three eigenvectors. Eigenvalues describe height of diffusion, while eigenvectors account for directions of diffusion. In Diffusion tensor imaging (DTI), every

voxel of the brain is given a tensor. The resulting map of diffusion also enables the reconstruction of WM tracts by following streamlines of diffusion properties. Fractional anisotropy (FA) is a frequently used DWI variable of interest describing directivity of diffusion. In ALS research, reduced FA is associated with loss of WM tract integrity (Menke et al., 2012). In FLAIR imaging, the excitatory RF impulse is preceded by a 180° pulse (Bitar et al., 2006). The time window between those two pulses is crucial and called inversion recovery time. By the use of specific inversion recovery times, signal of certain fluids (e.g. CSF) can be elucidated. This method enables the detailed investigation of anatomical details at the borders of the CSF and in the brainstem (Hajnal et al., 1992). In neurodegenerative diseases like multiple sclerosis (MS), local hyperintensity signal in FLAIR images may be interpreted as WM lesions (Gawne-Cain, Silver, Moseley, & Miller, 1997).

Neuroimaging has provided new insights into the pathogenesis of ALS and has raised many potential biomarkers for either presymptomatic or manifested ALS (Turner & Verstraete, 2015). The most frequently used MRI techniques in ALS are T1, DWI, FLAIR, functional MRI (fMRI) and magnetic resonance spectroscopy (MRS) (Grolez et al., 2016; see Table 1.3). Alterations of structure and function of corticospinal tract (CST), motor cortex and spinal cord are most consistently reported in ALS (Grolez et al., 2016). However, MRI alterations also involve non-motor areas. GM morphometric studies based on T1-weighted imaging reveal regional atrophy of the precentral cortex (Chiò et al., 2014). However, alterations in volume (Grosskreutz et al., 2006) or cortical thickness (Agosta et al., 2012) are not consistently reported in all studies. WM degeneration as detected by DWI is considered to be a rather consistent marker for ALS (Chiò et al., 2014). Studies have revealed reduced FA (Kassubek et al., 2014) and enhanced mean diffusivity (Ellis et al., 1999) along the CST and in extra-motor WM areas (Grolez et al., 2016). FLAIR imaging as a conventional MRI technique is primarily assessed to exclude ALS mimics like MS (Chiò et al., 2014). Despite detection of hyperintensity in CST and corpus callosum (Fabes et al., 2017) the specificity and sensitivity of FLAIR imaging for ALS is still a matter of debate (Chiò et al., 2014). FMRI has been used to detect alterations in the activity of the motor cortex (Mohammadi et al., 2011) or in functional connectivity of the sensorimotor network and frontoparietal network (Agosta et al., 2011, 2013). MRS has revealed deviations in metabolic concentrations, especially of N-acetyl aspartate and choline in the motor cortex (Lombardo et al., 2009). Despite biomarker potential of fMRI and MRS, studies using these techniques are still sparse.

Table 1.3

Most frequently used MRI techniques, variables of interest, and exemplary findings in ALS research (see review Grolez et al., 2016). DWI: Diffusion weighted imaging, FLAIR: fluid-attenuated inversion recovery, fMRI: functional magnetic resonance imaging, MRS: magnetic resonance spectroscopy, FA: fractional anisotropy, MD: Mean diffusivity, CST: corticospinal tract.

MRI technique	Variables of interest	Findings
T1	Volume	Reduced precentral volume (Grosskreutz et al., 2006)
	Cortical thickness	Reduced precentral cortical thickness (Agosta et al., 2012)
DWI	FA	Reduced FA along the CST (Kassubek et al., 2014)
	MD	Enhanced MD along the CST (Ellis et al., 1999)
FLAIR	Hyperintensity signal	Hyperintensity of the CST and the corpus callosum (Fabes et al., 2017)
fMRI	Motor task fMRI	Elevated activity in the motor cortex (Mohammadi et al., 2011)
	Functional and structural connectivity	Alterations in the sensorimotor network and frontoparietal network (Agosta et al., 2011, 2013)
MRS	Metabolic concentration	Altered peaks of N-Acetylaspartate and choline in the motor cortex (Lombardo et al., 2009)

The current thesis focuses on GM morphometry, WM diffusion properties and FLAIR lesion detection as potential MRI biomarkers for ALS. Moreover, these MRI biomarkers are combined with clinical and neurophysiological biomarkers. Study 1 examines GM morphometry by combinatory biomarker use of precentral and postcentral cortical thickness with neurophysiological MUNIX and clinical scores. Study 2 investigates WM diffusion properties by FA of different WM types associated with clinical data. Study 3 evaluates a newly established toolbox for the detection and quantification of FLAIR alterations in ALS. Preparatory work and the background, methods, and findings of the three subprojects are described in the following chapter.

CHAPTER 2: PROJECTS

PREPARATORY WORK

INTRODUCTION TO NEUROPHYSIOLOGICAL MUNIX DATA

The thesis involves MRI biomarkers as well as clinical and neurophysiological biomarkers. Therefore, it is necessary to become acquainted with the analysis and interpretation of MUNIX data. MUNIX has primarily been assessed in the musculus abductor digiti minimi (ADM) of the hand. The ADM is a muscle innervated by the ulnar nerve and in charge of movement of the little finger (Muscolino, 2014). Preparatory analysis includes 17 ALS patients with MUNIX assessment in the left and right ADM. MUNIX scores averaged across left and right hands significantly correlate with corresponding ALSFRS-R sum scores (r = .569, p = .017) (Figure 2.1.1A). ALS patients exhibit variable baseline levels and different progression of MUNIX over time (Figure 2.1.1B). The heterogeneity of baseline levels and progression of MUNIX may be linked to different onsets of disease (arm, leg) or different involvement of UMN and LMN. These findings are relevant for study 1 combining MRI biomarkers with neurophysiological MUNIX and clinical ALSFRS-R.

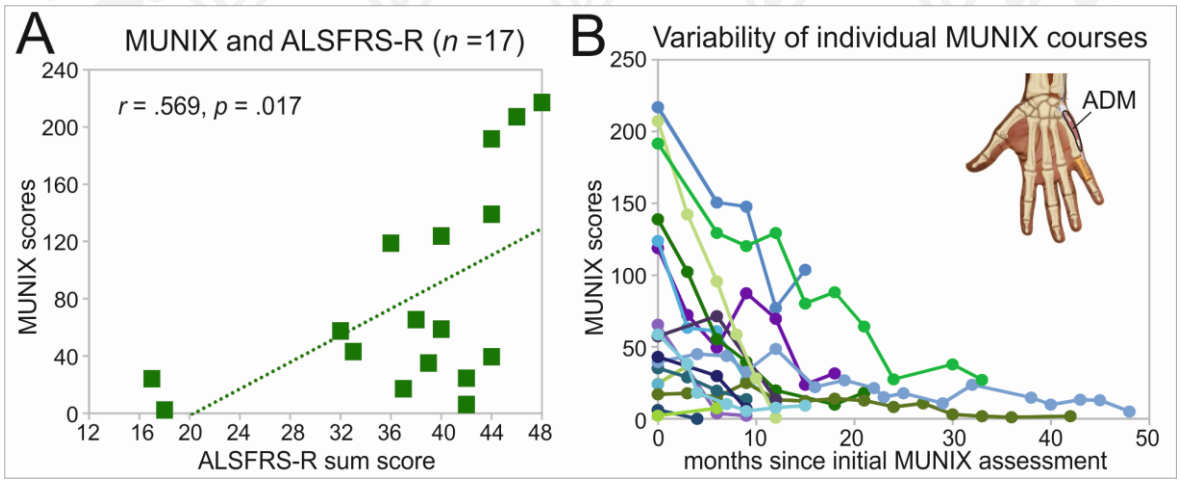

Figure 2.1.1. Preparatory study on MUNIX scores in 17 ALS patients. A) Correlation of MUNIX scores with ALSFRS-R scores at baseline. B) Variability of baseline level of MUNIX and progress of MUNIX decline over time in 17 individual patients. Illustration of the abductor digiti minimi (ADM) muscle of the right hand (adapted from Muscolino, 2014). MUNIX scores are averaged across left and right ADM.

PILOT TRIAL ON EDINBURGH COGNITIVE AND BEHAVIORAL ALS SCREEN

ALS patients may exhibit both motor deficits and cognitive impairment (Beeldman et al., 2016). Cognitive decline may involve speech, executive functions as well as social cognition. Frontal Assessment Battery (FAB; Dubois, Slachevsky, Litvan, & Pillon, 2000), Montreal Cognitive Assessment (MoCA, Nasreddine et al., 2005) or Mini Mental State Examination (MMSE; Tombaugh, McDowell, Kristjansson, & Hubley, 1996) are frequently used cognitive screening tools in clinical routine (Lulé et al., 2015). General cognitive decline (MMSE) and frontal cognitive impairment (FAB, MoCA) are predominantly detected in ALS patients with the behavioral variant of frontotemporal dementia (ALS-FTD) compared to healthy controls (Ohta et al., 2017). However, neuropsychological tools like MMSE, FAB, and MoCA may be biased by impaired motor performance of ALS patients (Heimrath et al., 2014; Lulé et al., 2015). The Edinburgh Cognitive and Behavioral ALS screen (ECAS) is a newly established cognitive screening tool, which enables a fast and reliable cognitive screening of ALS patients without motor biases (Lulé et al., 2015). It may be performed in either written or oral form. The ECAS is composed of a cognitive screen and a behavioral screen. The behavioral screen assesses behavioral disinhibition, apathy, empathy, behavioral abnormalities (perseverations, stereotypes, compulsive or ritualistic behaviour), nutrition, and includes a psychosis scale. The pilot trials focus on only the cognitive screen, as inclusion of the behavioral screen would have required more time and the presence of a caregiver (Lulé et al., 2015). The ECAS cognitive screen (Appendix 2) includes a so-called ALS-specific and ALS-nonspecific cognitive domain. ALS-specific cognitive deficits include language and executive functions. In contrast, memory or visuospatial abilities are considered to be preserved in ALS and account for ALS-nonspecific cognitive abilities. Two patients of the treatment program have been enrolled in a pilot estimation on ECAS use. These exams have been conducted to evaluate feasibility of this screening tool for prospective use. Both patients involved in this examination are male, limb-onset, leg-onset, and exhibit comparable education and professional background. Table 2.1.1 lists the results of the two pilot exams. ALSFRS-R sum scores at ECAS acquisition day were 29 score points for patient 1 and 34 score points for patient 2. ECAS assessment reveals no evident cognitive deficits of patient 1 in either ALS-specific or ALS-nonspecific cognitive domain. Patient 2 shows unremarkable cognitive skills in ALS-nonspecific domains. ALS-specific cognitive functions of patient 1 are estimated divergent in ALS-specific domains, especially in tasks concerning speech and verbal fluency. However, these results should be interpreted

carefully, as patient 2 is not a native speaker of German. In both patients, ECAS assessment was fast (approximately 15min), feasible, and well tolerated by the patients. However, scores for speech and verbal fluency may be biased by language skills of non-native speakers of German.

The thesis has initially been planned to include a prospective study using the ECAS and fMRI. Prolonged data analysis and still limited funding prohibited the conduction of a prospective randomized clinical trial (RCT). Thus, the thesis was limited to retrospective data acquired since 2010. Results of ECAS exams were incorporated in study 1.

Table 2.1.1

Scores of ECAS assessment in two patients of the named patient basis treatment program. The ECAS includes tasks for so-called ALS-specific domains (language, verbal fluency, executive functions) and ALS-nonspecific domains (memory, visuospatial functions).

	Domains	**Tasks**	**Patient 1**	**Patient 2**
ALS-specific	Language	Naming	7/8	8/8
		Comprehension	8/8	8/8
		Spelling	12/12	4/12
	Verbal fluency	S fluency	10/12	10/12
		G fluency	12/12	3/12
	Executive functions	Reverse Digit Span	12/12	4/12
		Alternation	12/12	12/12
		Sentence completion	12/12	10/12
		Social cognition	12/12	12/12
	Total		97/100	71/100
ALS-nonspecific	Memory	Immediate recall	7/10	4/10
		Delayed recall	10/10	10/10
		Delayed recognition	3/4	3/4
	Visuospatial functions	Dot counting	4/4	4/4
		Cube counting	4/4	4/4
		Number location	4/4	4/4
	Total		32/36	29/36
Total score			129/136	100/136

PROJECT 1: GREY MATTER MORPHOMETRY

Combinatory Biomarker Use of Cortical Thickness, MUNIX, and ALSFRS-R at Baseline and in Longitudinal Courses of Individual Patients with Amyotrophic Lateral Sclerosis

Wirth, A. M., Khomenko, A., Baldaranov, D., Kobor, I., Hsam, O., Grimm, T., Johannesen, S., Bruun, T.-H., Schulte-Mattler, W., Greenlee, M. W., Bogdahn, U.

Author-produced version of an article published after peer-review on July 30th 2018 in Frontiers in Neurology, Frontiers, Lausanne, Switzerland. Reprinted with permission.

ABSTRACT

Amyotrophic lateral sclerosis (ALS) is a progressive neurodegenerative process affecting upper and lower motor neurons as well as non-motor systems. In this study, precentral and postcentral cortical thinning detected by structural magnetic resonance imaging (MRI) were combined with clinical (ALS-specific functional rating scale revised, ALSFRS-R) and neurophysiological (motor unit number index, MUNIX) biomarkers in both cross-sectional and longitudinal analyses. The unicenter sample included 20 limb-onset classical ALS patients compared to 30 age-related healthy controls. ALS patients were treated with standard Riluzole and additional long-term G-CSF (Filgrastim) on a named patient basis after written informed consent. Combinatory biomarker use included cortical thickness of atlas-based dorsal and ventral subdivisions of the precentral and postcentral cortex, ALSFRS-R, and MUNIX for the musculus abductor digiti minimi (ADM) bilaterally. Individual cross-sectional analysis investigated individual cortical thinning in ALS patients compared to age-related healthy controls in the context of state of disease at initial MRI scan. Beyond correlation analysis of biomarkers at cross-sectional group level (n = 20), longitudinal monitoring in a subset of slow progressive ALS patients (n = 4) explored within-subject temporal dynamics of repeatedly assessed biomarkers in time courses over at least 18 months. Cross-sectional analysis demonstrated individually variable states of cortical thinning, which was most pronounced in the ventral section of the precentral cortex. Correlations of ALSFRS-R with cortical thickness and MUNIX were detected. Individual longitudinal biomarker monitoring in four slow progressive ALS patients revealed evident differences in individual disease courses and temporal dynamics of the

biomarkers. A combinatory use of structural MRI, neurophysiological and clinical biomarkers allows for an appropriate and detailed assessment of clinical state and course of disease of ALS.

INTRODUCTION

ALS is a rapidly progressive neurodegenerative disorder affecting upper and lower motor neurons as well as non-motor systems (Riva, Agosta, Lunetta, Filippi, & Quattrini, 2016). The degeneration of motor neurons results in muscular fasciculation, progressive weakness, and eventual paralysis (Calvo et al., 2014). Average survival in ALS is 3–5 years, but patients evidently vary in phenotype and disease progression (Calvo et al., 2014, Rosenfeld & Strong, 2015). The great clinical heterogeneity in ALS is reflected by different phenotypes with variability regarding the involvement of UMN and LMN signs, site of onset (bulbar, limb), rate of progression, and involvement of neurobehavioral deficits (Calvo et al., 2014; Chiò et al., 2011). Therefore, clinical and biological biomarkers are helpful in describing disease severity and progression (Rosenfeld & Strong, 2015). MRI has produced potential biomarkers that clarify the role of brain structure and function in the progress of the disease (Agosta et al., 2010; Simon et al., 2014). In structural morphometric studies, cortical thickness compared to surface and volume was most sensitive to disease-related changes (Turner & Verstraete, 2015). A variety of studies investigating structural surface-based morphometry showed reduced cortical thickness primarily in the precentral cortex (Agosta et al., 2012; De Albuquerque et al., 2017; Kwan, Meoded, Danielian, Wu, & Floeter, 2012; Mezzapesa et al., 2013; Roccatagliata, Bonzano, Mancardi, Canepa, & Caponnetto, 2009; Schuster et al., 2013, 2014; Verstraete et al., 2012; Walhout et al., 2015). Cortical thinning was not restricted to the primary motor cortex. Several studies reported cortical thinning to spread to non-motor cortex areas like the temporal, frontal, parietal, and postcentral cortex (Agosta et al., 2012; Kwan et al., 2012; Verstraete et al., 2012). However, not all published MRI studies detected alterations in the cortical thickness (Cardenas-Blanco et al., 2016) or cortical volume (Ellis et al., 2001; Mezzapesa et al., 2007) of the precentral cortex of ALS patients. Essentially, precentral cortical thinning was reported to be focal, and dependent on the clinical phenotype, rate of progression, and age (Agosta et al., 2012; Mezzapesa et al., 2013; Schuster et al., 2013). Additionally, several longitudinal MRI studies revealed no further cortical thinning of the precentral cortex in the course of disease (Cardenas-Blanco et al., 2016; De Albuquerque et al., 2017; Schuster et al., 2014; Verstraete et al., 2012; Walhout

et al., 2015). In addition to MRI, clinical and electrophysiological biomarkers are among the most currently used and prominent biomarkers (Benatar et al., 2016). The widely used ALS-specific functional rating scale revised (ALSFRS-R) and its subscales are correlated with survival (Rosenfeld & Strong, 2015). However, correlations between precentral cortical thickness and ALSFRS-R scores were rather weak (Cosottini et al., 2016; Kwan et al., 2012) or not detected in several neuroimaging studies so far (De Albuquerque et al., 2017; Roccatagliata et al., 2009; Schuster et al., 2013; Thorns et al., 2013; Walhout et al., 2015). While MRI is considered a suitable biomarker for UMN function, neurophysiological motor unit number estimation (MUNE) and motor unit number index (MUNIX) are treated as biomarkers for the estimation of functional lower motor units (Stein, Kobor, Bogdahn, & Schulte-Mattler, 2016; Van Es et al., 2017). MUNE is calculated from the division of maximal compound muscle action potential (CMAP) by the mean surface single motor unit action potential (SMUP) (Gooch et al., 2014). In contrast, MUNIX is derived from a mathematical model based on CMAP and electromyographic surface interference patterns (SIP) (Grimaldi et al., 2017). MUNE and MUNIX scores are inter-correlated in ALS patients (Stein et al., 2016). As the acquisition of MUNIX is easier and less time consuming than that of MUNE, MUNIX has become a promising biomarker of motor unit loss (Grimm & Schulte-Mattler, 2017; Escorcio-Bezerra et al., 2016). MUNIX scores were correlated with ALSFRS-R scores (Grimaldi et al., 2017), but they declined faster than ALSFRS-R scores over time in ALS patients (Neuwirth et al., 2017). Only few studies investigated the relationship between neurophysiological biomarkers and cortical thickness and failed to find a significant correlation with MUNE or other motor evoked potential indices (Cosottini et al., 2016; Mitsumoto et al., 2007). To our knowledge, no published study investigated correlations between cortical thickness and MUNIX as a biomarker potentially affected by both lower and UMN function (Stein et al., 2016).

Aim of the study was to investigate individual states of cortical thinning of the precentral and postcentral cortex in a limb-onset ALS sample with respect to young-onset, and slow disease progression. It is the first study to analyze combinatory biomarker use of MRI cortical thickness, neurophysiological MUNIX, and routine ALSFRS-R in both cross sectional group analysis of the whole sample, and in longitudinal monitoring exploring differences in temporal dynamics between biomarkers in a subgroup of slow progressive ALS patients.

METHODS

Participants

Cross-sectional group analysis included 20 limb-onset classical ALS patients (5 females, *M* = 48 years, *SD* = 11) compared to 30 age-related healthy controls (14 females, *M* = 45 years, *SD* = 13). Mean age of ALS patients was lower than that reported in other ALS studies, as the sample included several young-onset patients. Mean ALSFRS-R score across all 20 patients at the time point of first MRI scan was 36 score points (*SD* = 8; range: 23–48). The sample included both slow and fast progressive ALS patients indicated by disease progression rates (*M* = 0.51, *SD* = 0.27; range: 0.00–1.00). The presence of both UMN and LMN signs in all patients allowed no clear differentiation in UMN or LMN predominance of disease. Patients' characteristics are summarized in Table 2.2.1. These included age (in ranges of years), ALSFRS-R sum scores and neurophysiological MUNIX scores for left and right ADM upon initial MRI scan, time interval between symptom onset and initial T1 MRI scan (in months), onset of disease (arm, leg), and progression rates ((48-ALSFRSR)/ months since symptom onset) (Agosta et al., 2012).

Genetic background of ALS was exhibited in one patient only (patient 8). All other patients were diagnosed as sporadic ALS. All patients received standard Riluzole treatment and additional G-CSF (granulocyte-colony stimulating factor, Filgrastim) treatment on a named patient basis. Application modes and doses of G-CSF were individually adapted, treatment duration was up to 7 years. For safety and monitoring of progression, structural MRI and MUNIX were assessed every 3 months. ALSFRS-R scores were acquired monthly, but were integrated in the analysis only at the time points of MRI scanning. MRI cortical thickness was combined with ALSFRS-R sum scores, and MUNIX scores for left and right ADM in both cross-sectional analysis and longitudinal biomarker monitoring. The unicenter project was carried out in accordance with the Declaration of Helsinki (World Medical Association) and approved by the ethics committee at the University of Regensburg (ethics approval: 15-101-0106). Written informed consent was obtained prior to participation in all participants.

Table 2.2.1

*Patients' characteristics at baseline. Summary of characteristics of all 20 limb-onset ALS patients including age (in ranges of yrs), ALSFRS-R sum score upon initial MRI scan (48 in clinical non affected), neurophysiological MUNIX scores for left and right ADM upon initial MRI scan, the length of time span between symptom onset and initial MRI scan in months, onset of disease (arm, leg), and progression rate. In four out of 20 ALS patients (marked with *), neurophysiological assessment was still conducted using MUNE technique (patient 4: left MUNE = 2, right MUNE = 1; patient 7: left MUNE =3, MUNE right = 77; patient 13: left MUNE = 275, right MUNE = 85; patient 15: left MUNE = 240, right MUNE = 120). No MUNIX scores were obtained in these four patients. Progression rates were calculated by (48 – ALSFRS-R sum score / months since symptom onset) (see Agosta et al., 2012). Neuropsychological assessment using the Edinburgh Cognitive and Behavioral ALS Screen (ECAS) was conducted only in patient 3 (129/136 score points) and patient 9 (100/136 score points).*

#	Range of age	ALSFRS-R [0 48]	MUNIX Left	MUNIX Right	Time span since onset	Onset	Progression rate
1	21-25	30	6.63	10.43	49	Arm	0.37
2	26-30	35	8.20	29.21	28	Arm	0.46
3	31-35	24	6.94	2.83	28	Leg	0.86
4	41-45	24	*	*	28	Leg	0.86
5	41-45	41	54.12	38.00	19	Leg	0.37
6	41-45	28	4.85	0.70	38	Arm	0.53
7	41-45	46	*	*	16	Arm	0.13
8	46-50	39	138.40	41.88	56	Leg	0.16
9	46-50	48	170.10	187.30	19	Leg	0.00
10	46-50	24	48.37	18.51	24	Arm	1.00
11	46-50	46	213.60	193.00	3	Leg	0.67
12	46-50	40	114.50	97.18	21	Leg	0.38
13	46-50	38	*	*	25	Leg	0.40
14	51-55	42	27.25	21.62	7	Arm	0.86
15	51-55	35	*	*	33	Leg	0.39
16	56-60	38	123.90	101.60	29	Leg	0.34
17	56-60	44	126.90	0.00	13	Leg	0.31
18	61-65	42	83.10	119.00	10	Leg	0.60
19	61-65	24	12.34	9.66	33	Leg	0.73
20	66-70	21	6.94	2.83	36	Leg	0.75

Data acquisition

Structural MRI was conducted at a 1.5 Tesla clinical scanner (Aera, Siemens Medical, Erlangen, Germany). For each patient, a high-resolution T1-weighted structural scan was obtained by a magnetization prepared rapid gradient echo sequence (MPRAGE; time-to-repeat TR: 2220ms, time-to-echo TE: 5.97ms, flip angle FA: 15◦, voxel size: 1 × 1 × 1 mm3, field of view FOV: 256 × 256 mm², 176 sagittal slices covering the whole brain). MUNIX estimates the number of motor units in a muscle by a mathematical algorithm involving both the compound muscle action potentials (CMAP) and the continuous electromyographic surface interference pattern (SIP) of the muscles (Stein et al., 2016; Grimm & Schulte-Mattler, 2017). In contrast to original MUNIX, MUNIX recordings of this project implicated continuous SIP recordings during increasing muscle contraction. SIP data were modified by baseline correction, filter settings, rectifications, and SIP intervals. Artifacts were corrected by exclusion of SIP intervals below a specified baseline threshold. As MUNIX was introduced more recently as a neurophysiological biomarker, four out of 20 ALS patients received the assessment of MUNE only (see Table 2.2.1).

MRI Data Processing

T1-weighted structural images were reconstructed by Freesurfer software version 5.3 (Martinos Center for Biomedical Imaging, Charlestown, MA). The reconstruction procedure included automatic segmentation of gray matter and subcortical white matter (Fischl et al., 2002) and tessellation and registration of the cortical surface to a spherical atlas (Fischl, Sereno, Tootell, & Dale, 1999).). For group analysis, T1- weighted images of the 20 individual patients' brains were registered to the Freesurfer average structural brain by using the Freesurfer linear and non-linear image registration tools (FLIRT, FNIRT).

ROI Definition

Cortical thickness analysis focused on precentral and postcentral regions of interest (ROI) as defined by the Desikan-Killiany parcellation atlas (Desikan et al., 2006, see Figure 2.2.1A). Dorsal and ventral subdivisions of the sensorimotor network were defined by a resting-state-functional MRI (fMRI) data-based atlas (Yeo et al., 2011) in volumetric MNI (Montreal Neurological Institute) space. These ROIs were subsequently registered to the Freesurfer volumetric space and then to the Freesurfer average brain surface (see Figure 2.2.1B). As all ROIs were mapped upon the Freesurfer average brain space, ROIs were identically sized in each patient and healthy control.

Computation of Cortical Thickness

Cortical thickness was computed according to a workflow recommended by Freesurfer software. Individual surface-based cortical thickness data were mapped upon the Freesurfer average brain surface. By the use of a segmentation statistical tool of Freesurfer software, cortical thickness in each of the four ROIs (PreD: precentral dorsal, PreV: precentral ventral, PoD: postcentral dorsal, PoV: postcentral ventral, see Figure 2.2.1C) was calculated and extracted as a mean value across vertices.

Cross-Sectional Group Analysis

Group-analysis of mean cortical thickness was conducted using a repeated measures ANOVA with the within-subject factors region (PreD, PreV, PoD, PoV) and hemisphere (left vs. right), and the between-subject factors group (ALS vs. controls), gender (male vs. female), and the covariate age. Differences in cortical thickness between regions were investigated by paired *t*-tests and differences between patients and controls were analyzed using independent-samples *t*-tests. *T*-tests were corrected by Bonferroni correction. Correlation analyses were conducted to investigate relations between cortical thickness, ALSFRS-R sum scores and subscores, and MUNIX by the Bravais-Pearson correlation coefficient. Significance level was set to $p < 0.05$. Multiple comparison errors were controlled by Bonferroni correction procedure in post-hoc analyses.

Individual Cortical Thickness Analysis

In addition to cross-sectional group analysis, this project focused on the interindividual variability of cortical thinning. For this purpose, we compared the cortical thickness of all 20 patients to age-related controls, resulting in individual z-transformed deviations of cortical thickness from healthy control level. As age effects on cortical thickness are well described (Salat et al., 2004), ALS patients were compared to one out of two possible age groups. Based on the mean age of ALS patients, the 30 healthy controls were differentiated into two comparably sized subgroups (1: age <48 years, $n = 17$; 2: age ≥48 years, $n = 13$). Furthermore, z-transformed deviations of cortical thickness from healthy controls as well as biomarkers MUNIX and ALSFRS-R were monitored in four individual slow progressive ALS patients over a time course of at least 18 months (patient 1, 2, 8, 9, see Table 2.2.1). All other patients exhibited MRI time courses of a maximum of 9 months only (3 scans: $n = 2$; 2 scans $n = 6$; 1 scan: $n = 8$) due to high disability and lack of T1 MRI data.

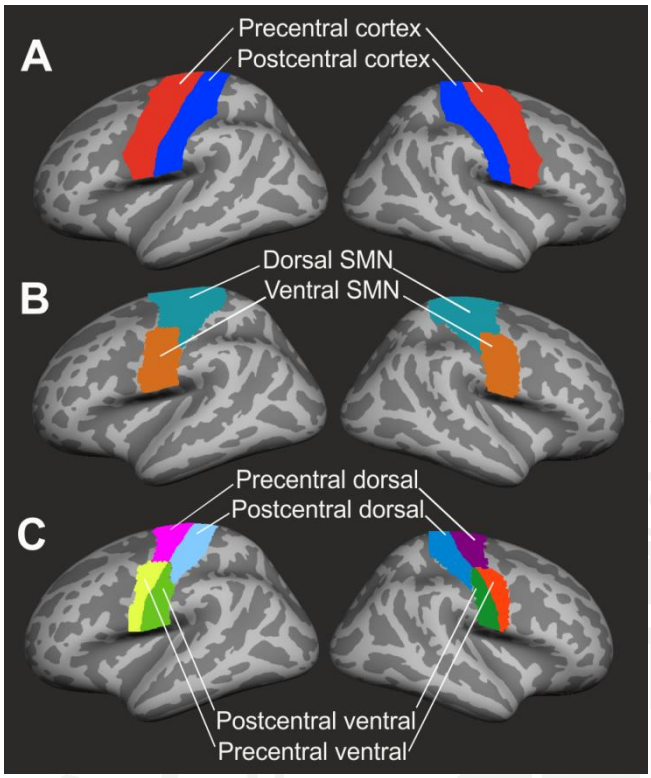

Figure 2.2.1. Definition of regions of interest. A) Precentral (red) and postcentral (blue) cortex were identified by the Desikan-Killiany parcellation atlas (Desikan et al., 2006). B) The resting-state-fMRI based atlas of Yeo et al. (2011) was used to define dorsal (marine blue) and ventral (brown) segments of the sensorimotor network (SMN). C) Final subdivision of the precentral and postcentral cortex into dorsal and ventral segments resulted in four ROIs (precentral dorsal, precentral ventral, postcentral dorsal, postcentral ventral) in both left and right hemisphere. ROIs were mapped upon the Freesurfer average brain surface.

RESULTS

Cross-Sectional Group Analysis

As Mauchly's test indicated that the assumption of sphericity was violated ($\chi^2(5) = 22.42$, $p < 0.001$), degrees of freedom were corrected using Greenhouse-Geisser estimates of sphericity ($\varepsilon = 0.79$). Cortical thickness was not significantly different between patients and healthy controls ($F(1, 45) = 1.314$; $p = 0.258$) at cross-sectional group level. Cortical thickness significantly varied across cerebral regions ($F(3, 135) = 23.351$, $p < 0.001$) and with respect to age ($F(1, 45) = 21.776$, $p < 0.001$). Cortical thickness was significantly higher in precentral than in postcentral regions in both ALS patients ($T(19) = 8.584$, $p < 0.05$, corrected), and healthy controls ($T(29) = 16.521$, $p < 0.05$, corrected) (Figure 2.2.2A). Ventral subdivisions of precentral and postcentral cortex showed greater cortical

thickness than dorsal subdivisions in both ALS patients ($T(19) = 9.906$, $p < 0.05$, corrected) and healthy controls ($T(29) = 12.389$; $p < 0.05$, corrected) (Figure 2.2.2B).

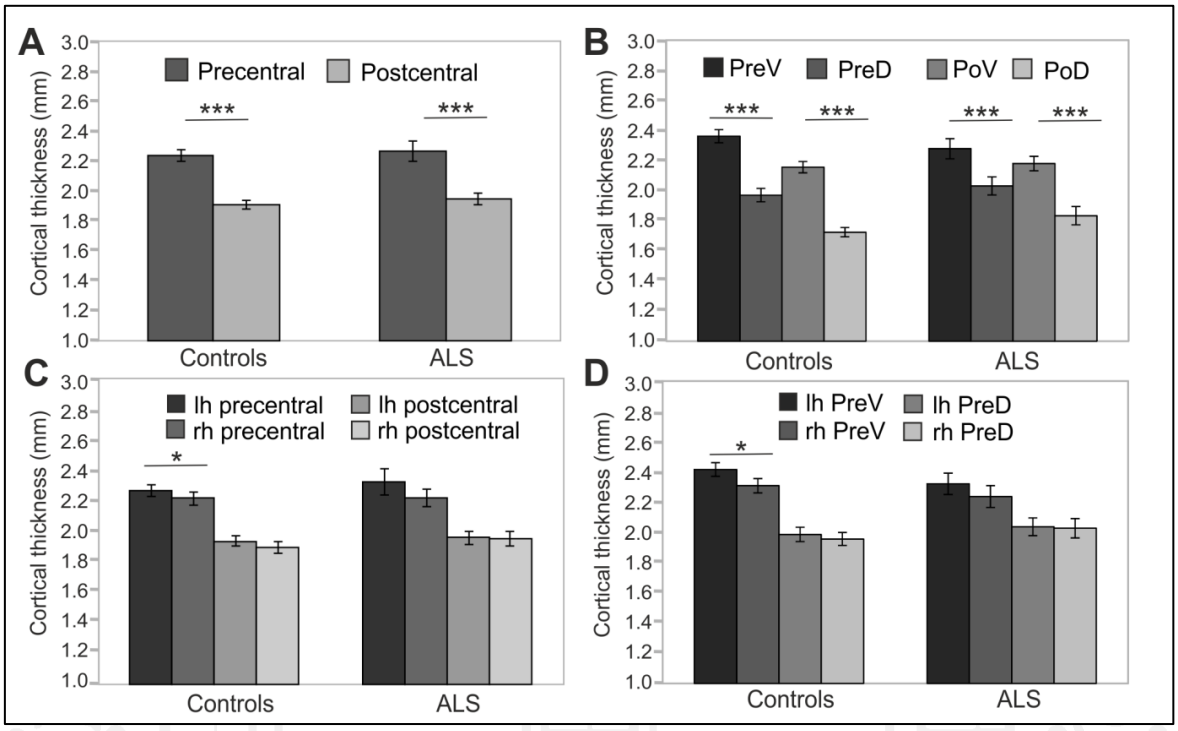

Figure 2.2.2. Precentral and postcentral cortical thickness. Cross-sectional analyses of cortical thickness of ALS patients (n = 20) and healthy controls (n = 30). A) Precentral cortical thickness averaged across left (lh) and right (rh) hemisphere was significantly higher than postcentral cortical thickness in both ALS patients and healthy controls. B) Cortical thickness of ventral segments of both precentral (PreV) and postcentral (PoV) cortex were similarly higher than in dorsal segments (PreD, PoD) in both ALS patients and healthy controls. Hemispheric differences were detected only in the precentral (C) and precentral ventral cortex (D) of healthy controls. Significance level was set to $p < .05$. Bonferroni correction was used for multiple comparisons. Lh = left hemisphere, Rh = right hemisphere, PreV = precentral ventral, PreD = precentral dorsal, PoV = postcentral ventral, PoD = postcentral dorsal.

The ANOVA revealed no significant main effect of hemisphere, as significant hemispheric differences in cortical thickness were restricted to the precentral ($T(29) = 3.445$, $p < 0.05$, corrected) (Figure 2.2.2C) and precentral ventral cortex ($T(29) = 3.596$, $p < 0.05$, corrected) of healthy controls (Figure 2.2.2D). ALSFRS-R sum scores correlated with cortical thickness of the precentral ventral cortex ($r = 0.570$, $p = 0.009$) and the postcentral ventral region ($r = 0.481$, $p = 0.032$). Cortical thickness did not significantly correlate with MUNIX scores for left and right ADM in any ROI. MUNIX scores for the left ($r = 0.767$, $p < 0.05$, corrected) and right ($r = 0.791$, $p < 0.05$, corrected) ADM correlated with ALSFRS-R sum scores. Highest correlations of cortical thickness with ALSFRS-R

subscores were found for turning (PreV: $r = 0.501$, $p = 0.024$; PoV: $r = 0.652$, $p = 0.002$), walking (PoV: $r = 0.603$, $p = 0.005$), and cutting (PreV: $r = 0.453$, $p = 0.045$). MUNIX scores predominantly correlated with ALSFRS-R subscores on handwriting (left ADM: $r = 0.637$, $p = 0.008$; right ADM: $r = 0.678$, $p = 0.005$), cutting (left ADM: $r = 0.840$, $p < 0.001$; right ADM: $r = 0.834$, $p < 0.001$), dressing (left ADM: $r = 0.793$, $p < 0.001$, right ADM: $r = 0.806$, $p < 0.001$), turning (left ADM: $r = 0.609$, $p = 0.012$; right ADM: $r = 0.663$, $p = 0.007$), and climbing stairs (left ADM: $r = 0.563$, $p = 0.023$; right ADM: $r = 0.611$, $p = 0.016$). ALS patients were separated post-hoc in arm-onset ($n = 7$) and leg-onset ($n = 13$) groups. Arm-onset patients showed significantly lower MUNIX scores for ADM (left: $M = 19$, $SD = 19$; right: $M = 16$, $SD = 11$) than leg-onset patients (left: $M = 95$, $SD = 69$; right: $M = 72$, $SD = 72$) (left ADM: $T(14) = -3.399$, $p < 0.05$, corrected; right ADM: $T(14) = -2.506$, $p = 0.029$). Arm-onset and leg-onset patients did not significantly differ in disease progression, ALSFRS-R sum scores and subscores.

Variability of Cortical Thinning

Thirty healthy controls were differentiated into two groups of age (1. age <48 years, 2. age ≥48 years, see section Individual Cortical Thickness Analysis). In each of the two subgroups, means of cortical thickness of all precentral and postcentral ROIs (see Table 2.2.2) were calculated.

Table 2.2.2

References values of cortical thickness. Cortical thickness (mm) of healthy control participants subdivided into two age groups (1: age < 48 yrs, 2: age ≥ 48 yrs). Mean age of the two subgroups: Group 1: M = 36, SD = 7, n = 17; Group 2: M = 52, SD = 15, n = 13. Lh = left hemisphere, Rh = right hemisphere, PreV = precentral ventral, PreD = precentral dorsal, PoV = postcentral ventral, PoD = postcentral dorsal.

		Lh PreV (mm)	**Rh PreV (mm)**	**Lh PreD (mm)**	**Rh PreD (mm)**	**Lh PoV (mm)**	**Rh PoV (mm)**	**Lh PoD (mm)**	**Rh PoD (mm)**
1	*M*	2.542	2.442	2.106	2.068	2.276	2.205	1.804	1.798
	SD	0.205	0.139	0.194	0.158	0.165	0.188	0.158	0.163
2	*M*	2.249	2.132	1.827	1.807	2.072	2.016	1.663	1.584
	SD	0.184	0.275	0.242	0.232	0.198	0.244	0.141	0.145

These mean values were used as reference values for the calculation of *z*-transformed deviations of ROI-specific cortical thickness of individual ALS patients (for patient numbers see Table 2.2.1) from healthy control level. Cortical thickness alterations below at least one deviation from healthy control level were detected in eleven out of twenty patients (patients 1, 2, 3, 4, 6, 10, 14, 16, 18, 19, 20) and marginally indicated in two patients (patients 5, 9). Cortical thinning was primarily observed in the precentral cortex, especially in the ventral segment (Figure 2.2.2A). Most pronounced cortical thinning in all precentral ROIs was detected in patient 10 and patient 19. Leg-onset patient 19 was characterized by older age (range: 61– 65 years), low ALSFRS-R score (24 score points), low MUNIX scores of ADM, and high disease progression rate (0.73). Patient 10 was much younger (range: 46–50 years), but showed low ALSFRS-R score (24 score points), and the highest progression rate (1.00) of the entire patient sample (see Table 2.2.1). The two youngest ALS patients (patients 1–2, age ranges: 21–25 and 26–30 years) shared similar patterns of cortical thinning, similar mode of disease (arm-onset), low ALSFRS-R scores, low MUNIX scores for ADM, and similar disease progression rates (see Table 2.2.1, see Figure 2.2.3A). Cortical thinning in the postcentral cortex was detected in four patients (patients 9, 10, 19, 20; Figure 2.2.3B). Three out of these four patients also exhibited evident precentral cortical thinning. Leg-onset patient 9 stood out of the sample with the highest ALSFRS-R score, high MUNIX scores for ADM, lowest progression rate (0.00), and more pronounced cortical thinning of the postcentral cortex than of the precentral cortex. Increased levels of cortical thickness above healthy control level were more prominent in the postcentral cortex than in the precentral cortex. Seven patients exhibited unremarkable levels of cortical thickness (patients 7, 8, 11, 12, 13, 15, 17). Six (patients 7, 8, 12, 13, 15, 17) out of these seven patients exhibited disease progression rates less or equal to 0.40 (see Table 2.2.1).

Longitudinal Monitoring of Cortical Thickness, ALSFRS-R, and MUNIX

Repeated long-term follow-up T1 MRI data exceeding 18months were available in two leg-onset patients (patients 8, 9) and two arm-onset patients (patients 1, 2). The four patients presented different initial levels and longitudinal courses of ALSFRS-R sum scores (Figure 2.2.4A), MUNIX scores (Figure 2.2.4B), and cortical thickness alterations (Figures 2.2.4C–F). Both patients 1 and 2 have in common young-onset (21–30 years), arm-onset diagnosis, low levels of ALSFRS-R scores (patient 1: 30 score points, patient 2: 35 score points) upon first MRI scan, low MUNIX scores for left and right ADM (see

Table 2.2.1), and similar progression rates (patient 1: 0.37, patient 2: 0.46). In both patients, ALSFRSR sum scores decreased over time (patient 1: blue; patient 2: green; Figure 2.2.4A).

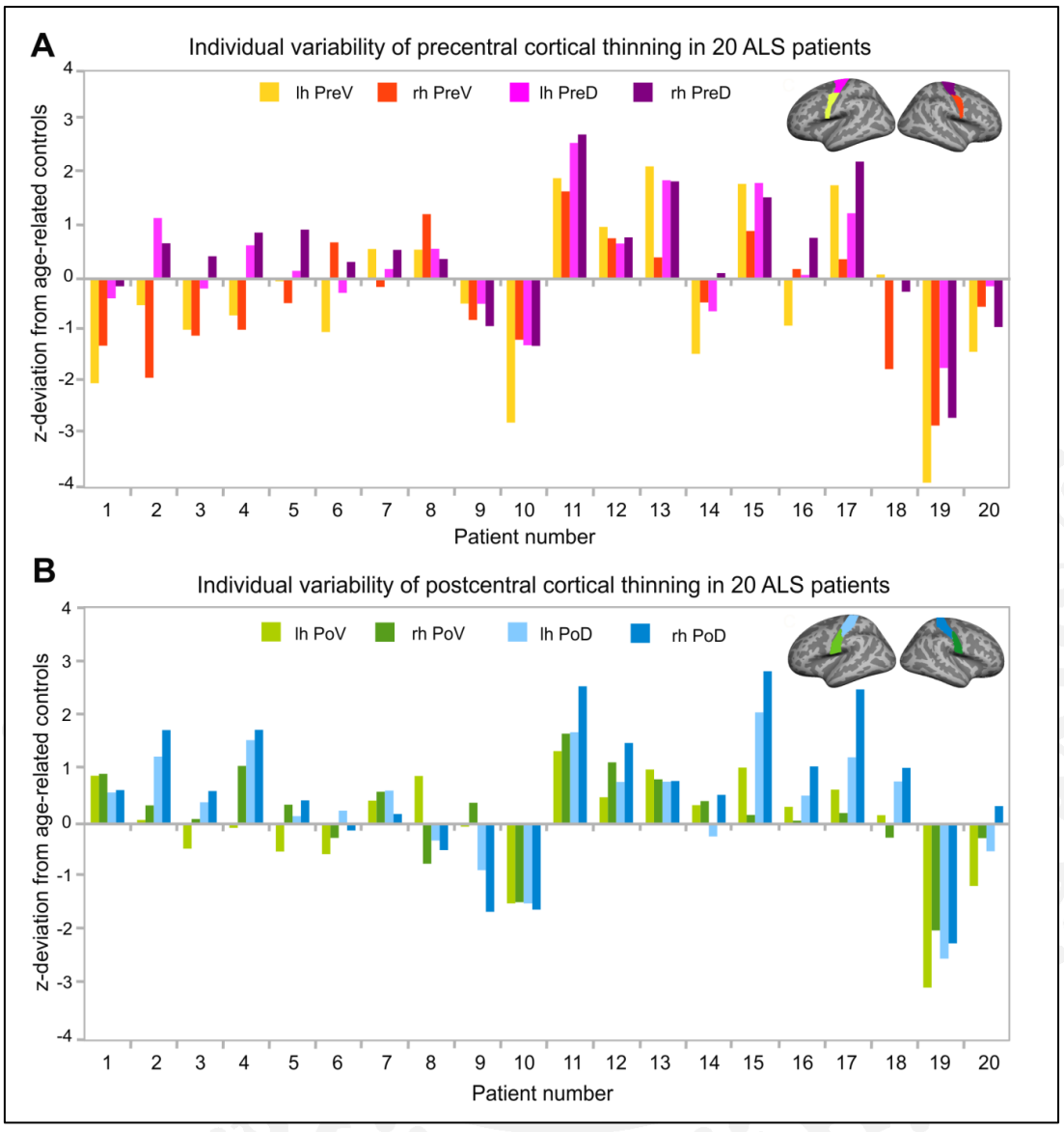

Figure 2.2.3. Individual variability of cortical thinning in ALS patients. Z-transformed deviation of cortical thickness from age-related healthy controls (see Table 2.2.2) in all 20 individual ALS patients. Patient numbers refer to Table 2.2.1. Patients were sorted by age. Z-transformed deviations of cortical thickness were considered relevant at least one deviation from healthy controls. A) Individual variability of cortical thickness of the left (lh, yellow) and right (rh, red) precentral ventral (PreV) and left (lh, pink) and right (rh, purple) precentral dorsal (PreD) ROIs. B) Deviations of individual cortical thickness of the left (lh, light green) and right (rh, dark green) postcentral ventral (PoV) and the left (lh, bright blue) and right (rh, dark blue) postcentral dorsal (PoD) region in the same 20 individual patients. Precentral (A) and postcentral (B) ROIs were visualized upon the Freesurfer average brain surface. Lh = left hemisphere, Rh = right hemisphere, PreV = precentral ventral, PreD = precentral dorsal, PoV = postcentral ventral, PoD = postcentral dorsal.

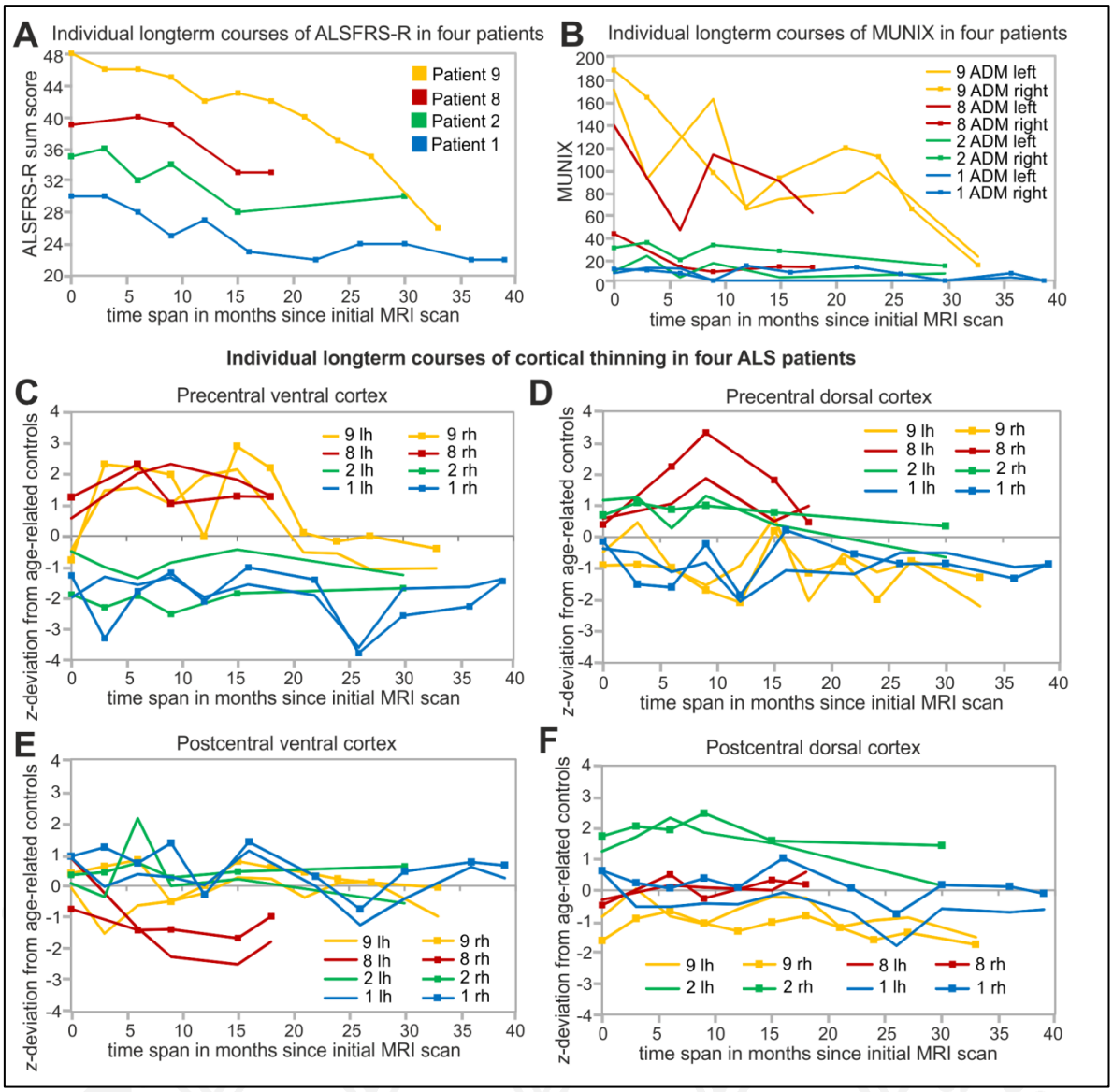

Figure 2.2.4. Individual and long-term biomarker monitoring over at least 18 months. Arm-onset and young-onset patients (patient 1, 2) showed higher progression rates (see Table 2.2.1) than leg-onset similarly aged patients 8 and 9. Patient 9 (yellow), Patient 8 (red), Patient 2 (green), patient 1 (blue) are sorted based on the initial levels of ALSFRS-R sum scores. (A) Courses of ALSFRS-R sum scores of the four individual patients starting at different baseline values and developed differently over the measured time span. (B) Long-term courses of MUNIX scores for the left and right ADM of the same four patients. Individual long-term monitoring of cortical thickness of these four patients in the precentral ventral (PreV, C) and dorsal cortex (PreD, D) and postcentral ventral (PoV, E) and dorsal (PoD, F) cortex of both hemispheres. Individual cortical thickness is *z*-transformed to age-related healthy control level (see Table 2.2.2). Lh = left hemisphere, rh = right hemisphere.

In contrast, MUNIX for left and right ADM stagnated at low level (patient 1: blue; patient 2: green; Figure 2.2.4B). Cortical thickness of the precentral ventral cortex persisted below healthy control level over time in both patients (patient 1: blue, patient 2: green; Figure

2.2.4C). Cortical thickness of the precentral dorsal cortex decreased below healthy control level in patient 1 in the longitudinal course (Figure 2.2.4D). No cortical thinning consistently below healthy control level was found for the postcentral ROIs in both patients 1 and 2 (Figures 2.2.4E, F). Patient 8 and 9 (both aged 46–50 years) were diagnosed with leg onset disease and obtained high ALSFRS-R sum scores at time point of initial MRI scan (Table 2.2.1). Progression rates of patient 8 (0.16) and 9 (0.00) were much lower than for patients 1 and 2. In both patients, ALSFRS-R sum scores declined over time (patient 8: red, patient 9: yellow, Figure 2.2.4A). MUNIX scores of patient 9 similarly decreased for the left and right ADM (yellow, Figure 2.2.4B). In patient 8, MUNIX scores for the left ADM started at much higher level than for the right ADM and showed a more pronounced decline of scores over time (red, Figure 2.2.4B). Patient 8 exhibited progressive cortical thinning only in the postcentral ventral cortex (Figure 2.2.4E). In patient 9, cortical thinning of the right precentral dorsal cortex spread to the left hemisphere over the time course (yellow, Figure 2.2.4D). Cortical thickness of the postcentral dorsal cortex further decreased over time (yellow, Figure 2.2.4F). Despite fluctuations, ventral sections of precentral and postcentral cortex of patient 9 persisted at healthy control level (yellow, Figures 2.2.4C,E).

DISCUSSION

Cortical thinning was heterogeneous and most pronounced in the precentral ventral cortex. ALSFRS-R sum score was associated with both cortical thickness and MUNIX scores. Individual longitudinal monitoring of clinical ALSFRS-R, neurophysiological MUNIX, and MRI cortical thickness indicated both interindividual differences among ALS patients as well as differences in temporal dynamics between biomarkers over the course of disease.

Cortical Thickness of the Precentral and Postcentral Cortex

Cortical thickness was highly age-dependent and significantly different between precentral and postcentral cortex as well as between ventral and dorsal subdivisions of precentral and postcentral cortex. Postmortem (Meyer et al., 1996) and MRI (Fischl & Dale, 2000; Sahin et al., 2016) studies showed approximately 1.5 times greater cortical thickness of the precentral compared to the postcentral cortex. The only study addressing gradients of postcentral cortical thickness in humans (Wagstyl, Ronan, Goodyer, & Fletcher, 2015)

reported greatest cortical thickness in the area defined as ventral segment in our study. Age effects on precentral and postcentral cortical thickness have been well described (Salat et al., 2004).

Variability of Cortical Thinning

Individual cross-sectional analysis revealed heterogeneous individual states of cortical thinning, which was more pronounced in the precentral than in the postcentral cortex. Postcentral cortical thinning was only present in four patients. Three out of these four patients also showed pronounced cortical thinning of the precentral cortex. These observations are consistent with studies reporting postcentral atrophy was rather less prominent or not detectable (Grosskreutz et al., 2006; Roccatagliata et al., 2009). Instead, postcentral atrophy was discussed to result from the spread of cortical degeneration in the course of disease (Brettschneider et al., 2013; Grosskreutz et al., 2006). With respect to the spread of disease, interestingly, individual longitudinal analysis revealed that patient 8 developed postcentral cortical thinning despite lack of precentral cortical thinning. Cortical thinning was most pronounced in the ventral segment of the precentral cortex. The precentral ventral cortex as defined here was also reported to exhibit alterations in ALS patients in other studies (Lillo et al., 2012; Schuster et al., 2014; Schuster, Hardiman, & Bede, 2017). Seven out of twenty patients exhibited no indications of cortical thinning. This finding is supported by a meta-analysis reporting cortical atrophy only in a percentage of ALS cases (Chen & Ma, 2010) and other MRI studies failing to find alterations in the precentral cortex of ALS patients (Cardenas-Blanco et al., 2016; Ellis et al., 2001; Mezzapesa et al., 2007). The lack of cortical thinning in ALS patients may be explained by low progression rates and young-onset. Cortical thinning was primarily observed in ALS patients with faster progression or advanced stage of disease (Meadowcroft et al., 2015). Six out of seven patients exhibiting no indications of cortical thinning were characterized with disease progression rates less or equal to 0.40. Moreover, the ALS sample of the current study was much younger than ALS patients involved in most MRI studies (Agosta et al., 2012, 2016; Cardenas-Blanco et al., 2016; Lillo et al., 2012; Schuster et al., 2013; Spinelli et al., 2016). Individual cross-sectional analysis also revealed enhanced levels of cortical thickness predominantly in the postcentral cortex. Future studies may investigate if enhanced levels of cortical thickness may be associated with processes of neuroplasticity or treatment effects. Finally, heterogeneous alterations in cortical thickness (including

increases and decreases) argue for the need of individual perspective on ALS patients beyond group averages (Simon et al., 2014).

Longitudinal Monitoring of Cortical Thickness, ALSFRS-R, and MUNIX

Longitudinal monitoring of cortical thickness in four patients revealed differences in temporal dynamics of clinical ALSFRS-R, neurophysiological MUNIX, and MRI cortical thickness in the same individual patients. The long-term biomarker monitoring was limited to the patients who survived for longer periods of time and who underwent more than three MRI scans. All other patients of the sample received three MRI scans or less due to short survival or lack of scan capability. Similar to Abhinav et al. (2014), patients showed very different baseline levels and various progression types of ALSFRS-R sum scores over time. While the decline of high-level ALSFRS-R sum scores of patient 9 (ALSFRS-R baseline: 48) was evidently observable, changes in ALSFRS-R sum scores of progressed stage patient 1 (ALSFRS-R baseline: 30) were less evident. These observations are consistent with ALSFRS-R being considered to be less sensitive for short-term time windows and slow disease progression (Rosenfeld & Strong, 2015; Rutkove, 2015; Van Es et al., 2017). ALSFRS-R is also regarded as a rather general severity summary scale without sensitivity for mode of disease (Cardenas-Blanco et al., 2016; Neuwirth et al., 2017). The unspecific character of ALSFRSR may also explain why correlations between ALSFRS-R and cortical thickness were weak or not detectable (Cosottini et al., 2016; De Albuquerque et al., 2017; Verstraete et al., 2012). In contrast to ALSFRS-R, MUNIX significantly differentiated between arm and leg-onset of disease. Corresponding to Grimaldi et al. (2017), MUNIX scores significantly correlated with ALSFRS-R scores, but showed much faster longitudinal dynamics than ALSFRS-R scores as reported by Neuwirth et al. (2017). Once at very low level MUNIX scores stagnated across time in arm-onset patients 1 and 2. The phenomenon of a floor effect of MUNIX measurements at low level in completely wasted muscles was described by Neuwirth et al. (2015). In contrast, higher level MUNIX scores for ADM in leg-onset patients 8 and 9 showed a fast decrease over time. Consistent with these observations, clinical markers are considered to be more sensitive to changes than MRI markers (Cardenas-Blando et al., 2016). Although MUNIX is considered a candidate biomarker like MUNE for LMN function (Van Es et al., 2017), MUNIX scores may be influenced by both lower and UMN function (Stein et al., 2016). Existing studies investigating correlations of cortical thickness to MUNE or other neurophysiological techniques failed to find significant correlations (Cosottini et al., 2016;

Mitsumoto et al., 2007). As the first study combining MRI cortical thickness with MUNIX, we also found no significant correlations. Differences in both individual state of disease and within-subject temporal dynamics of various biomarkers may explain the difficulty to find significant correlations in multimodal biomarker use.

Methodological limitations

Some methodological limitations need to be considered. First, the sample size was limited to 20 patients. As ALS MRI studies suffer from high costs and high drop-out rates due to increasing disability of patients (Rutkove, 2015), many published unicenter ALS MRI studies included samples smaller than 20 ALS patients (Cosottini et al., 2013; Grosskreutz et al., 2006; Roccatagliata et al., 2009; Verstraete et al., 2010). Second, the MRI magnetic field strength was 1.5T. Although MRI magnetic field strength of 3T may have been beneficial, 1.5T still was sufficient for the detection of gray matter alterations in ALS MRI studies (Grosskreutz et al., 2006; Mezzapesa et al., 2013; Roccatagliata et al., 2009; Tavazzi et al., 2015; Thorns et al., 2013). Third, by the use of a more conservative ROI based approach than a vertex-based approach, the study may have failed to detect very focal cortical thinning inside of the ROIs. However, this approach did not only reduce the influence of false positive results but still successfully detected cortical thinning. Fourth, MUNIX scores were not assessed in leg muscles. However, this study is the first cross-sectional and longitudinal study combining cortical thickness analysis with both ALSFRS-R and MUNIX with respect to the individual patient. Fifth, longitudinal monitoring of biomarkers was limited to four patients of the sample due to high disability (n = 6), death (n = 4), lack of T1 data (n = 6). Still, our long term biomarker monitoring analysis is unique, as to our knowledge, none of the published longitudinal MRI studies showed longitudinal courses of both MRI cortical thickness and MUNIX biomarkers using as many repeated measures in a time course longer than 18 months as presented in the current study. Moreover, most MRI studies focused on group analysis irrespective of the individual patient (Cardenas-Blanco et al., 2016; De Albuquerque et al., 2017; Kwan et al., 2012; Schuster et al., 2014; Verstraete et al., 2012; Walhout et al., 2015), although the individual perspective has been increasingly demanded in ALS neuroimaging research (Simon et al., 2014; Turner et al., 2013; Van Es et al., 2017; Verstraete & Foerster, 2015).

CONCLUSIONS

The present study demonstrated that MRI is a potential biomarker for the differentiation of individual states of cortical thinning in an ALS sample including young-onset and slow progressive patients. Longitudinal monitoring of MRI, clinical, and neurophysiological biomarkers in the same patient reveal substantial differences in temporal dynamics. Combinatory biomarker use contributes a substantial gain of information about individual state of disease beyond group averages. Future studies may expand the idea of combining neuroimaging techniques with other clinical or molecular biomarkers to deepen our understanding of multisystem/multifactorial ALS disease progression.

Contributions of authors:

AW: substantial contribution to the conception and the design of the study, acquisition, analysis, interpretation of the MRI data, and composition of the manuscript.

AK, DB: substantial contribution to the conception of the study, data acquisition, interpretation of the data, and revision of the manuscript.

IK, TG, SJ, SM, TB, UB: substantial contribution to the conception of the study, acquisition, analysis, and interpretation of clinical and neurophysiological data, and revision of the manuscript.

SJ, OH, AK, DB, SM, UB: care for ALS patients in outpatient clinic, treatment concept.

MG: substantial contribution to the conception of the study, supervision of MRI data analysis and data interpretation, and revision of the manuscript.

Funding

This work was supported by the German Federal Ministry of Education and Research (BMBF, Project GO-Bio, 031A386).

Conflict of Interest Statement:

The authors declare that the research was conducted in the absence of any commercial or financial relationships that could be constructed as a potential conflict of interest.

PROJECT 2: WHITE MATTER DIFFUSION PROPERTIES

Dying-forward or dying-back? White matter type-specific alterations of fractional anisotropy in classical Amyotrophic Lateral Sclerosis

Wirth, A. M., Khomenko, A., Johannesen, S., Baldaranov, D., Bruun, T.-H., Greenlee, M. W., Bogdahn, U.

Author-produced version of an article under peer-review for publication in Therapeutic Advances in Neurological Disorders (TAND), SAGE Publishing, London, UK

ABSTRACT

Background: Dying-forward and dying-back hypotheses propose different origins of the pathology of amyotrophic lateral sclerosis (ALS). The aim of this study was to investigate these hypotheses by fractional anisotropy (FA) of different white matter (WM) types in magnetic resonance imaging (MRI): brainstem WM (BS), projection fibers (PF), association fibers (AF), and commissural fibers (CF).

Methods: Diffusion-weighted imaging (DWI) data were acquired in 28 limb-onset classical ALS patients (9 females, mean age = 49 yrs, *SD* = 12yrs, mean ALSFRS-R score: 38, range: 21-48, mean disease progression rate: 0.89) and 34 age-related healthy controls (14 females, *M* = 45 yrs, *SD* = 12yrs). ALS patients were treated with standard Riluzole and additional long-term G-CSF (Granulocyte-Colony Stimulating Factor, Filgrastim) on a named patient basis with written informed consent. For safety and monitoring, MRI was conducted approximately every three months. Patients' raw FA values of 48 atlas-based WM ROIs were compared to the most suitable of two age groups of healthy controls resulting in *z*-transformed deviations. Alterations in FA of BS, PF, AF, and CF were investigated at baseline (*n* = 28) and in the longitudinal course of disease (*n* = 24). Propagation of FA alterations across WM types was associated with clinical data.

Results: FA alterations at initial MRI scan were significantly specific to region and type of WM. Most pronounced FA alterations were observed in the BS. Individual perspectives as well as group analysis revealed the spread of FA alterations across all WM types,

reflecting both cortico-fugal and cortico-petal propagation of disease. Patterns of spread resembling either dying-back or dying-forward processes were not significantly linked to ALSFRS-R, disease progression, onset of ALS, survival, age or gender.

Conclusions: Spread of FA alterations across WM types may serve as a biomarker for differentiation of dying-forward or dying-back propagation in classical ALS.

INTRODUCTION

Amyotrophic lateral sclerosis (ALS) is a complex neurodegenerative disease affecting both upper (UMN) and lower motor neurons (LMN) and non-motor systems (Al-Chalabi et al., 2016). ALS patients display a broad range of phenotypes including weakness and wasting of muscles and spasticity (Morgan & Orrell, 2016) as well as deficits in cognition and behavior (Ravits et al., 2013). Neither disease etiology nor pathogenesis is fully understood (Morgan & Orrell, 2016), and the development of pathological changes as either dying-forward or dying-back is a matter of discussion (Kiernan et al., 2011). The dying-back hypothesis indicates the origin of ALS in the LMN and neuromuscular junctions. The retrograde degeneration was supported by synaptic denervation processes before clinical onset of motor neuron degeneration (Chou & Norris, 1993). The dying-forward hypothesis proposes the origin of ALS in the UMN. The anterograde degeneration process is endorsed by cortical hyperexcitability in early stage ALS (Vucic et al., 2012). Dying-back and dying-forward processes may also occur independently (Kiernan et al., 2011).

MRI fractional anisotropy (FA) is considered a prominent biomarker for the estimation of WM integrity (Chiò et al., 2014). Alterations of FA were most consistently observed in the corticospinal tract, especially in the corona radiata, posterior limb of capsula interna, cerebral peduncles, and the pons (see review by Grolez et al., 2016). Moreover, FA alterations were reported in the cerebellum and extramotor areas such as corpus callosum, thalamic radiation, fornix, cingulum, and superior longitudinal fasciculus (Chapman, Jelsone-Swain, Johnson, Gruis, & Welsh, 2014; Douaud, Filippini, Knight, Talbot, & Turner, 2011; Filippini et al., 2010; Keil et al., 2012; Sach et al., 2004; Van der Graaff et al., 2011). Kassubek et al. (2014, 2017) proposed a four-stage (corticospinal tract, corticorubral/corticopontine pathway, corticostriatal pathway, perforant pathway) Diffusion tensor imaging (DTI)-model of WM degeneration based on the sequential spread of protein aggregations in post-mortem studies (Brettschneider et al., 2013). To date, the relevance of different functional types of WM tracts in ALS remains unclear: brainstem

WM (BS), projection fibers (PF), association fibers (AF), and commissural fibers (CF). Of these, CF are inter-hemispheric, whereas PF and AF are intra-hemispheric connections (Aralasmak et al., 2006). While PF connect subcortical with cortical areas, AF provide connections between cortical areas.

The aim of the study was to investigate FA alterations of different WM types at baseline and during disease progression. Patterns of spread of WM type degeneration were associated with clinical data of ALS patients. These analyses should then clarify the type and character of spread of disease in ALS.

METHODS

Participants

The uni-center project was carried out in accordance with the Declaration of Helsinki (World Medical Association) and approved by the ethics committee at the University of Regensburg (ethics approval: 15-101-0106). Written informed consent was obtained prior to participation. The sample included 28 limb-onset classical ALS patients (9 females, mean age = 49 yrs, *SD* = 12) compared to 34 age-related healthy controls (14 females, mean age = 45 yrs, *SD* = 12). Mean ALSFRS-R score at initial MRI scan was 38 (range: 21-48). Mean disease progression rate ((48 – ALSFRS-R score) / months since symptom onset) was 0.89 (range: 0 – 6.0). Characteristics of ALS patients including range of age, ALSFRS-R scores at baseline, time span between symptom onset and initial MRI, progression rate at baseline, and number of MRI scans are listed in Table 2.3.1. Genetic background of ALS was confirmed in one patient only (patient 7). All other ALS patients of the sample were diagnosed with sporadic ALS. Patients received standard Riluzole and additional G-CSF (granulocyte-colony stimulating factor, Filgrastim) treatment on *a named patient basis* from 2010 to present (Grassinger et al., 2014). Application modes and doses of G-CSF were individually adapted. Treatment duration was up to seven years. For safety and monitoring of progression, structural MRI data were assessed approximately every three months. ALSFRS-R scores were evaluated monthly. Repeated MRI scans were assessed in 24 patients. Different individual lengths of longitudinal courses in these 24 patients were indicated by different amounts of MRI scans (mean MRI time course: 16 months, range: 3 – 75 months, see Table 2.3.1). Four patients were not able to participate in more than one MRI scan due to high disability.

Table 2.3.1

Baseline characteristics of patients. Characteristics include range of age, ALSFRS-R sum score at initial MRI scan, time interval between symptom onset and initial MRI scan, progression rate ((48 – ALSFRS-R score at initial MRI scan) / months since symptom onset), and total number of MRI scans. DWI sequence change affected 17 out of 28 patients (*). In these patients, sequence-derived biases of FA raw values were corrected by multiplication factors.

#	Age [range]	ALSFRS-R [0 48]	Time symptom onset – first MRI scan [months]	Progression rate	Number of scans	Sequence change
1	26-30	33	22	0.68	19	*
2	26-30	44	7	0.57	12	*
3	31-35	36	8	1.50	2	*
4	31-35	24	28	0.86	2	
5	41-45	32	28	0.57	8	*
6	41-45	37	36	0.30	7	*
7	41-45	44	38	0.10	11	*
8	41-45	42	13	0.46	3	
9	41-45	48	19	0.00	12	
10	41-45	44	16	0.25	6	*
11	41-45	28	38	0.53	1	
12	46-50	29	20	0.95	2	
13	46-50	46	3	0.67	4	*
14	46-50	31	5	3.40	2	*
15	46-50	42	25	0.24	5	*
16	46-50	40	21	0.38	2	
17	46-50	33	60	0.25	1	*
18	51-55	42	7	0.86	2	
19	51-55	37	33	0.33	4	*
20	56-60	39	23	0.39	2	
21	56-60	48	14	0.00	6	*
22	61-65	41	12	0.58	4	*
23	61-65	42	3	2.00	3	

24	61-65	44	14	0.28	2	
25	61-65	29	16	1.19	1	*
26	66-70	36	2	6.00	2	*
27	66-70	21	26	1.04	1	
28	71-75	45	25	0.12	2	*

Data acquisition

Structural MRI was conducted at two 1.5 Tesla clinical scanners (Aera, Sonata, Siemens Medical, Erlangen, Germany). DWI data were acquired with single shot spin-echo echo-planar sequences. The initial diffusion sequence of six orientations (DWI6) (repetition time TR: 3500 ms, echo time TE: 83 ms, flip angle FA: 90°, field of view FOV: 230 x 230 mm, 5 mm slice thickness, 20 axial slices, *b*-value: 1000 s/mm², three *b0* images) was modified to 20 orientations (DWI20) (TR: 3500 ms, TE: 83 ms, FA: 90°, FOV: 230 x 230mm, 5 mm slice thickness, 20 axial slices, b-value: 1000 s/mm², three *b0* images) during data acquisition period. Possible biases caused by the change of DWI sequence were controlled for and corrected by a separate control analysis.

Data preprocessing

MRI data of both ALS patients and healthy controls were processed by a workflow (Figure 2.3.1) using Freesurfer software 5.3 (Martinos Center for biomedical imaging, Charlestown, MA) and Matlab **(**Release 2012b, The MathWorks, Inc., Natick, Massachusetts, United States)**.** DWI raw data were preprocessed and atlas-based ROIs were registered to individual DWI space (Figure 2.3.1A). Maps of DTI-based FA were estimated (Figure 2.3.1B). The Johns Hopkins University (JHU) WM atlas by Mori et al. (2008) defined 48 WM regions in Montreal Neurological Institute (MNI) DWI space (resolution: 2mm). Average DWI space was registered to individual DWI space by using linear and nonlinear registration tools (FLIRT, FNIRT). Registrations were visually inspected and carefully adapted if necessary. All 48 WM regions were transferred to the individual DWI space. Mean FA values for all regions were calculated across voxels in every individual patient and healthy control.

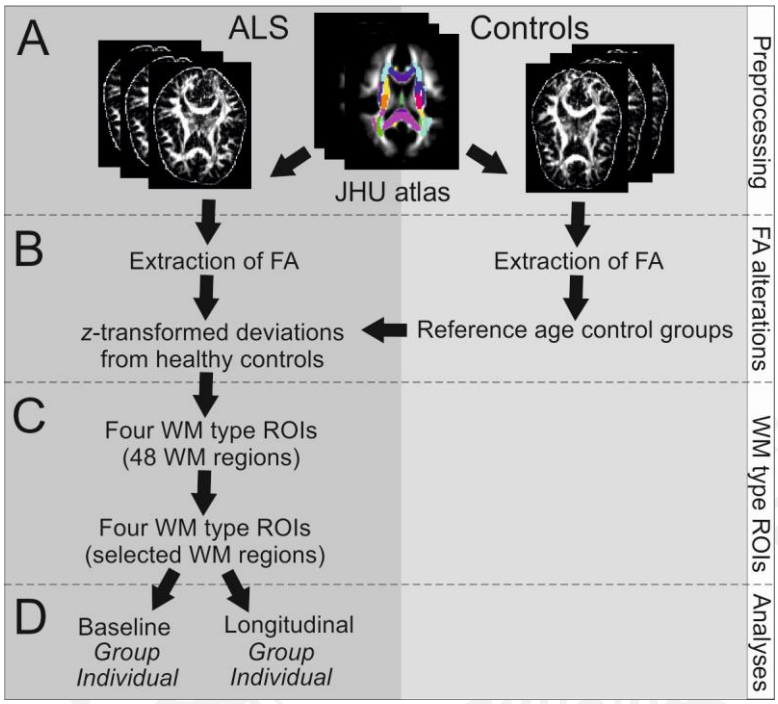

Figure 2.3.1. DWI workflow. A) Preprocessing of raw DWI data of both ALS patients (*n* = 28) and healthy controls (*n* = 34). Individual maps of FA were estimated based on DTI model. 48 atlas-based WM regions (Mori et al., 2008) were registered to the individual DWI space. B) Extraction of means of FA across voxels for each of the 48 WM regions. Healthy controls (*n* = 34) were differentiated into two reference age control groups. FA values of ALS patients for every WM region were compared to reference values of FA of the adequate control group resulting in *z*-transformed deviations. C) The 48 WM regions were differentiated into four WM types (BS, PF, AF, CF) based on Mori et al. (2008). The WM type ROIs including all 48 regions were modified by using only regions with FA alterations significantly below healthy control level (one-sample *t*-test) (see Table 2.3.2). D) The resulting specified WM type ROIs were used for baseline (*n* = 28) and longitudinal (*n* = 24) analyses with respect to both group level and individual patient.

Sequence-derived biases on fractional anisotropy

A subset of healthy controls (*n* = 22) was involved in a separate control analysis. These 22 healthy controls were assessed with both DWI sequences (DWI6, DWI20) on the same acquisition day. We calculated FA of the 48 WM regions in both DWI data sets. Possible bias effects of DWI sequence (DWI6, DWI20) were analyzed by a repeated-measures ANOVA. Raw FA values of DWI20 sequence were divided by raw FA values of DWI6 sequence resulting in one multiplication factor for every WM region. This multiplication factor enabled the correction of sequence-derived biases of FA in the 17 patients (see Table 2.3.1) assessed with DWI6 sequence. In all other patients, DWI20 sequence was consistently used and no FA correction was necessary.

Calculation of WM type-specific fractional anisotropy

ALS patients (n = 28) were compared to the whole sample of healthy controls (n = 34). Healthy controls were signed into two reference age control groups (Group 1: < 49 yrs, n = 20; Group 2: age ≥ 49 yrs, n = 14) (Figure 2.3.1B). In both groups, means of FA for every WM region served as reference values for the calculations of z-transformed deviations of FA of ALS patients from healthy control level. The differentiation of 48 regions into BS (corticospinal tract, pontine crossing tract, medial lemniscus, cerebellar peduncles), PF (capsula interna, corona radiata, cerebral peduncles, posterior thalamic radiation), AF (capsula externa, sagittal stratum, cingulum, superior longitudinal fasciculi, superior frontooccipital fasciculi, uncinate fasciculi, fornix) and CF (genu, body, splenium, tapetum) was based on Mori et al. (2008). For every WM type, medians of z-transformed deviations of FA alterations across the referred regions were calculated (Figure 2.3.1C). After the investigation of region-specific FA alterations, ROI definitions of the four WM types by all 48 WM regions were modified by only taking into account regions with FA alterations significant below zero (one sample t-tests, n = 28). FA alterations of the four WM types in ALS patients were analyzed at the time point of initial MRI scan (n = 28) and during disease progression (n = 24) at both group level and individual level (Figure 2.3.1D).

WM type-specific alterations of fractional anisotropy at baseline

Repeated-measures ANOVAs were used to investigate differences in ALS patients' z-transformed deviations of FA between different regions or types of WM (within-subject factors). Both ANOVAs included between-subject factor gender and covariate age. Individual perspective enabled the investigation of variability of WM type-specific FA alterations across patients.

Spread of WM type-specific FA alterations over time

Longitudinal FA analysis included 24 out of 28 patients. Four out of 28 patients were not able to participate in follow-up MRI due to high disability. Longitudinal courses of FA alterations of the four different WM types were assessed by the calculation of slopes of FA over time. Patients (n = 24) were divided in low level (z-deviation < -1) and normal level (z-deviation > -1) baseline FA alterations for most affected WM types. A repeated-

measures ANOVA including within-subject factor WM type (BS, PF, AF, CF), and between-subject factors baseline level of FA alterations (low, normal) and gender, and covariates age and time span of MRI follow-up helped to investigate potential effects of baseline FA levels on slopes of WM type-specific FA alterations over time. Significance levels of group analyses were set to $p < .05$. At individual level, spread of FA alterations across WM types was inspected for every single patient. Based on these patterns, patients were differentiated into either dying-back or dying-forward groups. Independent *t*-tests and chi-square tests for independence served to investigate differences in demographic and clinical characteristics between those two groups.

RESULTS

Control analysis of sequence-derived biases on FA

FA values for DWI20 sequence were significantly higher than those for DWI6 sequence consistently across all 48 WM regions ($F(1, 21) = 1019.11$, $p < .001$, $n = 22$ healthy controls). We corrected the sequence-derived bias of FA values by the calculation of a multiplication factor for every WM region, and thus were able to raise FA values of DWI6 to the level of DWI20. After this correction, the initial DWI sequence effect was no longer significant ($F(1, 21) = 0.447$, $p = .511$).

Region-specific and WM type-specific FA alterations at baseline

Deviations of FA of ALS patients from healthy control level were significantly specific to WM regions ($F(47, 1175) = 1.912$, $p < .001$). Repeated-measures ANOVA revealed no significant effects of gender ($F(1,25) = 2.693$, $p = .113$) or covariate age ($F(1, 25) = 0.998$, $p = .327$). Baseline FA alterations significantly below healthy control level were detected in specific WM regions of the BS, PF, AF, and CF (Table 2.3.2). Significant BS alterations involved the pontine crossing tract, the corticospinal tract, and the inferior cerebellar peduncles of the left and right hemispheres. Most pronounced FA alterations in the PF were observed in the bilateral cerebral peduncles and the posterior thalamic radiation. Alterations in AF were primarily detected in the fornix, the sagittal stratum, and the frontooccipital longitudinal fasciculus of the left hemisphere. Most affected WM regions of CF were callosal body and the left tapetum. ROIs of WM types (BS, PF, AF, CF) were redefined by taking into account only the WM regions listed in Table 2.3.2.

Table 2.3.2

Region-specific FA alterations at baseline. One-sample t-test (n = 28) testing FA alterations below threshold 0. BS = brainstem tracts, PF = projection fibers, AF = association fibers, CF = Commissural fibers, lh = left hemisphere, rh = right hemisphere. P-values refer to z-transformed deviations of FA significantly below zero at initial MRI scan. Significance level is set to p < .05 (uncorrected).

Type	**ROI**	***T***	***p***
BS	*Pontine crossing tract*	-3.580	.001
	Corticospinal tract rh	-7.277	< .001
	Corticospinal tract lh	-6.460	< .001
	Inferior cerebellar peduncle rh	-5.284	< .001
	Inferior cerebellar peduncle lh	-6.027	< .001
PF	*Cerebral peduncle rh*	-3.408	.002
	Cerebral peduncle lh	-4.796	< .001
	Posterior thalamic radiation rh	-3.675	.001
	Posterior thalamic radiation lh	-2.619	.014
AF	*Fornix*	-4.028	< .001
	Sagittal stratum lh	-3.278	.003
	Superior frontooccipital fasciculus lh	-3.996	< .001
CF	*Body*	-2.571	.016
	Tapetum lh	-2.546	.017

A repeated-measures ANOVA considering both initial and redefined WM type ROIs (Figure 2.3.2A) served as a control analysis. Modification of the WM type ROIs (BS, PF, AF, CF) by only ALS-relevant WM regions instead of using all 48 WM regions significantly improved the accuracy of detecting FA alterations, especially in the BS ($T(27) = 5.239$, $p < .001$), PF ($T(27) = 6.294$, $p < .001$), and CF ($T(27) = 4.439$, $p < .001$) ($F(3, 75) = 4.687$, $p = .005$) (Figure 2.3.2B). In both ROI models, FA alterations significantly differed between WM types ($F(3, 75) = 2.724$, $p = .05$). A separate repeated-measures ANOVA focusing on only redefined WM ROIs underlined the specificity of FA alterations to WM types ($F(3, 75) = 2.997$, $p = .036$). Deviations of FA of ALS patients from healthy control level were most pronounced in the BS (Figure 2.3.2B). No significant effects of

gender ($F(1, 25) = 3.728$, $p = .065$) or covariate age ($F(1, 25) = 1.299$, $p = .265$) were detected. Correlation analyses revealed rather weak or no significant correlations of WM type-specific FA alterations with baseline ALSFRS-R scores (BS: $r = -.148$, $p = .454$; PF: $r = -.080$, $p = .687$; AF: $r = -.058$, $p = .770$; CF: $r = .148$, $p = .451$) or disease progression rates (BS: $r = -.025$, $p = .900$; PF: $r = -.374$, $p = .050$; AF: $r = -.107$, $p = .589$; CF: $r = -.125$, $p = .527$).

Individual alterations of fractional anisotropy at baseline

Individual patient analysis revealed different states of FA alterations at baseline level (Figure 2.3.2C). The majority ($n = 19$) of 28 patients showed reduced FA baseline levels involving BS only ($n = 3$; *patients 17, 18, 19*), BS + PF only ($n = 3$, *patients 1, 12, 20*), BS + PF + AF only ($n = 4$; *patients 2, 3, 21, 24*), or in all four WM types as BS + PF + AF + CF ($n = 9$, *patients 5, 7, 9, 10, 14, 22, 25, 26, 28*). However, some patients showed alternative deviation patterns ($n = 7$, *patients 4, 6, 8, 11, 15, 23, 27*) or no FA alterations ($n = 2$, *patients 13, 16*) at baseline: Both patients without FA alterations exhibited ALSFRS-R scores higher than 40 scores points. Four out of the seven patients with alternative deviation patterns (*patient 6:* PF+CF, *patient 8:* BS + CF, *patient 11:* CF, *patient 15:* PF) shared low progression rates (range: 0.24 - 0.53). The other three patients (*patients 4, 23, 27*) exhibited particular clinical characteristics. Young-onset patient 4 showed FA alterations in the BS and AF, low ALSFRS-R score (24 score points) and average disease progression (0.86). Patient 23 exhibited FA alterations in all WM types except for the AF and fast disease progression (2.00). Patient 27 stood out of the sample by FA alterations in all WM types except for the BS, low ALSFRS-R score (21 score points), fast disease progression (1.04), and a time course of 26 months since symptom onset.

Spread of alterations of fractional anisotropy across WM types

We acquired longitudinal MRI data in 24 out of 28 patients. A repeated-measures ANOVA (within-subject factor: WM type; between-subject factors: baseline FA alterations of BS and PF, gender; covariates: age, time span of MRI follow-up) revealed no significant differences of slopes of FA alterations between WM types ($F(3, 42) = 1.768$, $p = .168$). Instead, slopes of WM type-specific FA significantly depended on age ($F(1,14) = 9.795$, $p = .007$), time span of MRI follow-up ($F(1, 14) = 7.829$, $p = .014$) and baseline levels of FA

alterations in the PF ($F(1, 14) = 5.702$, $p = .032$). In contrast, baseline levels of FA deviations in the BS had no significant impact on slopes of WM type-specific FA over time ($F(1, 14) = 0.066$, $p = .801$). Slopes of WM type-specific FA alterations did not significantly correlate with slopes of ALSFRS-R scores over time (BS: $r = -.087$, $p = .685$; PF: $r = .075$, $p = .728$; AF: $r = .131$, $p = .540$; CF: $r = .026$, $p = .906$).

Dying-back and Dying-forward in the context of clinical data

Individual courses of FA alterations over time were inspected for every single patient. Spread of FA alterations across WM types was observed in mainly two patterns resembling dying-back or dying-forward. Patient 2 is visualized as an example for potential dying-back propagation (Figure 2.3.2D). Here, FA alterations were most pronounced in the BS and propagated to PF, AF, and C. This pattern of FA decline was observed in 13 out of 24 patients with longitudinal courses. Ten out of 24 patients showed patterns of spread resembling dying-forward patterns as visualized in exemplary patient 9 (Figure 2.3.2E). This pattern of spread was characterized by no primary involvement of BS alterations (Figure 2.3.2E) but rather predominant FA alterations in the PF and CF. Fluctuations in FA hindered the classification of patient 13 (see Table 2.3.1) into one of the two groups. Patient groups of dying-back ($n = 13$) and dying-forward ($n = 10$) did not significantly differ in age ($T(21) = -1.648$, $p = .117$), baseline ALSFRS-R score ($T(21) = -0.599$, $p = .555$), ALSFRS-R slope over time ($T(21) = 1.533$, $p = .142$), or disease progression rate at baseline ($T(21) = -0.903$, $p = .384$). Patterns of spread were specific to neither gender ($\chi 2(1) = 0.710$, $p = .400$, $\varphi = .176$) or onset site ($\chi 2(1) = 0.006$, $p = .940$, $\varphi = .016$). Moreover, patients with different spread of FA did not significantly differ in survival since initial MRI scan ($T(15) = 0.693$, $p = .502$). Survival analysis was restricted to a sample size of $n = 17$ instead of $n = 23$, as six patients were alive and still participating in the study.

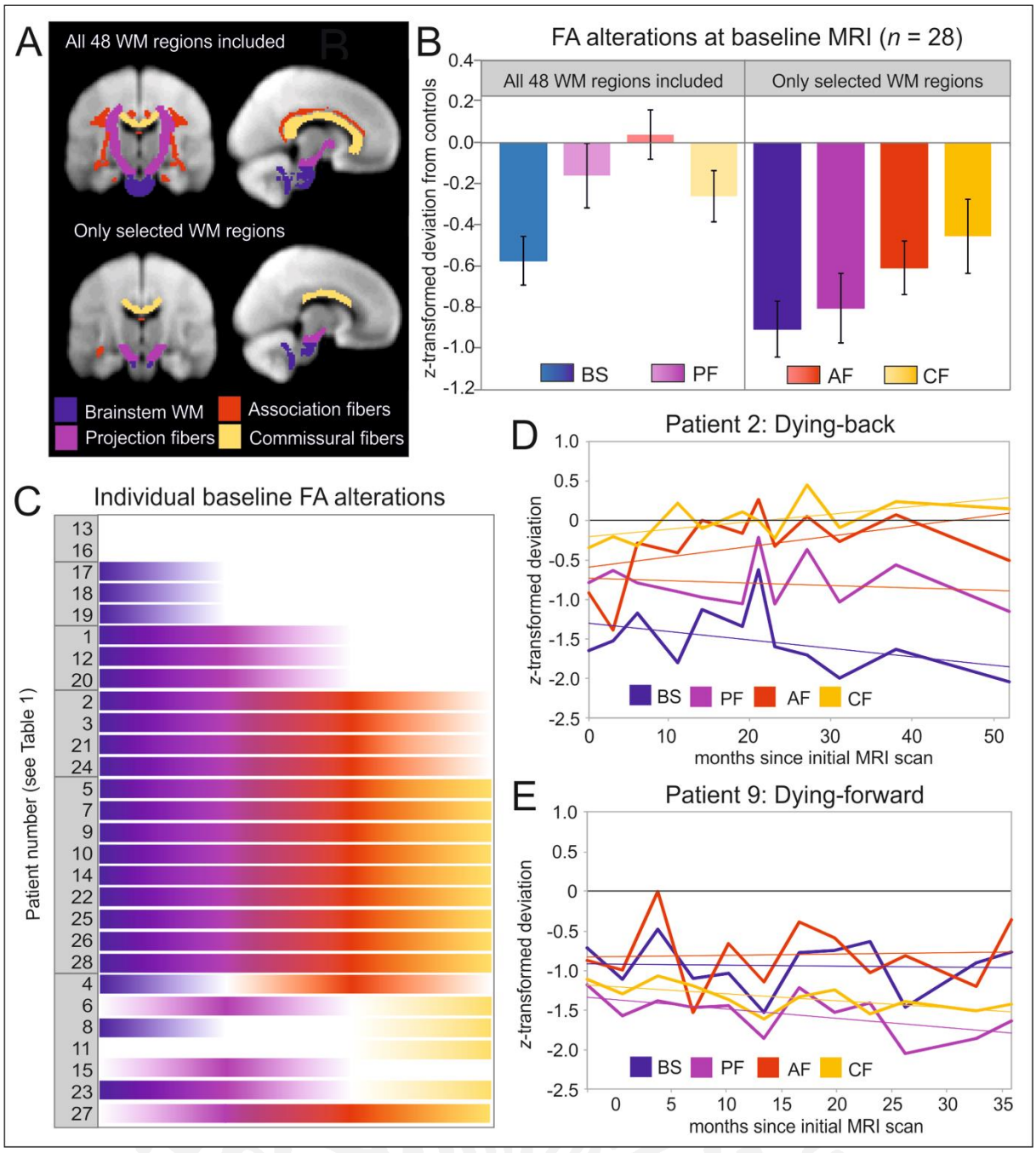

Figure 2.3.2. WM type-specific FA alterations. A) ROIs of WM types were defined by either all 48 atlas-based WM regions or only by regions with significant FA alterations below zero. B) FA alterations of WM types before and after ROI modification at baseline in 28 patients. C) Individual states of FA alterations at baseline level of 28 patients. Patient numbers refer to Table 2.3.1. Threshold for visualization of FA alterations (BS: blue, PF: pink, AF: red, CF: yellow) is -0.5. Longitudinal analysis differentiated patients (n = 24) into either dying-back (see patient 2, D) or dying-forward (see patient 9, E) patterns of spread. FA alterations are described by z-transformed deviations from healthy control level (zero, black line). Colors refer to BS (brainstem WM, blue), PF (projection fibers, pink), AF (association fibers, red), and CF (commissural fibers, yellow).

DISCUSSION

FA alterations of WM were specific to regions and types of WM in ALS patients. Compared to values from age-related controls, the most pronounced baseline FA alterations of ALS patients were detected in the BS. A spread of FA alterations between WM types was supported by both individual perspective and group analysis. Patients with classical ALS showed both dying-back and dying-forward patterns.

FA alterations in the WM of ALS patients compared to healthy controls were region-specific. This is consistent with the literature. At the BS level, significantly reduced FA levels of ALS patients compared to healthy controls were observed in the pontine crossing tract, corticospinal tract and inferior cerebellar peduncles as reported in several previous studies (Douaud et al., 2011; Karlsborg et al., 2004; Keil et al., 2012; Roccatagliata et al., 2009; Sach et al., 2004; Sage, Peeters, Görner, Robberecht, & Sunaert, 2007; Toosy et al., 2003). At PF level, FA alterations were detected in the cerebral peduncles and the posterior thalamic radiation. Observations of reduced FA of ALS patients in the cerebral peduncles (Metwalli et al., 2010; Prudlo et al., 2012; Roccatagliata et al., 2009) and in the thalamic radiations (Douaud et al., 2011; Prudlo et al., 2012) have been published. At AF level, we observed FA alterations in the fornix, sagittal stratum and the superior frontooccipital fasciculus. AF like fornix and longitudinal fasciculi were altered in ALS patients (Borsodi et al., 2017; Chapman et al., 2014; Prudlo et al., 2012; Sarica et al., 2014; Van der Graaff et al., 2011). Reduced FA in CF, especially in the callosal body, was frequently described (Chapman et al., 2014; Douaud et al., 2011; Filippini et al., 2010; Keil et al., 2012; Metwalli et al., 2010; Menke et al., 2012; Prudlo et al., 2012; Sach et al., 2004). The tapetum is defined as an area of the corpus callosum involving fibers of the splenium along the lateral ventricle (Sarikcioglu, Ozsoy, & Unver, 2007), but its structural and functional role is poorly understood.

Baseline FA alterations significantly depended on WM type and were most pronounced in the BS. This finding may support the dying-back hypothesis. However, individual perspective on every single ALS patient's WM type specific FA alterations at baseline revealed patterns of FA alterations without BS involvement (n = 7) or no FA alterations at all (n = 2). The absence of FA alterations could have different reasons such as early stage ALS, slow progression, dying-back process originating from the spinal cord (Nair et al., 2010) or by reduced sensitivity of method. As the WM atlas did not include cortex adjacent areas (e.g. motor cortex), the analysis may not directly endorse a cortical origin of

degeneration (dying-forward). Slopes of WM type-specific FA alterations significantly depended on age, time span of MRI follow-up and baseline levels of PF. Although FA is considered to be less susceptible to age effects than cortical thickness (Pfefferbaum, Adalsteinsson, Rohlfing, & Sullivan, 2008), age may be an important prognostic factor in ALS (Chiò et al., 2009). Meta-analysis of Zhang et al. (2018) reported no significant correlations between age and FA decrease. Age effects in our study may be explained by the broad range of age in an ALS sample including also young-onset patients. Length of MRI follow-up was replicated to be crucial as it may bias results of longitudinal MRI studies by slow-progressive cases (Menke, Proudfoot, Talbot, & Turner, 2017). BS alterations at baseline were observed in the majority of ALS patients but were no crucial factor for slopes of FA of other WM types over time. As reported in other studies (Borsodi et al., 2017; Roccatagliata et al., 2009; Sage et al., 2007; Toosy et al., 2003) FA alterations at baseline and their slopes over time did not significantly correlate with ALSFRS-R scores themselves or disease progression rates derived from ALSFRS-R scores. The lack of correlation may be explained by the influence of not only UMN but also LMN involvement on ALSFRS-R scores (Simon et al., 2014), whereas MRI may predominantly reflect UMN affection. Moreover, lack of correlations may be explained by the suggestion that ALSFRS-R may be more sensitive for disease-related changes than diffusion properties (Cardenas-Blanco et al., 2016).

13 out of 24 ALS patients showed longitudinal spread of FA alterations resembling dying-back. In these patients, BS involvement preceded FA alterations of other WM types. In 10 out of 24 patients, FA alterations were more pronounced in the PF, AF, and C without primary involvement of BS. One patient could not be sorted in either dying-forward or dying-back patterns of spread due to high fluctuations of FA alterations. Fluctuations of FA deviations of WM types may result from data quality or focal FA alterations within WM types. ALS patients with different spread of FA alterations did not significantly differ in age, ALSFRS-R baseline or slope, disease progression rate, and survival. Moreover, dying-back or dying-forward propagation of FA alterations were not associated with gender or onset of disease. These findings indicate that both patterns of spread may independently exist in classical ALS (Kiernan et al., 2011).

Some methodological limitations need to be considered. First, sample size was limited to 28 ALS patients. Still, sample sizes of 20-30 patients were shown to be adequate for MRI analysis in unicenter ALS studies published since 2010 (Borsodi et al., 2017; Douaud et al., 2011; Fillippi et al., 2010; Keil et al., 2012; Metwalli et al., 2010). Second, slice thickness

of DWI sequence was relatively large. Facing this issue, we chose a ROI approach using larger atlas-based ROI definitions (Mori et al., 2008) instead of voxel-based approaches or fiber tractography. Third, DWI sequence was changed during the period of data acquisition. When dealing with different MRI scanners, FA is the most robust DTI estimate (Fox et al., 2012). We replicated sequence-derived biases on FA values (Wang, Abdi, Bakhadirov, Diaz-Arrastia, & Devous, 2011) and corrected these biases by a separate control analysis. As the study design included no ALS control sample without G-CSF treatment, therapeutic effects may not be deduced from this study.

Conclusions

We demonstrated that FA alterations of WM in limb-onset ALS patients are specific to both region and type of WM. They were most pronounced in the BS. FA decline spread between different WM types indicating retro- and anterograde patterns of spread supporting both dying-forward and dying-back hypotheses. Future studies may expand upon the idea of spread of degeneration between different WM types in different phenotypes of motor neuron disease.

Contributions of authors:

AW: conception and the design of the study, acquisition, analysis, interpretation of the MRI data, and composition of the manuscript.

AK, DB: contribution to the conception of the study, data acquisition, interpretation of the data, and revision of the manuscript.

SJ, TB, UB: contribution to the conception of the study, acquisition, analysis, and interpretation of clinical data, and revision of the manuscript.

SJ, AK, DB, UB: care for ALS patients in outpatient clinic, treatment concept.

MG: contribution to the conception of the study, supervision of MRI data analysis and data interpretation, and revision of the manuscript

Funding:

This work was supported by the German Federal Ministry of Education and Research (BMBF, Project GO-Bio, 031A386).

Conflict of Interest Statement:

The authors declare that the research was conducted in the absence of any commercial or financial relationships that could be constructed as a potential conflict of interest.

PROJECT 3: WHITE MATTER LESION DETECTION

Value of Fluid-Attenuated Inversion Recovery MRI data analyzed by the Lesion Segmentation Toolbox in Amyotrophic Lateral Sclerosis

---

Wirth, A. M., Khomenko, A., Baldaranov, D., Hsam, O., Johannesen, S., Bruun, T.-H., Greenlee, M. W., Bogdahn, U.

Author-produced version of an article accepted for publication on October 30th 2018 in Journal of Magnetic Resonance Imaging (JMRI), Wiley Online Library, New York, USA.

ABSTRACT

Background: MRI Fluid-Attenuated Inversion Recovery (FLAIR) studies reported hyperintensity in the corticospinal tract and corpus callosum of patients with Amyotrophic Lateral Sclerosis (ALS). Purpose: To evaluate the Lesion segmentation toolbox (LST) for the objective quantification of FLAIR lesions in ALS patients. Study type: Retrospective. Population: 28 ALS patients (eight females, mean age: 50 range: 24-73, mean ALSFRS-R sum score: 36) were compared to 31 age-matched healthy controls (12 females, mean age: 45, range: 25-67). ALS patients were treated with Riluzole and additional G-CSF (Granulocyte-colony stimulating factor) on a named patient basis. Field strength/ sequence: 1.5T, FLAIR, T1-weighted MRI. Assessment: The Lesion Prediction Algorithm (LPA) of the LST enabled the extraction of individual binary lesion maps, total lesion volume (TLV) and number (TLN). Location and overlap of FLAIR lesions across patients were investigated by registration to FLAIR average space and an atlas. ALS-specific functional rating scale revised (ALSFRS-R), disease progression and survival since diagnosis served as clinical correlates. Statistical tests: Univariate ANOVA, Repeated-measures ANOVA, *T*-test, Bravais-Pearson correlation, Chi-square test of independence, Kaplan-Meier analysis, Cox-regression analysis. Results: Both ALS patients and healthy

controls exhibited FLAIR alterations. TLN significantly depended on age ($F(1, 54) = 24.659$; $p < .001$) and sex ($F(1,54) = 5.720$, $p = .020$). ALS patients showed higher TLN than healthy controls depending on sex ($F(1,54) = 5.720$, $p = .020$). FLAIR lesions were small and most pronounced in male ALS patients. FLAIR alterations were predominantly detected in the superior and posterior corona radiata, anterior capsula interna and posterior thalamic radiation. Patients with pyramidal tract (PT) lesions exhibited significantly inferior survival than patients without PT lesions ($p = .013$). Covariate age exhibited strong prognostic value for survival ($p = .015$). Data conclusion: LST enables the objective quantification of FLAIR alterations and is a potential prognostic biomarker for ALS.

INTRODUCTION

Amyotrophic Lateral Sclerosis (ALS) is a progressive neurodegenerative disease involving both upper motor neurons (UMN) and lower motor neurons (LMN) as well as non-motor areas like the frontotemporal cortex (Al-Chalabi et al., 2016). The diagnostic process for this disorder is delayed by the great clinical heterogeneity of ALS phenotypes due to variability of onset (limb or bulbar), extent of UMN and LMN involvement and affected site (upper or lower limbs, distal or proximal muscles). Facing the psychological impact of a life-threatening diagnosis precise ALS diagnosis requires the reliable exclusion of other disorders (Tao & Wu, 2017). Electromyography, lumbar puncture, and MRI may provide promising biomarkers improving the classification of ALS and the identification of mimic disorders (Al-Chalabi et al., 2016; Tao & Wu, 2017).

MRI findings like cortical thinning of the precentral cortex as well as reduced fractional anisotropy of the corticospinal tract (CST) and corpus callosum (CC) are promising biomarkers for ALS (Bede, Querin, & Pradat, 2018). CST involvement in ALS may be detected by brain MRI as well as spinal cord MRI (Cohen-Adad et al., 2013). Conventional Fluid-Attenuated Inversion Recovery (FLAIR) imaging is a T2-weighted MRI sequence that eliminates signals derived from free cerebrospinal fluid (Gramsch et al., 2015). FLAIR imaging enables the detection of cortical, subcortical and paraventricular lesions and is considered a crucial sequence for multiple sclerosis (MS) (Gawne-Cain, et al., 1997; Hajnal et al., 1992). In ALS, FLAIR imaging studies could show pathological signal increase in the CST (Fabes et al., 2017; Gupta, Nguyen, Chakraborty, & Bourque, 2014; Hecht et al., 2001; Jin, Hu, Zhang, Jia, & Dang, 2016; Schweitzer et al., 2015) and the CC (Fabes et al., 2017). However, the sensitivity and specificity of FLAIR imaging for ALS

are controversial as FLAIR hyperintensity is also detectable in healthy controls (Thorpe et al., 1996; Zhang et al., 2003) and was predominantly found in ALS patients with disease progress (Protogerou et al., 2011). Only a few studies using FLAIR imaging objectively quantified FLAIR alterations in ALS (Fabes et al., 2017; Hecht et al., 2001, 2002; Schweitzer et al., 2015). The automated Lesion Segmentation Toolbox (LST) established in MS research enables the objective and time-saving quantification of white matter (WM) lesions in FLAIR images (Schmidt et al., 2012).

Thus the aim of this study was to evaluate the potential of LST in the detection of FLAIR lesions in ALS patients. We investigated the localization and overlap of FLAIR lesions across patients and potential correlations to clinical data.

METHODS

Participants

The uni-center project was carried out in accordance with the Declaration of Helsinki (World Medical Association) and approved by the local ethics committee (ethics approval: 15-101-0106). Written informed consent was obtained prior to participation. The sample of this study was composed of 28 ALS patients compared to 31 age-matched healthy controls. Overall, 25 patients were diagnosed classical limb-onset ALS, whereas another three patients exhibited bulbar-onset of disease. All ALS patients received Riluzole standard therapy and additional G-CSF (granulocyte-colony stimulating factor, Filgrastim) on a named patient basis. Application modes and doses of G-CSF were individually adapted; treatment duration was up to 7 years. Safety and monitoring of ALS patients required the assessment of ALSFRS-R scores every month and MRI acquisition every three months.

Data acquisition

Structural FLAIR MRI was performed on two 1.5 Tesla clinical scanners using identical settings (Aera, Sonata, Siemens Medical, Erlangen, Germany) with 2D-axial orientation (TR = 7530 ms, TE = 110 ms, TI = 2300 ms, FA: 180°, 21 slices, slice thickness: 5mm, gap: 0.2, number of averages: 1, matrix: 256 x 196). A FLAIR average template (resolution: 2mm, n = 853 subjects) (http://brainder.org) served as a reference for the transfer of regions of interest (ROI). T1-weighted structural images were assessed in all healthy controls and a subset of ALS patients (n = 20) using a magnetization prepared rapid

gradient echo sequence (MPRAGE) (TR: 2220 ms, TE: 5.97 ms, FA: 15°, voxel size: 1 x 1 x 1 mm^3, FOV: 256 x 256 mm^2, 176 sagittal slices covering the whole brain).

Lesion segmentation toolbox

Individual FLAIR data were analyzed by Lesion Prediction Algorithm (LPA; Schmidt, 2017) included in the freeware LST version 2.0.15 (www.statistical-modelling.de/lst.html) for SPM (SPM12, Matlab Version 2015b). LPA involves a binary classifier based on the logistic regression model developed on data from 53 patients with severe MS lesions (Schmidt, 2017). The model involves lesion belief maps and considers spatial covariates. Based on the model, lesions are segmented by calculation of lesion probabilities for each voxel. Raw FLAIR data were preprocessed and lesion probability maps were estimated. Values of interest like TLV (total lesion volume in ml) and TLN (number of lesions) were extracted by thresholding individual lesion probability maps. Threshold kappa was set to $\kappa = 0.5$ as this threshold was recommended for LPA SPM12 use (Egger et al., 2016). Binary lesion maps thresholded by κ enabled the visualization of individual patients' FLAIR lesions. T1 data are not required for LPA use. However LPA provides the possibility for T1 registration in case of low resolution FLAIR images (Schmidt, 2017). A separate control analysis involving all healthy controls and a subset of ALS patients ($n = 20$) investigated effects of precedent T1 registration on LPA results.

Locations and Overlap of FLAIR lesions

Individual FLAIR images of ALS patients were registered to the FLAIR average template (http://brainder.org) by linear and nonlinear registration tools (FLIRT, FNIRT) of FSL (Freesurfer Version 3.2). Individual binary lesion maps were transferred to an average FLAIR template. Localization of FLAIR lesions was performed by the use of a WM atlas (Mori et al., 2008). The atlas defines 48 WM areas in average Diffusion weighted imaging (DWI) space. Masks of these WM regions were registered from average DWI space to average FLAIR space by FLIRT and enabled the description of locations of FLAIR lesions. Addition of individual binary lesion maps across ALS patients enabled the investigation of size and distribution of FLAIR lesions across individual ALS patients.

Quantitative and visual evaluation of FLAIR images

Results of the LST are compared to visual evaluation in three exemplary patients. Visual evaluation was performed by two neuroradiologists with long professional experience (S.G.: >30yrs; W.C.: 8yrs). The choice of patients includes one patient evaluated with inconspicuous FLAIR images, one patient with unspecific FLAIR lesions and one patient with ALS-specific FLAIR lesions in the pyramidal tracts (PT).

Separate control analysis on T1 registration

A separate control analysis was conducted to investigate effects of preceding T1 registration on LPA results. The healthy control group (n = 31) and a subset of patients (n = 20) were included in this control analysis. Control analysis in patients was restricted to a subgroup due to lack of T1 data in eight patients. Threshold κ was set to 0.5 in both groups.

Statistical analysis

Two univariate ANOVAs (TLV, TLN) took into account factors group (ALS, controls), sex, and covariate age and investigated differences in TLV and TLN between all 28 ALS patients and all 31 healthy controls. ANOVA effects were analyzed by independent and dependent t-tests. Bravais-Pearson correlation analyses examined the relation of TLV and TLN to age, ALSFRS-R scores, disease progression rates and elapsed time since diagnosis. Chi-square tests of independence were applied to analyze differences in frequencies of FLAIR lesions between ALS patients and healthy controls in most affected WM regions. Survival since diagnosis was analyzed by the Kaplan-Meier log-rank test. Seven out of 28 ALS patients were still alive and considered as censored data. In these seven patients, survival was calculated as time span between diagnosis and MRI scan. Cox-regression analysis was used to investigate effects of potential prognostic factors (age, sex, ALSFRS-R scores, disease progression rates) on survival. Separate control analysis examined effects of precedent T1 registration on LST results. This control analysis was performed using repeated-measures ANOVAs including a within-subject factor (with or without preceding T1 registration), between subject factors group (ALS, controls) and sex, and the covariate age for both TLV and TLN. Significance level was set to $p < .05$. Multiple comparison errors were controlled for by use of Bonferroni correction.

RESULTS

Participants

28 ALS patients (8 females) were compared to 31 age-matched controls (12 females). The characteristics of ALS patients and healthy controls are summarized in Table 2.4.1. ALS patients did not significantly differ from healthy controls in age ($T(57) = -1.560$; $p = .124$). No sex-specific differences in age were detected either between ALS patients and healthy controls (females: $T(18) = -.826$, $p = .420$; males: $T(37) = -1.307$, $p = .199$) or within groups (ALS: $T(26) = .268$, $p = .792$; controls: $T(29) = .076$, $p = .940$).

Table 2.4.1

Characteristics of ALS patients (n = 28) and age-matched healthy controls (n = 31). ALS patients are described by median ALSFRS-R score, median disease progression rate ((48 – ALSFRS-R) / months since symptom onset), and elapsed time between diagnosis and MRI scan (months).

	n	**Mean age (yrs)**	**Median ALSFRS-R**	**Median disease progression rate**	**Time since diagnosis (months)**
ALS	28	50 .10 [24-73]	37.50 [21-48]	0.47 [0-4]	11 [1-43]
Controls	31	45.06 [25 – 67]			

Total lesion number and volume

Two univariate ANOVAs (ALS $n = 28$, healthy controls $n = 31$) revealed highly significant effects of covariate age on both TLV ($F(1, 54) = 22.171$; $p < .001$) and TLN ($F(1, 54) = 24.659$; $p < .001$). These findings were supported by highly significant correlations of age with TLV ($r = .529$, $p < .001$, corrected) and TLN ($r = .554$, $p < .001$, corrected). TLN was significantly dependent on sex ($F(1,54) = 5.720$, $p = .020$) and tended to be higher in male compared to female participants ($T(57) = 2.261$, $p = .028$, uncorrected). Age was not significantly different between male and female participants ($T(57) = 0.374$, $p = .711$). ALS patients showed a significant increase in TLN compared to healthy controls dependent on sex ($F(1, 54) = 5.076$, $p = .028$) (Figure 2.4.1a). FLAIR lesions were

significantly more frequent in male ALS patients than in female ALS patients ($T(26) = 3.879$, $p < .001$, corrected; males: $n = 20$, $M = 8.55$, $SD = 5.978$, females: $n = 8$, $M = 2.375$; $SD = 2.44$) and tended to be more common than in male healthy controls ($n = 19$) ($T(37) = -2.020$, $p = .051$). TLN did not significantly differ between female ALS patients and female healthy controls ($n = 12$) ($T(18) = 1.237$, $p = .233$) or between female and male healthy controls ($T(29) = 0.136$, $p = .893$). No significant differences in age were observed between female and male ALS patients ($T(26) = 0.268$, $p = .792$), between male controls and male ALS patients ($T(37) = -1.307$, $p = .199$) and between female controls and female ALS patients ($T(18) = -0.826$, $p = .420$). Most pronounced levels of TLN were observed in two patients with bulbar-onset.

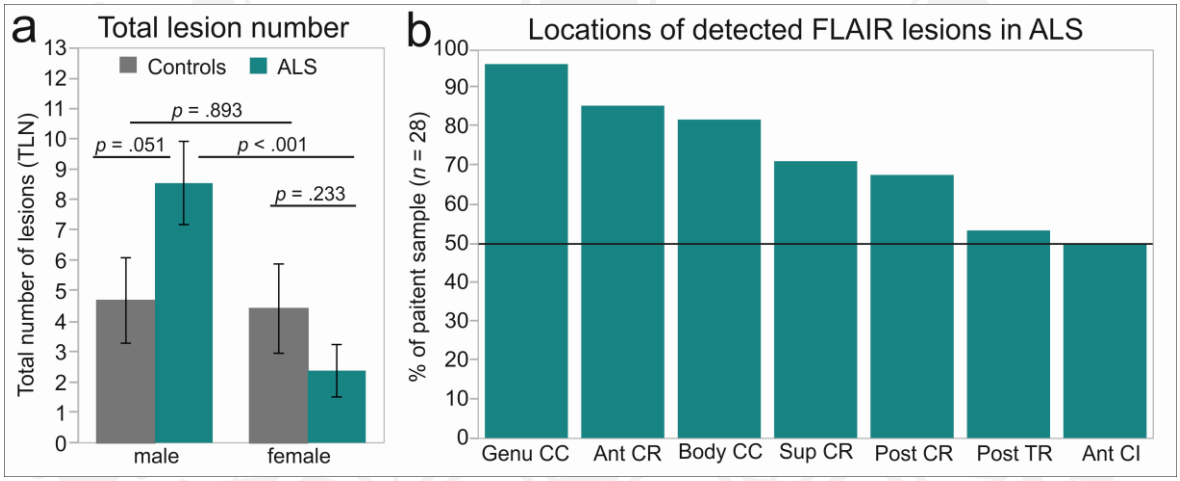

Figure 2.4.1. Total lesion number and locations of FLAIR lesions detected by LPA. A) Total lesion number (TLN) of healthy controls (grey, male: $n = 19$, female: $n = 12$) and ALS patients (cyan, male: $n = 20$, female: $n = 8$). B) % of ALS patients showing FLAIR lesions in the most affected WM regions. Ant CR = anterior corona radiata, sup CR = superior corona radiata, post CR = posterior corona radiata, post TR = posterior thalamic radiation, ant CI = anterior capsula interna. P-values refer to two-sample t-tests.

TLV did not significantly differ between ALS patients and healthy controls ($F(1, 54) = 1.407$, $p = .241$) or between sex ($F(1, 54) = 1.639$; $p = .206$). No significant interaction effect of sex with group (ALS, controls) was observed for TLV ($F(1, 54) = 1.562$, $p = .202$). TLN and TLV were strongly intercorrelated ($r = .790$, $p < .001$, corrected).

Characteristics of FLAIR lesions

Individual binary lesion maps of ALS patients (n = 28) revealed most frequent FLAIR lesions in the *callosal genu* (n = 27) and *body* (n = 23), the *anterior* (n = 24), *superior* (n = 20), and *posterior* (n = 19) *corona radiata*, *posterior thalamic radiation* (n = 15) and the anterior *capsula interna* (n = 14) (Figure 2.4.1b). Healthy controls (n = 31) exhibited similar frequency of FLAIR alterations in the *genu* ($\chi^2(1) = 0.253$, $p = .615$, $\varphi = 0.065$), *body* ($\chi^2(1) = 1.015$, $p = .314$, $\varphi = 0.131$) and the *anterior corona radiata* ($\chi^2(1) = .024$, $p = .877$, $\varphi = 0.020$). However, FLAIR lesions in the *superior* ($\chi^2(1) = 6.345$, $p = 0.012$, $\varphi = 0.328$) and *posterior corona radiata* ($\chi^2(1) = 7.460$, $p = 0.006$, $\varphi = 0.356$), *posterior thalamic radiation* ($\chi^2(1) = 6.042$, $p = 0.014$, $\varphi = 0.320$), and marginally in the *anterior capsula interna* ($\chi^2(1) = 3.683$, $p = 0.055$, $\varphi = 0.250$) were significantly more frequent in ALS patients than in healthy controls. FLAIR lesions at the ventricular borders were detected in ALS patients as well as in healthy controls. Individual binary lesion maps across all ALS patients were accumulated into an overlap lesion map (Figure 2.4.2). FLAIR lesions of ALS patients were small (TLV: M = 0.72ml, SD = 0.22) and diffuse. 65% of voxels with FLAIR alterations showed no overlap between ALS patients.

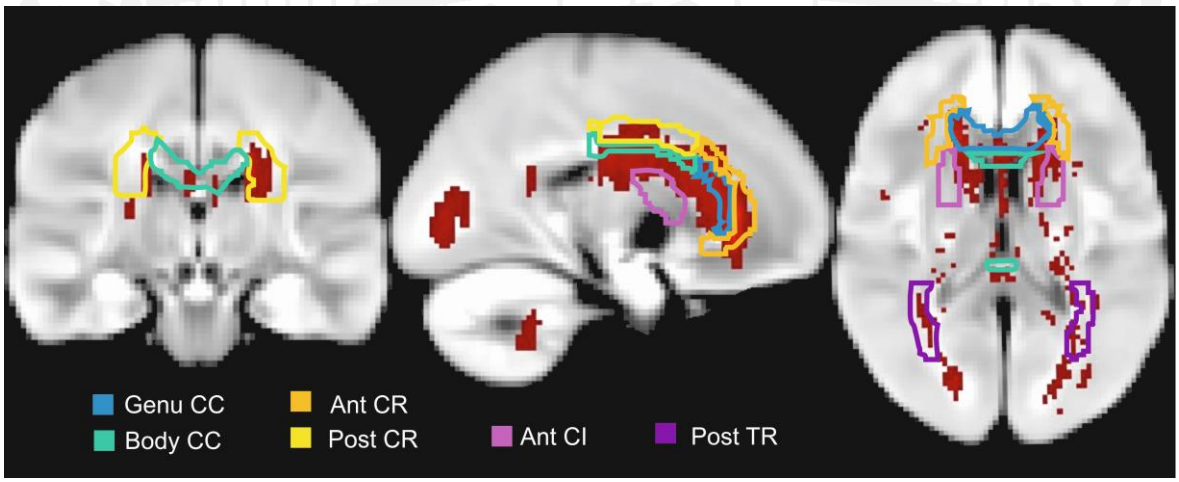

Figure 2.4.2. Localization and distribution of FLAIR lesions in ALS patients. Overlap of individual binary lesion maps summed up across all ALS patients (n = 28). Ant CR = anterior corona radiata, sup CR = superior corona radiata, post CR = posterior corona radiata, post TR = posterior thalamic radiation, ant CI = anterior capsula interna.

Quantitative and subjective evaluation of FLAIR images

Results of LST were compared to visual evaluation of FLAIR images by two experienced neuroradiologists (Figure 2.4.3). Both neuroradiologists classified the FLAIR images of patient 1 (Figure 2.4.3a) as age-related without abnormalities. LST only marked regions at the ventricular border. Patient 2 (Figure 2.4.3b) was evaluated with multiple small and unspecific WM lesions but weak to no evidence for pathological signal change in PTs. Consistent with this visual evaluation, LST detected no lesions in PTs but the presence of unspecific WM lesions (white arrow, Figure 2.4.3b). Patient 3 (Figure 2.4.3c) was evaluated with symmetrical signal change along the PTs in both LST and visual evaluation of the two neuroradiologists. Increased FLAIR signal in the PTs was not evaluated as an artifact, as it was persistent across the following brain slices (Figure 2.4.3d). Signal changes along the PTs as visualized in patient 3 were marked by LST in 14 out of 28 ALS patients.

Clinical correlations

LST variables did not significantly correlate with disease progression rates (TLV: r = .045, p =.820; TLN: r = -.101, p = .608). ALSFRS-R scores at baseline significantly correlated with elapsed time between diagnosis and MRI scan (r = -.520, p = .005, corrected). However, ALSFRS-R sum scores only weakly correlated with TLV of ALS patients (r = -.417, p = .027, uncorrected) and showed no significant correlation with survival since diagnosis (r = .136, p =.569). A tendency towards association between TLN and survival (r = -.445, p = .050, uncorrected) led to the following post-hoc analysis: Patients were differentiated into patients with (n = 14) or without (n = 14) PT lesions as detected by the LST. Overall estimated mean survival time was 29.08 months since diagnosis (95% CI 23.31-34.85 months). Kaplan-Meier log-rank test revealed significantly inferior survival since diagnosis for patients with PT lesions (95% CI 16.5-27.7 months) compared to those without PT lesions (95% CI 26.51-43.04 months) (p = .013) (Figure 2.4.4). Cox-regression analysis showed the prognostic value of age (Hazard ratio: 1.067, CI: 1.01-1.12; p = .015) for survival. No prognostic value was observed for ALSFRS-R scores (p = .964), disease progression rates (p = .154) or sex (p = .245).

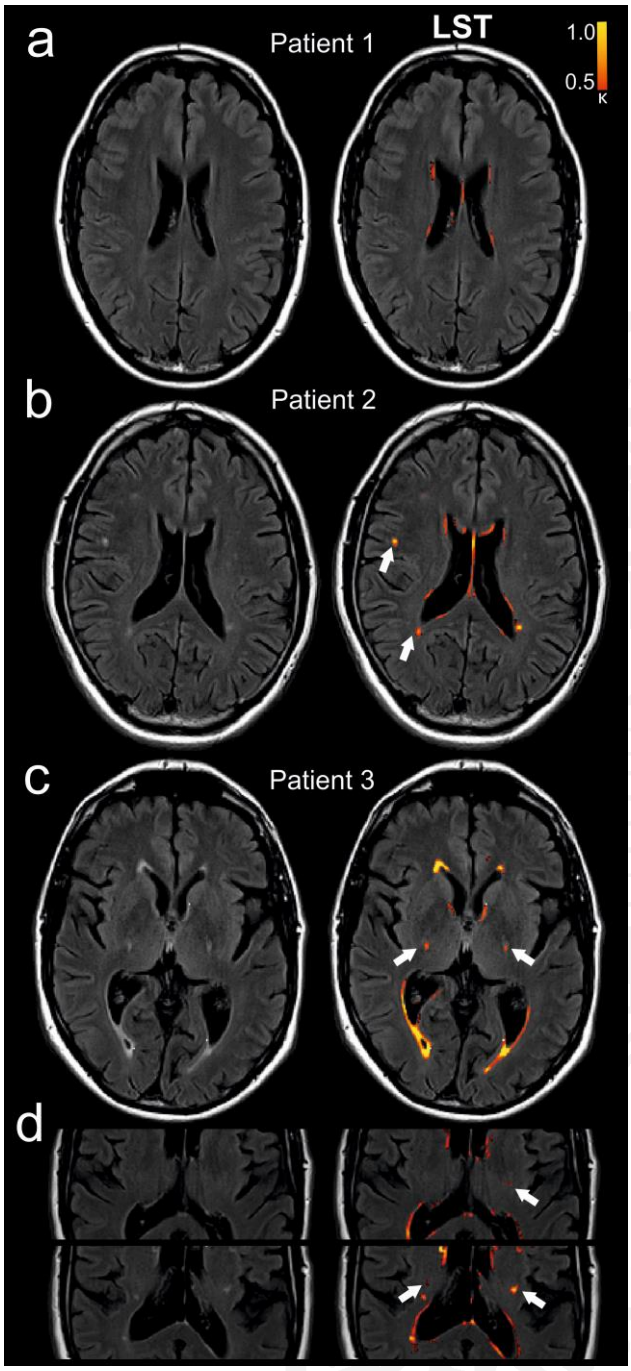

Figure 2.4.3. Lesion segmentation in three exemplary patients. MRI slices of three limb-onset patients' (patient 1: 46 yo, male, ALSFRS-R: 39; patient 2: 46 yo, male, ALSFRS-R: 48, patient 3) 69 yo, male, ALSFRS-R: 21) FLAIR images were evaluated by two experienced neuroradiologists and LST (red). A) Patient 1 evaluated with age-related FLAIR images. B) Slice of FLAIR images of patient 2 described by unspecific WM lesions and weak to no evidence for pathological signal change in the PTs. LST successfully detected unspecific WM lesions (white arrows). C) Evaluation of symmetric hyperintensity signal in the PTs of patient 3 by both LST and visual evaluation of two neuroradiologists. D) Persistent hyperintensity in the PT across the following MRI slices of patient 3. Threshold for lesion probability was κ = .50. PT = pyramidal tract.

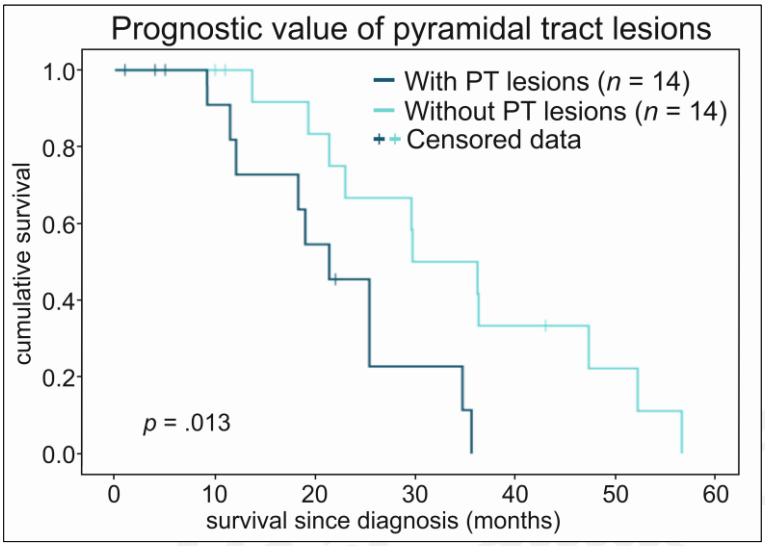

Figure 2.4.4. Prognostic value of pyramidal tract lesions for survival since diagnosis. Pyramidal tract (PT) lesions were detected by the LST in 14 out of 28 patients. Kaplan-Meier analysis revealed significantly inferior survival prognosis for patients with PT lesions (dark cyan) compared to those without PT lesions (bright cyan)(p = .013). Seven out of 28 patients were still participating in the study and were marked as censored data.

Control analysis on preceding T1 registration

A separate control analysis (ALS n = 20, controls n = 31) investigated bias effects of precedent T1 registration on LPA lesion segmentation. Registration to T1 images did not significantly affect TLN (F(1, 46) = .008, p = .930). In contrast, TLV was significantly increased if LPA was preceded by registration of FLAIR images to T1 images (F(1, 46) = 7.538, p = .009).

DISCUSSION

LST revealed enhanced frequency of FLAIR alterations in male ALS patients. FLAIR lesions were small and diffuse and more frequent in ALS patients than in healthy controls in the superior and posterior corona radiata, posterior thalamic radiation and anterior capsula interna. The presence of PT lesions as detected by the LST was associated with inferior survival.

FLAIR lesions may be interpreted as loss of myelination in fibers (Schmidt et al., 2012). In healthy subjects, FLAIR alterations were observed to increase with age (Gawne-Cain et al., 1997). Consistent with this finding, we detected distinct effects of age on TLN and TLV. LST revealed FLAIR hyperintensity in both ALS patients and healthy controls, as reported

in other studies (Hecht et al., 2001; Thorpe et al., 1996; Vázquez-Costa et al., 2018; Zhang et al., 2003). FLAIR lesions were observed to be dependent on sex and more frequent in male ALS patients than in female ALS patients as well as male healthy controls. In contrast, healthy controls showed no sex-specific differences in FLAIR alterations, as reported by Gawne-Cain et al. (1997). Sex-specific differences in FLAIR lesions were reported for MS patients despite balanced age and disease duration (Klistorner et al., 2016). In ALS research, effects of sex on FLAIR hyperintensity were not detected (Vázquez-Costa et al., 2018) or not analyzed (Fabes et al., 2017; Hecht et al., 2001, 2002; Ignjatović, Stević, Lavrnić, Daković, & Bačić, 2013; Ngai, Tang, Du, & Stuckey, 2007; Schweitzer et al., 2015; Zhang et al., 2003). Sex-specific differences may be due to outliers with low TLN in the small sample size of female ALS patients (n = 8). Consistent with this consideration, several studies failed to detect FLAIR alterations in all ALS patients of the sample (Hecht et al., 2002; Ignjatović et al., 2013; Ishikawa, Nagura, Yokota, & Yamaouchi, 1993; Rocha et al., 2004; Thorpe et al., 1996). FLAIR alterations were discussed to occur predominantly in patients with progressed stage of ALS (Huynh et al., 2016; Ignjatović et al., 2013; Thorpe et al., 1996). The two patients with the highest TLN had bulbar-onset of disease. This finding is consistent with Vazques-Costa et al. (2018) reporting more pronounced FLAIR signal change of the CST in bulbar- compared to limb-onset patients. Total lesion volumes in ALS patients were comparable to that of healthy controls and much lower than in other neurological diseases such as MS (Egger et al., 2016). These findings are consistent with previous studies reporting the dominant role of frequency rather than volumes of FLAIR alterations in ALS (Thorpe et al., 1996; Zhang et al., 2003).

FLAIR lesions in ALS patients were most prominent in the corona radiata and body and genu of the CC. These findings are consistent with a study (Fabes et al., 2017) reporting most pronounced FLAIR hyperintensity of classical ALS in corona radiata of the CST and the body of the CC. Similarly, we observed FLAIR lesions to be more frequent in ALS patients than in healthy controls in the superior and posterior corona radiata. FLAIR alterations in the CC were shared in both ALS patients and healthy controls. These findings may indicate that detected callosal FLAIR lesions may be age-related (Gawne-Cain et al., 1997) or may result from FLAIR artifacts (Krupa & Bekiesińska-Figatowska, 2015). Moreover, FLAIR alterations were detected at the ventricular borders. FLAIR hyperintensity visualized as thin lines surrounding ventricles is a frequently observed phenomenon also in healthy controls (Gawne-Cain et al., 1997) and may be associated

with cerebrospinal fluid/vascular pulsation artifacts (Krupa & Bekiesińska-Figatowska, 2015) or artifacts originating from incomplete signal inversion (Hajnal, Oatridge, Herlihy, & Bydder, 2001). However, structural changes at the ventricular borders may as well indicate processes in the region of neurogenesis (subventricular zone) (Bergmann, Spalding, & Frisén, 2015). LST detected FLAIR alterations at the PT in 14 out of 28 patients. These lesions often appeared to be symmetric across hemispheres as reported in Cheung et al. (1995). The good correspondence of LST results to findings of visual evaluation (Hecht et al., 2001; Klistorner et al., 2016; Schweitzer et al., 2015; Thorpe et al., 1996) and quantitative evaluation (Fabes et al., 2017; Hecht et al., 2001; Schweitzer et al., 2015) argue for the potential of LST use. The interpretation of numerical TLN and TLV should be careful, as LST may be biased by hyperintensity derived from incomplete signal inversion along the ventricular walls resulting in CSF-ventricular-border-artifacts. Still, LST was capable in the fast and objective detection of intracerebral lesions.

Correlations of both ALSFRS-R and disease progression rates with LST variables were rather weak or not detectable. Lack of correlation between FLAIR intensity and clinical data was frequently reported in both visual evaluation studies (Gupta et al., 2014; Jin et al., 2016; Peretti-Viton et al., 1999) and quantitative studies (Hecht et al., 2001, 2002). Kaplan-Meier analysis detected inferior survival for patients with PT lesions compared to patients without PT lesions. Thus, LST may not only help to monitor intracerebral lesions but may also contribute to prognosis and diagnosis of different ALS phenotypes. Cox-regression analysis revealed significant prognostic value of age for survival. This is consistent with Pupillo, Messina, Logroscino & Beghi (2014) showing age as one of the most relevant prognostic factors of ALS survival. Baseline ALSFRS-R score significantly correlated to elapsed time between diagnosis and MRI scan but had no predictive value for the survival of patients. Prognostic values of sex, ALSFRS-R scores, and disease progression rates on survival were less consistently reported than that of age (Chiò et al., 2009).

Several methodological limitations may be considered. First, sample size was limited to n = 28 patients. The subset of female patients did not show severe FLAIR lesions potentially affecting group statistics. Still, sample size was adequate to detect higher frequency of FLAIR lesions in male patients at group level. Second, the sample included both limb-onset and bulbar onset patients. Lack of balanced sample sizes (limb-onset: n = 25, bulbar-onset: n = 3) allowed for no statistical test for ALS onset. A separate control analysis revealed that TLV was biased by precedent T1 registration. TLN was stable in T1

registration. Thus, precedent registration of lower resolution FLAIR data to higher resolution T1 images may bias size of detected FLAIR lesions.

Conclusion

In conclusion, LST is an accessible and time-saving tool for objective quantification of FLAIR alterations in ALS. The predictive value of FLAIR alterations for survival prognosis underlines the relevance of monitoring FLAIR images in ALS patients and its potential for the classification of ALS phenotypes. Future studies may explore FLAIR alterations detected by LST in different ALS subtypes and ALS mimic disorders to underline ALS-specificity of these FLAIR lesions.

Contributions of authors:

Wirth: conception and design of the study, acquisition, analysis, interpretation of MRI data, and composition of the manuscript.

Johannesen, Bruun, Bogdahn: contribution to the conception of the study; acquisition, analysis, and interpretation of clinical data, and revision of the manuscript.
Khomenko, Baldaranov: data acquisition and revision of the manuscript.
Johannesen, Khomenko, Baldaranov, Bogdahn: care for ALS patients in outpatient clinic, treatment concept.

Schuierer, Wendl: MRI data acquisition and visual evaluation of MRI data

Greenlee: contribution to the conception of the study, supervision of MRI data analysis and data interpretation, and revision of the manuscript.

Acknowledgements:

This work was supported by the German Federal Ministry of Education and Research (BMBF, Project GO-Bio).

Conflict of Interest Statement:

The authors declare no commercial or financial conflicts of interest.

CHAPTER 3: CONCLUDING REMARKS

SUMMARY OF FINDINGS OF THIS THESIS

The aim of the thesis is to evaluate the potential of candidate MRI biomarkers for ALS. The subprojects focus on structure of both WM and GM of the brain using T1-weighted imaging, DWI, and FLAIR MRI. The analysis of candidate MRI biomarkers includes conventional cross-sectional group analysis but also focuses on the individual patient perspective and specifically longitudinal monitoring. Combinatory biomarker use is emphasized by the association of MRI biomarkers with clinical and neurophysiological biomarkers.

Study 1 reveals that cortical thinning of the precentral cortex is a prominent but not omnipresent feature of ALS patients. Precentral cortical thinning is linked to age and disease progression. Combinatory biomarker use of MRI, clinical, and neurophysiological biomarkers underlines the potential gain of information. Moreover, study 1 reveals substantial differences in the temporal dynamics of specific biomarkers challenging the detection of correlations between them. Precentral cortical thinning cannot be used as a diagnostic criterion for ALS per se. However, cortical thinning may be used as a *monitoring biomarker* capable of the differentiation of ALS patients in different disease and progression types. Moreover, the combinatory biomarker use with neurophysiological MUNIX may help to describe levels of involvement of UMN and LMN in complex classical ALS and therefore help to establish definite ALS diagnosis.

Study 2 shows that FA alterations are specific to region and type of WM in ALS patients. Reduced levels of FA are primarily detected in the CST and non-motor WM areas. FA alterations are predominant in the brainstem and spread to other types of WM. Spread of WM alterations is observed to occur in both dying-forward and dying-back manner. Still, patients with either dying-forward or dying-back patterns of disease spreading do not significantly differ in clinical scores, disease progression, or survival. Moreover, dying-forward or dying-back spread is not associated with gender or onset of disease in classical ALS. The findings indicate that both patterns of disease spread may exist in classical ALS. Therefore, FA may be used as a *diagnostic biomarker* potentially contributing to the

understanding and the differentiation of ALS disease propagation mechanisms and individual phenotype.

Study 3 underlines the great potential of the LST for the fast and objective evaluation of FLAIR images in ALS. LST is highly sensitive to intracerebral lesions and corresponds well to the visual evaluation of FLAIR images. LST may be considered a promising and easily accessible tool enabling one step beyond visual evaluation studies. FLAIR imaging does not appear to provide a strict diagnostic criterion for ALS. However, LST may help to standardize quantification of FLAIR hyperintensity signal as a highly relevant *exclusive biomarker* of ALS mimics. Moreover, FLAIR lesions of the PTs are associated with inferior survival. These findings reveal the hidden potential of conventional FLAIR imaging as a source for *prognostic biomarkers* for ALS.

In summary, structural MRI may contribute to the *diagnosis* (FA), the *monitoring of disease progression* (cortical thickness, FA), and the *prognosis* (FLAIR hyperintensity) of ALS. All structural MRI biomarkers investigated in this thesis show their potential to add to the understanding of pathogenesis of ALS.

THE CHANGING SCENE OF MRI BIOMARKERS

The last decade of ALS research has changed the perspective on ALS and its neuroimaging biomarkers. The following three emerging aspects of MRI biomarker research have had an essential influence on the aims and the study designs of this thesis: understanding neurodegenerative disease, multimodal MRI use, and individual perspective.

First, biomarkers are not only needed to enlarge ALS-specific diagnostic criteria, but also more generally to deepen our understanding of neurodegenerative diseases. Biomarkers enable the differentiation of ALS from so-called mimic disorders (Agosta et al., 2010). However, biomarkers may as well help to find commonalities with other neurodegenerative diseases (Eisen et al., 2014). Similar to other neurodegenerative diseases, ALS is characterized by a long presymptomatic period (Eisen et al., 2014), frequent genetic background (Calvo et al., 2014) and fast disease propagation (Ludolph & Brettschneider, 2015). Moreover, ALS is considered to potentially overlap with the behavioral variant of frontotemporal dementia (Zago, Poletti, Morelli, Doretti, & Silani, 2011). The accumulation and spread of protein aggregations in the brain are considered

communalities of ALS with Parkinson's disease and Alzheimer's disease (Ludolph & Brettschneider, 2015). These findings have lead to the controversial discussion of ALS being a spreading prion-like disease (Ludolph & Brettschneider, 2015). Spread of WM degeneration has been investigated by stage-wise degeneration of specific WM tracts (Kassubek et al., 2014). Study 2 makes a further step by investigating dying-forward and dying-back hypotheses as reflected in the spread of WM type-specific FA alterations.

Second, it is not essential to find the one and only MRI biomarker for ALS but rather an MRI footprint of ALS by multimodal MRI use (Ferraro et al., 2017). Routine anatomical imaging like T2-weighted imaging and FLAIR are useful for the exclusion of MRI mimic disorders (Agosta et al., 2010). However, advanced techniques like DWI and voxel-based morphometry appear to be more promising biomarkers for disease progression and ALS diagnosis (Wijesekera & Leigh, 2009). Both GM and WM pathology have been detected (Zhang et al., 2014). However, MRI studies have revealed more consistent WM than GM involvement in ALS (e.g. Cardenas-Blanco et al., 2016, Christidi et al., 2018). Bede & Hardiman (2014) discuss that WM alterations may be detectable earlier in disease than GM changes suggesting that WM alterations may be more helpful as monitoring biomarkers. Consistent with this theory, the current thesis detects common FA alterations, but precentral cortical thinning only in about half of the patient cohort. Consistent with Ferraro et al. (2017), multimodal MRI biomarker use of cortical thickness, FA, and FLAIR hyperintensity in the same patient cohort results in a substantial gain of information. The thesis fulfils these criteria, as it has assessed multimodal MRI techniques in the same patient cohort.

Third, ALS is no longer considered a single disease but rather as a spectrum of various syndromes of MND (Turner et al., 2013; Wijesekera & Leigh, 2009). ALS includes complex variations of phenotypes, onsets, and progression types (Eisen et al., 2014). The latest version of El Escorial criteria enables the coarse categorization into possible, probable and definite ALS (Costa et al., 2012). However, El Escorial criteria cannot cope with the heterogeneity of ALS phenotypes, which may have a substantial impact on the prospects of success of clinical trials (Al-Chalabi et al., 2016). Biomarkers like neuroimaging may improve diagnosis and classification of ALS (Verstraete & Foerster, 2015). For this purpose, future studies need to include detailed descriptions of ALS phenotypes in their samples (Al-Chalabi et al., 2016). Most importantly, MRI studies in ALS may go beyond group averages and focus on the individual patient (Turner et al.,

2013). Accordingly, a special focus of this thesis is set on the detailed description of the individual patients of the sample.

MRI research of the last decades has been further developed and has contributed to the current understanding of ALS (Al-Chalabi et al., 2016; Chiò et al., 2014). Still, MRI biomarker research is challenged by a number of technical and methodological caveats. These challenges have also influenced the methodological approaches of this thesis.

CHALLENGES OF MRI BIOMARKER RESEARCH

MRI biomarker research for ALS includes various MRI approaches, heterogeneous cohorts of ALS phenotypes, and various clinical correlates. These manifold approaches may offer broad perspectives, but may as well challenge comparability of findings (Chiò et al., 2014).

Variability of MRI approaches. MRI studies may involve conventional MRI like FLAIR (e.g. Ishikawa et al., 1993), T1-weighted imaging (e.g. Großkreutz et al., 2006) or advanced imaging techniques like DWI, fMRI, and MRS (Agosta et al., 2010). Morphometric studies may investigate cortical thickness (e.g. Walhout et al., 2015), volumes (e.g. Bede et al., 2013) or areas (e.g. Verstraete, Veldink, Mandl, van den Berg, & van den Heuvel, 2011) of the precentral cortex. In turn, cortical thickness may be assessed by either vertex-based approaches (e.g. Walhout et al., 2015) or ROI-based approaches (e.g. Bede et al., 2013). ROI-based approaches are usually based on atlas definitions (e.g. Desikan et al., 2006). DWI has given rise to the investigation of diffusion properties of the CST. FA and MD are the most commonly investigated diffusion properties in ALS research (Chiò et al., 2014). However, several DWI studies have also included the analysis of radial diffusivity and axial diffusivity (e.g. Metwalli et al., 2010). DWI variables may be approached by either voxel-based (Chapman et al., 2014) or ROI-based methods (Keil et al., 2012). The ROI of CST may be defined by either an atlas (e.g. Kwan et al., 2012) or DTI tractography (Kassubek et al., 2014). The DTI model enables approaches for deterministic or probabilistic tractography (Descoteaux et al., 2009). Both deterministic (e.g. Kassubek et al., 2014) and probabilistic (Steinbach et al., 2015) tractography have revealed alterations in the CST of ALS patients. Probabilistic tractography is considered to be more sensitive and specific than the deterministic approach (Thomas et al., 2014). However, no study has yet investigated differences in findings between deterministic and

probabilistic tractography in the same ALS sample. The choice of tractography thresholds and seed procedures are among the crucial factors for comparability of tractography methods (Zhan et al., 2015). The CST may be defined by tracking from seed regions in either the pons (e.g. Steinbach et al., 2015) or the capsula interna (e.g. Ciccarelli et al., 2006), respectively. In FLAIR imaging, studies on visual evaluation including rating scales and independent raters broadly dominate the field (e.g. Hecht et al., 2001). However, new methods of objective quantification of FLAIR signal open up new vistas for FLAIR imaging (Fabes et al., 2017). In summary, MRI research in ALS provides a broad range of different methods and restrictions but also with various perspectives and possibilities. Detailed description of MRI approaches may ease their comparison and enable their combination in ALS cohort studies (Ferraro et al., 2017).

Variability of patient cohorts. Comparing findings of different MRI studies is challenged by variable patient cohorts with different clinical characteristics and demography (Chiò et al., 2014). MRI biomarker studies may be restricted to specific ALS phenotypes (e.g. primary lateral sclerosis; Kuipers-Upmeijer, Jager, Hew, Snoek, & van Weerden, 2001) or may compare between different ALS phenotypes (e.g. Mezzapesa et al., 2013). Patient subgroups may differ in genetic background (e.g. Westeneng et al., 2016), onset of disease (e.g. Cardenas-Blanco et al., 2014), extent of UMN and LMN involvement (Van der Graaff et al., 2011), or in overlap with frontotemporal dementia (Omer et al., 2017). Moreover, ALS subtypes may be compared to ALS mimic disorders (e.g. Walhout et al., 2015). Patient cohorts of different MRI studies may vary in duration of disease (1/2 year – 15 years, Chiò et al., 2014), mean age (e.g. 52 yrs: Thivard et al., 2007; 64 yrs: Cosottini et al., 2005), or mean baseline ALSFRS-R score (e.g. 40 score points: Verstraete et al., 2011; 23 score points: Meadowcraft et al., 2015). Moreover, ALS patient samples may differ in ethnic origin (e.g. China: Tang et al., 2015; Germany: Grosskreutz et al., 2006). Ethnic background may be crucial, as population-based registers reveal ethnic differences in prevalence and incidence of ALS (Hardiman et al., 2017). Variability of patient samples challenges the comparison between studies and their generalization (Chiò et al., 2014). However, failures of several clinical trials indicate that response to treatment may depend on ALS phenotypes (Mitsumoto et al., 2014). Therefore, the focus on specific ALS phenotypes may be trend-setting for improving ALS classification (Al-Chalabi et al., 2016) and for understanding the manifold pathogenic processes of ALS (Grad, Rouleau, Ravits, & Cashman, 2017).

Choice of clinical correlates. Disease-related changes in structure and function are considered to affect clinical outcome (Chiò et al., 2014). Therefore, MRI biomarker research needs to involve clinical correlates. ALSFRS-R is the most commonly used clinical correlate in MRI studies (e.g. Rutkove, 2015). ALSFRS-R is prominent in clinical routine and is considered a reliable clinical score for the severity of disease (Rosenfeld & Strong, 2015). However, correlations of ALSFRS-R with MRI candidate biomarkers like precentral cortical thinning (e.g. De Albuquerque et al., 2016), reduced FA of the CST (e.g. Borsodi et al., 2017) or FLAIR hyperintensity (e.g. Hecht et al., 2002) are rather weak or not at all detected. These results may be explained by ALSFRS-R being a rather general severity scale influenced by both UMN and LMN signs (Cardenas-Blanco et al., 2016). In addition to ALSFRS-R, prominent clinical correlates of MRI studies include disease duration, disease progression rate, survival, or burden scales (Grolez et al., 2016). The increasing interest in ALS-FTD overlap and cognitive deficits in ALS has led to the recommendation of neuropsychological assessment in clinical trials (Dorst et al., 2018) and MRI studies (Christidi et al., 2018). The inclusion of a broad range of valid clinical correlates may contribute to a detailed description and differentiation of ALS patient cohorts (Grolez et al., 2016).

The subprojects of this thesis have been challenged by a variety of methodological challenges which have also affected the majority of MRI studies in ALS research: small sample sizes, restricted data quality, adequacy of control samples, lack of standardization, and statistical shortcomings (Chiò et al., 2014).

Small sample sizes. Only very few published studies exhibit sample sizes greater than 30 subjects per group (Grolez et al., 2016). Small sample sizes may be due to flow occurrence of ALS cases (Nagel, Unal, Rosenbohm, Ludolph, & Rothenbacher, 2013) or high MRI drop-out rates (Grolez et al., 2016), among other factors. MRI is a time-consuming technique associated with patient discomfort (Benatar et al., 2016). ALS patients often drop out of studies due to respiratory problems, increasing disability, or even death (Grolez et al., 2016). Small sample sizes do not only lead to variable results, but also challenge subgroup analysis. Facing the problems of sample sizes in unicenter studies, the Neuroimaging Society in Amyotrophic Lateral Sclerosis (NiSALS) has initiated the cooperation of MRI research units for an international and multicenter investigation of MRI biomarkers (Filippi et al., 2015).

Lack of standardization. Comparability and reproducibility of MRI studies in ALS research are often challenged by the variability of imaging sequences and analytical methods (Verstraete & Foerster, 2015). Additionally, several studies lack a detailed description of MRI equipment, sequence parameters, and data processing (Chiò et al., 2014). As MRI scanners and sequences are highly heterogeneous between centers, multicenter MRI research as proposed by Filippi et al. (2015) include general guidelines for the acquisition and analysis of good quality and comparable MRI data in ALS.

Data quality. One major issue in clinical MRI research is pragmatism (Benatar et al., 2016). MRI assessment requires technical equipment, expertise, and high costs. Most MRI studies on ALS before 2010 used MRI scanners with 1.5T field strength. MRI scanners with 3T or even 7T are not available in every hospital (Bede & Hardiman, 2014). Reduction of MRI acquisition time may decrease patient discomfort and lead to lower drop-out rates (Hollingsworth, 2015). However, reduced scan acquisition time may lead to MRI images with lower resolution or reduced number of orientations in DWI (e.g. 5mm resolution and six DWI orientations: Abe et al., 2004). This data quality may not be sufficient for advanced imaging data analysis like probabilistic tractography (Behrens, Berg, Jbabdi, Rushworth, & Woolrich, 2007) or voxel-based morphometry (Ashburner & Friston, 2000). Another problem in clinical MRI research is the change of scanner types or sequences within a study. Therefore, technical equipment and sequence parameters should be described in detail (Chiò et al., 2014).

Inappropriate control samples. Control samples are often small (Grolez et al., 2016) and not adequate as controls for ALS samples (Chiò et al., 2014). Specifically, control samples frequently suffer from an insufficient match of age and gender, and often miss detailed description (e.g. cognitive status). Inclusion of age and gender correction in statistical models may help to overcome this caveat (Bede & Hardiman, 2014). Moreover, the inclusion of disease control samples like e.g. ALS mimics may be trend-setting to investigate specificity of MRI biomarkers for ALS (e.g. Ferraro et al., 2017).

Statistical shortcomings. Reliability and reproducibility are enormously challenged by statistical shortcomings in neuroimaging (Zugman, Sato, & Jackowski, 2016). MRI studies facing low sample sizes often struggle with limited statistical power (Nagel et al., 2013) resulting in no significant differences between ALS patients and controls and weak correlations with clinical variables. This leads to the following dilemma: On the one hand, liberal statistical testing (e.g. lack of multiple comparison correction) may lead to false

positive results (Bede & Hardiman, 2014). On the other hand, conservative statistical testing may increase risk of neglecting positive results or potential tendencies (Bennett, Wolford, & Miller, 2009). The key to solve this problem may be the plain description of positive as well as negative results and a critical interpretation of both.

The three subprojects of this thesis have handled these challenges by adapting their methods, aims, and study designs. The following section discusses the benefits and drawbacks of these methods.

DISCUSSION OF METHODS AND DESIGNS OF THIS THESIS

Restriction to retrospective data. The data analysis of the treatment program is limited to the time window of 2010 – 2017. No additional patients have been included into MRI data acquisition after this period. These conditions exacerbated the collection of an adequate ALS sample of more than five patients for prospective studies. Therefore, the thesis focuses on retrospective patient data acquired since 2010. Retrospective data enables the analysis of longitudinal time courses of MRI biomarkers and fulfils the aim of ALS sample sizes of at least 20 patients.

Choice of MRI approaches due to restricted data quality. Retrospective data dates back to 2010, when MRI technology was ruled by different standards than used in recent MRI studies (Bede & Hardiman, 2014). All data sets were acquired with 1.5T MRI scanners with low resolution of DWI and FLAIR data. A slice thickness of 5mm in DWI and FLAIR data hinderes the conduction of voxel-based approaches. Thus, all projects of this thesis use ROI-approaches base on atlas definitions (Mori et al., 2008; Yeo et al., 2011). Moreover, ROIs are rather large (Study 1: ventral and dorsal precentral/postcentral cortex) or summed up to larger ROIs (Study 2: WM types). The low resolution of MRI data is carefully discussed in the methodological limitations of the subprojects. Another caveat of data quality is the change of DWI sequence during the study period. Modification of DWI sequence from six to 20 orientations challenges both cross-sectional and longitudinal data analysis. A control analysis of 22 healthy controls scanned with both DWI sequences on the same acquisition day has revealed evident bias effects of DWI sequence change on FA values (Supplementary figure 1A, Appendix 3). Ignoring these biases may have led to erroneous results and interpretations. DWI sequence change within the time course of a

single patient would have induced the analysis and fatal interpretation of FA increase over time (Supplementary figure 1B, Appendix 3). Calculation of multiplication factors for every WM region overcomes these bias effects and enables the conduction of cross-sectional and longitudinal analysis without excessive drop-out of data sets. Even after modification of DWI sequence, DWI data quality restricts DWI data analysis. Probabilistic tractography is considered to require at least 30 orientations of DWI data (Behrens et al., 2007). Deterministic tractography would have been possible with DWI20. Still, slice thickness of 5mm of DWI data is not adequate for tractographic analysis. Therefore, DWI data analysis is restricted to basic methods like extraction of mean FA for specific ROIs.

Variability of patient cohorts. The ALS patient cohort of this thesis includes 28 limb-onset and three bulbar-onset patients. Both bulbar-onset and limb-onset ALS patients are characterized by UMN and LMN signs. Unbalanced sample sizes for bulbar and limb-onset ALS patients do not allow for subgroup analysis. However, ALS patients are differentiated into either arm or leg onset. The ALS sample of this thesis differs from other MRI studies with respect to the younger age of our patients. Usually, ALS patient cohorts are aged 60 years in average (64 yrs in Cosottini et al., 2005). Here, our ALS sample is aged 50 years on average and includes several young-onset patients. Young-onset ALS is associated with better prognosis (Chiò et al., 2011) and slow disease progression (Orban, Devon, Hayden, & Leavitt, 2007). Consistent with these findings, the two youngest ALS patients exhibit slow disease progression and longitudinal survival. Facing high drop-out rates in MRI studies, slow progressive patients enable the longitudinal monitoring of MRI biomarkers (Menke et al., 2017). On the one hand, these patients may represent only a small subtype of ALS and challenge generalizability of findings. On the other hand, ALS research of the past 10 years has underlined that the focus on homogenous subtypes of ALS may be the key towards understanding and treating ALS (Al-Chalabi et al., 2106; Mitsumoto et al., 2014). For this purpose, the subprojects provide detailed clinical data of ALS cohorts and emphasize the perspective on the individual patient as recommended by Chiò et al. (2014) and Simon et al. (2014).

Choice of clinical correlates. Detailed description of ALS cohorts requires the acquisition of numerous clinical correlates. Most MRI studies in ALS research involve clinical correlates like ALSFRS-R sum scores and subscores, disease duration and disease progression rates (Grolez et al., 2016). All three subprojects of the thesis fulfil the inclusion of these basic clinical correlates. Still, the thesis may have benefited from acquisition of further clinical correlates like UMN burden scale (Mezzapesa et al., 2013),

UMN rapidity index (Iwata et al., 2011), spasticity scale (Ellis et al., 1999) or muscular strength (Poujois et al., 2013). One major caveat of this thesis is the lack of neuropsychological data. The relevance of neuropsychological assessment for clinical trials (Mitsumoto et al., 2014), and multidisciplinary care of ALS patients (Hogden, Foley, Henderson, James, & Aoun, 2017) has gradually increased over the last ten years. Still, neuropsychological evaluation is underrepresented in MRI ALS research (Christidi et al., 2018). Survival is considered a standard outcome variable in ALS clinical trials although survival may not be an adequate correlate for disease progression (Rutkove, 2015). Still, survival is considered an important clinical correlate for the evaluation of MRI as a prognostic biomarker. Consistent with this notion, study 3 detects prognostic value of FLAIR imaging for ALS survival.

Small sample sizes. The thesis has been challenged by a small sample size of ALS patients. In total, the treatment program involves 36 ALS patients. Some of these patients have dropped out of the studies due to exclusion from MRI acquisition or lack of specific MRI sequences. While DWI and FLAIR data have consistently been acquired since 2010, T1-weighted imaging has been included into the standard MRI protocol as recently as 2013. Therefore, study 1 may have included the same patients as in study 2 or 3 at a later stage of disease. All projects account for these possible bias effects by taking into account the current severity of disease (ALSFRS-R), disease progression rates, and time elapse since diagnosis at the time point of so-called baseline MRI scan. A greater number of ALS patients would have enabled subgroup analysis (e.g. limb-onset, bulbar-onset). Still, ALS is a rare disease and sample size is comparable to those of other unicenter MRI studies (e.g. Cosottini et al., 2013; Grosskreutz et al., 2006; Roccatagliata et al., 2009; Verstraete et al., 2010).

Inappropriate control samples. Recruitment and MRI acquisition of age-related healthy controls are main aspects of the thesis. As most of these healthy controls are clinical staff or related to the research unit, the control sample may have been influenced by selection bias. Still, these participants serve as an age-matched control group for ALS patients and enable methodological control analyses (e.g. DWI sequence change). The thesis may have benefited from a control sample without G-CSF treatment or control groups with other neurological diseases. An ALS control sample without G-CSF treatment would have enabled the investigation of potential effects of G-CSF. However, the acquisition of this control sample has not been part of the treatment program. Additional control samples with other neurodegenerative diseases would have underlined the ALS-specificity of results.

However, the ethics-committee approval has been restricted to MRI acquisition in ALS patients and healthy controls.

Lack of standardization. The three studies included in this thesis use different MRI approaches. Study 1 investigates T1-weighted imaging. Study 2 focuses on DWI, whereas study 3 examines FLAIR imaging. Still, different MRI sequences of this thesis enable the differentiated evaluation of MRI as a biomarker in the same preselected cohort. MRI variables of interest (cortical thickness, FA) are transformed to *z*-transformed deviations of age-related healthy controls. This standardization procedure facilitates the comparison of findings of this thesis. Bias effects of change of DWI sequence on FA are controlled for and corrected by multiplication factors and *z*-standardization. All projects of this thesis have been conducted using the same software programs (Freesurfer 5.3, SPM, Matlab).

Statistical shortcomings. Increased sample size of ALS patients may have enhanced statistical power and may have rendered a broader range of statistical analyses possible (e.g. cluster analysis). Thus, the subprojects of this thesis have been restricted to rather basic statistical analyses like ANOVA, *t*-test, chi-square tests for independence, correlation analyses, Kaplan-Meier analysis and Cox-regression. While projects 1 and 3 include multiple comparison correction, region-specific *t*-tests of project 2 does not. The choice of WM regions for WM type ROIs is based on results of uncorrected *t*-tests. This procedure has to be used as multiple comparison correction may have eliminated the full choice of WM regions for commissural WM and may have led to no ROI definition of WM type CF at all.

In summary, the thesis may have benefited from better MRI data quality, increased ALS sample size, and additional correlates and control samples. Still, handling common challenges of MRI ALS research marks this thesis as a worthwhile approach towards the evaluation of potential MRI biomarkers in clinical routine ALS data.

CONCLUSION AND FUTURE OUTLOOK

In conclusion, this thesis may increase awareness for both the potential and the challenges of MRI biomarker research in a rare, complex and heterogeneous disease like ALS. GM and WM structure of ALS patients are investigated using different MRI sequences and approaches. Candidates of MRI biomarkers are associated with neurophysiological and

clinical biomarkers and monitored in the individual patient and in longitudinal courses of disease.

The findings of this thesis underline that MRI biomarkers may have great potential in diagnosis (DWI FA), prognosis (FLAIR), and longitudinal monitoring (cortical thickness) of ALS disease. Moreover, they may reveal potential propagation mechanisms and contribute to etiopathological understanding of ALS. Combination of different MRI modalities in the same patient may be rather more promising than searching for the unique MRI biomarker. Moreover, MRI biomarkers should be associated with other types of biomarkers (clinical, neurophysiological, molecular etc.). Multimodal biomarker use, detailed description of ALS phenotypes, and an individual perspective may contribute to the characterization of biomarker fingerprints of ALS subtypes.

The thesis has been conducted on behalf of a treatment program on a named patient basis for G-CSF. The results of this thesis may contribute to the evaluation of MRI approaches for prospective MRI biomarker studies in the treatment program. Moreover, the thesis may help to plan the set-up of MRI in a potential future clinical trial or broader application of G-CSF.

Future MRI research on ALS may try to bridge two challenges of ALS: ALS MRI research may aim at an improvement of data quality, enhanced sample sizes, adequate control samples, detailed description of ALS phenotypes, and a broad range of clinical correlates. Still, useful MRI biomarkers may be characterized by validity, applicability, feasibility, and above all: tolerability for the patients. By solving this dilemma, MRI biomarkers may help to take a further step towards the understanding and the cure of ALS disease. In addition, MRI biomarkers may help to bridge the huge time gap between an initially effective systemic medical treatment and the by far delayed functional benefits for the patient, when healthier neurons will restructure spinal cord and spinal nerves including the connected musculature.

BIBLIOGRAPHY

Abe, O., Yamada, H., Masutani, Y., Aoki, S., Kunimatsu, A., Yamasue, H.,. . . Ohtomo, K. (2004). Amyotrophic lateral sclerosis: diffusion tensor tractography and voxel-based analysis. *NMR in biomedicine*, *17*, 411–416. doi:10.1002/nbm.907

Abhinav, K., Yeh, F.-C., El-Dokla, A., Ferrando, L.M., Chang, Y.-F., Lacomis, D., Friedlander, R.M. & Fernandez-Miranda, J.C. (2014). Use of diffusion specrum imaging in preliminary longitudinal evaluation of amyotrophic lateral sclerosis: development of an imaging biomarker. *Front Hum Neurosci*, *8*, 270. doi:10.3389/fnhum.2014.00270

Adly, A. M. (2010). Oxidative Stress and Disease: An Updated Review. *Research Journal of Immunology*, *3*, 129-145

Agosta, F., Chiò, A., Cosottini, M., Stefano, N. de, Falini, A., Mascalchi, M.,. . . Filippi, M. (2010). The present and the future of neuroimaging in amyotrophic lateral sclerosis. *American journal of neuroradiology*, *31*, 1769–1777. doi:10.3174/ajnr.A2043

Agosta, F., Valsasina, P., Absinta, M., Riva, N., Sala, S., Prelle, A.,. . . Filippi, M. (2011). Sensorimotor functional connectivity changes in amyotrophic lateral sclerosis. *Cerebral cortex*, *21*, 2291–2298

Agosta, F., Valsasina, P., Riva, N., Copetti, M., Messina, M. J., Prelle, A.,. . . Filippi, M. (2012). The cortical signature of amyotrophic lateral sclerosis. *PloS one*, *7*. doi:10.1371/journal.pone.0042816

Agosta, F., Canu, E., Valsasina, P., Riva, N., Prelle, A., Comi, G. & Filippi, M. (2013). Divergent brain network connectivity in amyotrophic lateral sclerosis. *Neurobiology of aging*, *34*, 419–427

Agosta, F., Ferraro, P. M., Riva, N., Spinelli, E. G., Chiò, A., Canu, E.,. . . Filippi, M. (2016). Structural brain correlates of cognitive and behavioral impairment in MND. *Human brain mapping*, *37*, 1614–1626. doi:10.1002/hbm.23124

Agosta, F., Spinelli, E. G. & Filippi, M. (2018). Neuroimaging in amyotrophic lateral sclerosis: current and emerging uses. *Expert review of neurotherapeutics*, *18*, 395–406. doi:10.1080/14737175.2018.1463160

Albuquerque, M. de, Branco, L. M. T., Rezende, T. J. R., Andrade, H. M. T. de, Nucci, A. & França, M. C. (2017). Longitudinal evaluation of cerebral and spinal cord damage in Amyotrophic Lateral Sclerosis. *NeuroImage Clinical*, *14*, 269–276. doi:10.1016/j.nicl.2017.01.024

Al-Chalabi, A., Hardiman, O., Kiernan, M. C., Chiò, A., Rix-Brooks, B. & van den Berg, L. H. (2016). Amyotrophic lateral sclerosis: moving towards a new classification system. *The Lancet Neurology*, *15*, 1182–1194. doi:10.1016/S1474-4422(16)30199-5

Aralasmak, A., Ulmer, J. L., Kocak, M., Salvan, C. V., Hillis, A. E. & Yousem, D. M. (2006). Association, commissural, and projection pathways and their functional deficit reported in literature. *Journal of computer assisted tomography*, *30*, 695–715. doi:10.1097/01.rct.0000226397.43235.8b

Ashburner, J. & Friston, K. J. (2000). Voxel-based morphometry--the methods. *NeuroImage*, *11*, 805–821. doi:10.1006/nimg.2000.0582

Bede, P., Bokde, A., Elamin, M., Byrne, S., McLaughlin, R. L., Jordan, N.,. . . Hardiman, O. (2013). Grey matter correlates of clinical variables in amyotrophic lateral sclerosis (ALS): a neuroimaging study of ALS motor phenotype heterogeneity and cortical focality. *Journal of neurology, neurosurgery, and psychiatry*, *84*, 766–773. doi:10.1136/jnnp-2012-302674

Bede, P. & Hardiman, O. (2014). Lessons of ALS imaging: Pitfalls and future directions - A critical review. *NeuroImage Clinical*, *4*, 436–443. doi:10.1016/j.nicl.2014.02.011

Bede, P., Querin, G. & Pradat, P.-F. (2018). The changing landscape of motor neuron disease imaging: the transition from descriptive studies to precision clinical tools. *Current opinion in neurology*, *31*, 431–438. doi:10.1097/WCO.0000000000000569

Beeldman, E., Raaphorst, J., Klein Twennaar, M., Visser, M. de, Schmand, B. A. & Haan, R. J. de (2016). The cognitive profile of ALS: a systematic review and meta-analysis update. *Journal of neurology, neurosurgery, and psychiatry*, *87*, 611–619. doi:10.1136/jnnp-2015-310734

Behrens, T. E., Berg, H. J., Jbabdi, S., Rushworth, M. F. & Woolrich, M. W. (2007). Probabilistic diffusion tractography with multiple fibre orientations: What can we gain. *Neuroimage*, *34*(1), 144-155

Benatar, M., Boylan, K., Jeromin, A., Rutkove, S. B., Berry, J., Atassi, N. & Bruijn, L. (2016). ALS biomarkers for therapy development: State of the field and future directions. *Muscle & nerve*, *53*, 169–182. doi:10.1002/mus.24979

Bennett, C. M., Wolford, G. L. & Miller, M. B. (2009). The principled control of false positives in neuroimaging. *Social cognitive and affective neuroscience*, *4*, 417–422. doi:10.1093/scan/nsp053

Bergmann, O., Spalding, K. L. & Frisén, J. (2015). Adult Neurogenesis in Humans. *Cold Spring Harbor perspectives in biology*, *7*. doi:10.1101/cshperspect.a018994

Bhandari, R. & Kuhad, A. (2018). Edaravone: a new hope for deadly amyotrophic lateral sclerosis. *Drugs Today (Barc)*, *54*, 349–360. doi:10.1358/dot.2018.54.6.2828189

Bicchi, I., Emiliani, C., Vescovi, A. & Martino, S. (2015). The Big Bluff of Amyotrophic Lateral Sclerosis Diagnosis: The Role of Neurodegenerative Disease Mimics. *Neuro-degenerative diseases*, *15*, 313–321. doi:10.1159/000435917

Bitar, R., Leung, G., Perng, R., Tadros, S., Moody, A. R., Sarrazin, J.,. . . Roberts, T. P. (2006). MR pulse sequences: what every radiologist wants to know but is afraid to ask. *Radiographics : a review publication of the Radiological Society of North America, Inc*, *26*, 513–537. doi:10.1148/rg.262055063

Borsodi, F., Culea, V., Langkammer, C., Khalil, M., Pirpamer, L., Quasthoff, S.,. . . Ropele, S. (2017). Multimodal assessment of white matter tracts in amyotrophic lateral sclerosis. *PloS one*, *12*. doi:10.1371/journal.pone.0178371

Bozzoni, V. (2016). Amyotrophic lateral sclerosis and environmental factors. *Functional Neurology*, *31*(1), 7-19. doi:10.11138/FNeur/2016.31.1.007

Brettschneider, J., Del Tredici, K., Toledo, J. B., Robinson, J. L., Irwin, D. J., Grossman, M.,. . . Trojanowski, J. Q. (2013). Stages of pTDP-43 pathology in amyotrophic lateral sclerosis. *Annals of neurology*, *74*, 20–38. doi:10.1002/ana.23937

Brooks, B. R. (1994). El Escorial World Federation of Neurology criteria for the diagnosis of amyotrophic lateral sclerosis. Subcommittee on Motor Neuron Diseases/Amyotrophic Lateral Sclerosis of the World Federation of Neurology Research Group on Neuromuscular Diseases and the El Escorial "Clinical limits of amyotrophic lateral sclerosis" workshop contributors. *Journal of the neurological sciences*, *124*, 96–107

Calvo, A. C., Manzano, R., Mendonça, D. M. F., Muñoz, M. J., Zaragoza, P. & Osta, R. (2014). Amyotrophic lateral sclerosis: a focus on disease progression. *BioMed research international*, *2014*, 925101. doi:10.1155/2014/925101

Cardenas-Blanco, A., Machts, J., Acosta-Cabronero, J., Kaufmann, J., Abdulla, S., Kollewe, K.,. . . Nestor, P. J. (2014). Central white matter degeneration in bulbar- and limb-onset amyotrophic lateral sclerosis. *Journal of neurology*, *261*, 1961–1967. doi:10.1007/s00415-014-7434-4

Cardenas-Blanco, A., Machts, J., Acosta-Cabronero, J., Kaufmann, J., Abdulla, S., Kollewe, K.,. . . Nestor, P. J. (2016). Structural and diffusion imaging versus clinical assessment to monitor amyotrophic lateral sclerosis. *NeuroImage Clinical*, *11*, 408–414. doi:10.1016/j.nicl.2016.03.011

Carvalho, T. L., Almeida, L. M. S. de, Lorega, C. M. A., Barata, M. F. O., Ferreira, M. L. B., Brito-Marques, P. R. de & Correia, C. d. C. (2016). Depression and anxiety in individuals with amyotrophic lateral sclerosis: a systematic review. *Trends in psychiatry and psychotherapy*, *38*, 1–5. doi:10.1590/2237-6089-2015-0030

Cedarbaum, J. M., Stambler, N., Malta, E., Fuller, C., Hilt, D., Thurmond, B. & Nakanishi, A. (1999). The ALSFRS-R: a revised ALS functional rating scale that incorporates assessments of respiratory function. BDNF ALS Study Group (Phase III). *Journal of the neurological sciences*, *169*(1-2), 13–21

Chapman, M. C., Jelsone-Swain, L., Johnson, T. D., Gruis, K. L. & Welsh, R. C. (2014). Diffusion tensor MRI of the corpus callosum in amyotrophic lateral sclerosis. *Journal of magnetic resonance imaging*, *39*, 641–647. doi:10.1002/jmri.24218

Charcot, J. M. (1869). Deus cas d'atrophie musculaire progressive avec lesions de la substance grise et des faisceaux antéro-latérale. *Arch Physiol*, *2*, 354–367

Cheah, B. C., Vucic, S., Krishnan, A. V., Boland, R. A. & Kiernan, M. C. (2011). Neurophysiological index as a biomarker for ALS progression: validity of mixed effects models. *Amyotrophic lateral sclerosis: official publication of the World Federation of Neurology Research Group on Motor Neuron Diseases*, *12*, 33–38. doi:10.3109/17482968.2010.531742

Chen, Z. & Ma, L. (2010). Grey matter volume changes over the whole brain in amyotrophic lateral sclerosis: A voxel-wise meta-analysis of voxel based morphometry studies. *Amyotrophic lateral sclerosis: official publication of the World Federation of Neurology Research Group on Motor Neuron Diseases*, *11*, 549–554. doi:10.3109/17482968.2010.516265

Chen, X. & Shang, H.-F. (2015). New developments and future opportunities in biomarkers for amyotrophic lateral sclerosis. *Translational neurodegeneration*, *4*, 17. doi:10.1186/s40035-015-0040-2

Cheung, G., Gawel, M. J., Cooper, P. W., Farb, R. I., Ang, L. C. & Gawal, M. J. (1995). Amyotrophic lateral sclerosis: correlation of clinical and MR imaging findings. *Radiology*, *194*, 263–270. doi:10.1148/radiology.194.1.7997565

Chiò, A., Logroscino, G., Hardiman, O., Swingler, R., Mitchell, D., Beghi, E. & Traynor, B. G. (2009). Prognostic factors in ALS: A critical review. *Amyotrophic lateral sclerosis : official publication of the World Federation of Neurology Research Group on Motor Neuron Diseases*, *10*, 310–323

Chiò, A., Calvo, A., Moglia, C., Mazzini, L. & Mora, G. (2011). Phenotypic heterogeneity of amyotrophic lateral sclerosis: a population based study. *Journal of neurology, neurosurgery, and psychiatry*, *82*, 740–746. doi:10.1136/jnnp.2010.235952

Chiò, A., Pagani, M., Agosta, F., Calvo, A., Cistaro, A. & Filippi, M. (2014). Neuroimaging in amyotrophic lateral sclerosis: insights into structural and functional changes. *The Lancet Neurology*, *13*, 1228–1240. doi:10.1016/S1474-4422(14)70167-X

Chiò, A., Mora, G. & Lauria, G. (2017). Pain in amyotrophic lateral sclerosis. *The Lancet Neurology*, *16*, 144–157. doi:10.1016/S1474-4422(16)30358-1

Chou, S. M. & Norris, F. H. (1993). Amyotrophic lateral sclerosis: lower motor neuron disease spreading to upper motor neurons. *Muscle & nerve*, *16*, 864–869. doi:10.1002/mus.880160810

Christidi, F., Karavasilis, E., Ferentinos, P., Xirou, S., Velonakis, G., Rentzos, M.,. . . Evdokimidis, I. (2018). Investigating the neuroanatomical substrate of pathological laughing and crying in amyotrophic lateral sclerosis with multimodal neuroimaging techniques. *Amyotrophic lateral sclerosis & frontotemporal degeneration*, *19*, 12–20. doi:10.1080/21678421.2017.1386689

Ciccarelli, O., Behrens, T. E., Altmann, D. R., Orrell, R. W., Howard, R. S., Johansen-Berg, H.,. . . Thompson, A. J. (2006). Probabilistic diffusion tractography: a potential tool to assess the rate of disease progression in amyotrophic lateral sclerosis. *Brain*, *129*, 1859–1871. doi:10.1093/brain/awl100

Cohen-Adad, J., Mendili, M.-M. E., Morizot-Koutlidis, R., Lehéricy, S., Meininger, V., Blancho, S.,. . . Pradat, P.-F. (2013). Involvement of spinal sensory pathway in ALS and specificity of cord atrophy to lower motor neuron degeneration. *Amyotrophic Lateral Sclerosis and Frontotemporal Degeneration*, *14*, 30–38. doi:10.3109/17482968.2012.701308

Corcia, P., Pradat, P.-F., Salachas, F., Bruneteau, G., Le Forestier, N., Seilhean, D.,. . . Meininger, V. (2008). Causes of death in a post-mortem series of ALS patients. *Amyotrophic lateral sclerosis : official publication of the World Federation of Neurology Research Group on Motor Neuron Diseases*, *9*, 59–62. doi:10.1080/17482960701656940

Cosottini, M., Giannelli, M., Siciliano, G., Lazzarotti, G., Michelassi, M. C., Del Corona, A., Bartolozzi, C. & Murri, L. (2005). Diffusion-tensor MR imaging of corticospinal tract in amyotrophic lateral sclerosis and progressive muscular atrophy. *Radiology, 237*(1), 258-264.

Cosottini, M., Cecchi, P., Piazza, S., Pesaresi, I., Fabbri, S., Diciotti, S.,. . . Bonuccelli, U. (2013). Mapping cortical degeneration in ALS with magnetization transfer ratio and voxel-based morphometry. *PloS one*, *8*, e68279. doi:10.1371/journal.pone.0068279

Cosottini, M., Donatelli, G., Costagli, M., Caldarazzo Ienco, E., Frosini, D., Pesaresi, I.,. . . Tosetti, M. (2016). High-Resolution 7T MR Imaging of the Motor Cortex in Amyotrophic Lateral Sclerosis. *American journal of neuroradiology*, *37*, 455–461. doi:10.3174/ajnr.A4562

Costa, J., Swash, M. & Carvalho, M. de. (2012). Awaji criteria for the diagnosis of amyotrophic lateral sclerosis:a systematic review. *Archives of neurology*, *69*, 1410–1416. doi:10.1001/archneurol.2012.254

da Rocha, A. J., Oliveira, A. S. B., Fonseca, R. B., Maia, A. C. M., Buainain, R. P. & Lederman, H. M. (2004). Detection of corticospinal tract compromise in amyotrophic lateral sclerosis with brain MR imaging: relevance of the T1-weighted spin-echo magnetization transfer contrast sequence. *American journal of neuroradiology*, *25*(9), 1509–1515

Descoteaux, M., Deriche, R., Knösche, T. R. & Anwander, A. (2009). Deterministic and probabilistic tractography based on complex fibre orientation distributions. *IEEE transactions on medical imaging*, *28*, 269–286

Desikan, R. S., Ségonne, F., Fischl, B., Quinn, B. T., Dickerson, B. C., Blacker, D.,. . . Killiany, R. J. (2006). An automated labeling system for subdividing the human cerebral cortex on MRI scans into gyral based regions of interest. *NeuroImage*, *31*, 968–980. doi:10.1016/j.neuroimage.2006.01.021

Dorst, J., Ludolph, A. C. & Huebers, A. (2018). Disease-modifying and symptomatic treatment of amyotrophic lateral sclerosis. *Therapeutic advances in neurological disorders*, *11*, 1756285617734734. doi:10.1177/1756285617734734

Douaud, G., Filippini, N., Knight, S., Talbot, K. & Turner, M. R. (2011). Integration of structural and functional magnetic resonance imaging in amyotrophic lateral sclerosis. *Brain*, *134*, 3470–3479. doi:10.1093/brain/awr279

Dubois, B., Slachevsky, A., Litvan, I. & Pillon, B. (2000). The FAB: a Frontal Assessment Battery at bedside. *Neurology*, *55*(11), 1621–1626

Duning, T., Schiffbauer, H., Warnecke, T., Mohammadi, S., Floel, A., Kolpatzik, K.,. . . Schäbitz, W. R. (2011). G-CSF prevents the progression of structural disintegration of white matter tracts in amyotrophic lateral sclerosis: a pilot trial. *PloS one*, *6*. doi:10.1371/journal.pone.0017770

Egger, C., Opfer, R., Wang, C., Kepp, T., Sormani, M. P., Spies, L.,. . . Schippling, S. (2016). MRI FLAIR lesion segmentation in multiple sclerosis: Does automated segmentation hold up with manual annotation? *NeuroImage Clinical*, *13*, 264–270. doi:10.1016/j.nicl.2016.11.020

Eisen, A., Kiernan, M., Mitsumoto, H. & Swash, M. (2014). Amyotrophic lateral sclerosis: a long preclinical period? *Journal of neurology, neurosurgery, and psychiatry*, *85*, 1232–1238. doi:10.1136/jnnp-2013-307135

Ellis, C. M., Simmons, A., Jones, D. K., Bland, J., Dawson, J. M., Horsfield, M. A.,. . . Leigh, P. N. (1999). Diffusion tensor MRI assesses corticospinal tract damage in ALS. *Neurology*, *53*(5), 1051–1058

Ellis, C. M., Suckling, J., Amaro, E., Bullmore, E. T., Simmons, A., Williams, S. C. & Leigh, P. N. (2001). Volumetric analysis reveals corticospinal tract degeneration and extramotor involvement in ALS. *Neurology*, *57*(9), 1571–1578

Escorcio-Bezerra, M. L., Abrahao, A., Castro, I. de, Chieia, M. A. T., Azevedo, L. A. de, Pinheiro, D. S.,. . . Manzano, G. M. (2016). MUNIX: Reproducibility and clinical correlations in Amyotrophic Lateral Sclerosis. *Clinical neurophysiology*, *127*, 2979–2984. doi:10.1016/j.clinph.2016.06.011

Fabes, J., Matthews, L., Filippini, N., Talbot, K., Jenkinson, M. & Turner, M. R. (2017). Quantitative FLAIR MRI in Amyotrophic Lateral Sclerosis. *Academic radiology*, *24*, 1187–1194. doi:10.1016/j.acra.2017.04.008

Ferraro, P. M., Agosta, F., Riva, N., Copetti, M., Spinelli, E. G., Falzone, Y.,. . . Filippi, M. (2017). Multimodal structural MRI in the diagnosis of motor neuron diseases. *NeuroImage Clinical*, *16*, 240–247. doi:10.1016/j.nicl.2017.08.002

Filippi, M., Agosta, F., Grosskreutz, J., Benatar, M., Kassubek, J., Verstraete, E. & Turner, M. R. (2015). Progress towards a neuroimaging biomarker for amyotrophic lateral sclerosis. *The Lancet Neurology*, *14*, 786–788. doi:10.1016/S1474-4422(15)00134-9

Filippini, N., Douaud, G., Mackay, C. E., Knight, S., Talbot, K. & Turner, M. R. (2010). Corpus callosum involvement is a consistent feature of amyotrophic lateral sclerosis. *Neurology*, *75*, 1645–1652. doi:10.1212/WNL.0b013e3181fb84d1

Fineberg, N. A., Haddad, P. M., Carpenter, L., Gannon, B., Sharpe, R., Young, A. H.,. . . Sahakian, B. J. (2013). The size, burden and cost of disorders of the brain in the UK. *Journal of psychopharmacology*, *27*, 761–770. doi:10.1177/0269881113495118

Fischl, B., Sereno, M. I., Tootell, R. B. & Dale, A. M. (1999). High-resolution intersubject averaging and a coordinate system for the cortical surface. *Human brain mapping*, *8*(4), 272–284

Fischl, B. & Dale, A. M. (2000). Measuring the thickness of the human cerebral cortex from magnetic resonance images. *Proceedings of the National Academy of Sciences of the United States of America*, *97*, 11050–11055. doi:10.1073/pnas.200033797

Fischl, B., Salat, D. H., Busa, E., Albert, M., Dieterich, M., Haselgrove, C.,. . . Dale, A. M. (2002). Whole brain segmentation: automated labeling of neuroanatomical structures in the human brain. *Neuron*, *33*(3), 341–355

Fox, R. J., Sakaie, K., Lee, J.-C., Debbins, J. P., Liu, Y., Arnold, D. L.,. . . Fisher, E. (2012). A validation study of multicenter diffusion tensor imaging: reliability of fractional anisotropy and diffusivity values. *American journal of neuroradiology*, *33*, 695–700. doi:10.3174/ajnr.A2844

Garbuzova-Davis, S., Thomson, A., Kurien, C., Shytle, R. D. & Sanberg, P. R. (2016). Potential new complication in drug therapy development for amyotrophic lateral sclerosis. *Expert review of neurotherapeutics*, *16*, 1397–1405. doi:10.1080/14737175.2016.1207530

Gawne-Cain, M. L., Silver, N. C., Moseley, I. F. & Miller, D. H. (1997). Fast FLAIR of the brain: the range of appearances in normal subjects and its application to quantification of white-matter disease. *Neuroradiology*, *39*, 243–249. doi:10.1007/s002340050402

Goldstein, L. H. & Abrahams, S. (2013). Changes in cognition and behaviour in amyotrophic lateral sclerosis: nature of impairment and implications for assessment. *The Lancet Neurology*, *12*, 368–380

Gooch, C. L., Doherty, T. J., Chan, K. M., Bromberg, M. B., Lewis, R. A., Stashuk, D. W.,. . . Daube, J. R. (2014). Motor unit number estimation: a technology and literature review. *Muscle & nerve*, *50*, 884–893. doi:10.1002/mus.24442

Gordon, P. H., Miller, R. G. & Moore, D. H. (2004). ALSFRS-R. *Amyotrophic lateral sclerosis and other motor neuron disorders : official publication of the World Federation of Neurology, Research Group on Motor Neuron Diseases*, *5*, 90–93. doi:10.1080/17434470410019906

Grad, L. I., Rouleau, G. A., Ravits, J. & Cashman, N. R. (2017). Clinical Spectrum of Amyotrophic Lateral Sclerosis (ALS). *Cold Spring Harbor perspectives in medicine*, *7*. doi:10.1101/cshperspect.a024117

Gramsch, C., Nensa, F., Kastrup, O., Maderwald, S., Deuschl, C., Ringelstein, A.,. . . Schlamann, M. (2015). Diagnostic value of 3D fluid attenuated inversion recovery sequence in multiple sclerosis. *Acta radiologica*, *56*, 622–627. doi:10.1177/0284185114534413

Grassinger, J., Khomenko, A., Hart, C., Baldaranov, D., Johannesen, S. W., Mueller, G.,. . . Bogdahn, U. (2014). Safety and feasibility of long term administration of recombinant human granulocyte-colony stimulating factor in patients with amyotrophic lateral sclerosis. *Cytokine*, *67*, 21–28. doi:10.1016/j.cyto.2014.02.003

Grimaldi, S., Duprat, L., Grapperon, A.-M., Verschueren, A., Delmont, E. & Attarian, S. (2017). Global motor unit number index sum score for assessing the loss of lower motor neurons in amyotrophic lateral sclerosis. *Muscle & nerve*, *56*, 202–206. doi:10.1002/mus.25595

Grimm, T. & Schulte-Mattler, W. (2017). Update – Neurophysiologische Methoden zur Bestimmung der Anzahl motorischer Einheiten in menschlichen Muskeln. *Klinische Neurophysiologie*, *48*, 144–150. doi:10.1055/s-0043-115149

Grolez, G., Moreau, C., Danel-Brunaud, V., Delmaire, C., Lopes, R., Pradat, P. F.,. . . Devos, D. (2016). The value of magnetic resonance imaging as a biomarker for amyotrophic lateral sclerosis: a systematic review. *BMC neurology*, *16*, 155. doi:10.1186/s12883-016-0672-6

Grosskreutz, J., Kaufmann, J., Frädrich, J., Dengler, R., Heinze, H.-J. & Peschel, T. (2006). Widespread sensorimotor and frontal cortical atrophy in Amyotrophic Lateral Sclerosis. *BMC neurology*, *6*, 17. doi:10.1186/1471-2377-6-17

Grover, V. P. B., Tognarelli, J. M., Crossey, M. M. E., Cox, I. J., Taylor-Robinson, S. D. & McPhail, M. J. W. (2015). Magnetic Resonance Imaging: Principles and Techniques: Lessons for Clinicians. *Journal of clinical and experimental hepatology*, *5*, 246–255. doi:10.1016/j.jceh.2015.08.001

Gupta, A., Nguyen, T. B., Chakraborty, S. & Bourque, P. R. (2014). Accuracy of Conventional MRI in ALS. *Canadian Journal of Neurological Sciences*, *41*(1), 53–57

Hajnal, J. V., Bryant, D. J., Kasuboski, L., Pattany, P. M., Coene, B. de, Lewis, P. D.,. . . Bydder, G. M. (1992). Use of fluid attenuated inversion recovery (FLAIR) pulse sequences in MRI of the brain. *Journal of computer assisted tomography*, *16*(6), 841–844

Hajnal, J. V., Oatridge, A., Herlihy, A. H. & Bydder, G. M. (2001). Reduction of CSF artifacts on FLAIR images by using adiabatic inversion pulses. *AJNR. American journal of neuroradiology*, *22*(2), 317–322

Hardiman, O., Al-Chalabi, A., Brayne, C., Beghi, E., van den Berg, L. H., Chiò, A.,. . . Rooney, J. (2017). The changing picture of amyotrophic lateral sclerosis: lessons from European registers. *Journal of neurology, neurosurgery, and psychiatry*, *88*, 557–563. doi:10.1136/jnnp-2016-314495

Hecht, M. J., Fellner, F., Fellner, C., Hilz, M. J., Heuss, D. & Neundörfer, B. (2001). MRI-FLAIR images of the head show corticospinal tract alterations in ALS patients more frequently than T2-, T1- and proton-density-weighted images. *Journal of the neurological sciences*, *186*(1-2), 37–44

Hecht, M. J., Fellner, F., Fellner, C., Hilz, M. J., Neundörfer, B. & Heuss, D. (2002). Hyperintense and hypointense MRI signals of the precentral gyrus and corticospinal tract in ALS: a follow-up examination including FLAIR images. *Journal of the neurological sciences*, *199*(1-2), 59–65

Heimrath, J., Gorges, M., Kassubek, J., Müller, H.-P., Birbaumer, N., Ludolph, A. C. & Lulé, D. (2014). Additional resources and the default mode network: Evidence of increased connectivity and decreased white matter integrity in amyotrophic lateral sclerosis. *Amyotrophic lateral sclerosis & frontotemporal degeneration*, *15*, 537–545. doi:10.3109/21678421.2014.911914

Hogden, A., Foley, G., Henderson, R. D., James, N. & Aoun, S. M. (2017). Amyotrophic lateral sclerosis: improving care with a multidisciplinary approach. *Journal of multidisciplinary healthcare*, *10*, 205–215. doi:10.2147/JMDH.S134992

Hollingsworth, K. G. (2015). Reducing acquisition time in clinical MRI by data undersampling and compressed sensing reconstruction. *Physics in medicine and biology*, *60*, 297-322. doi:10.1088/0031-9155/60/21/R297

Hrastelj, J. & Robertson, N. P. (2016). Ice bucket challenge bears fruit for amyotrophic lateral sclerosis. *Journal of neurology*, *263*, 2355–2357. doi:10.1007/s00415-016-8297-7

Huynh, W., Simon, N. G., Grosskreutz, J., Turner, M. R., Vucic, S. & Kiernan, M. C. (2016). Assessment of the upper motor neuron in amyotrophic lateral sclerosis. *Clinical neurophysiology*, *127*, 2643–2660. doi:10.1016/j.clinph.2016.04.025

Ignjatović, A., Stević, Z., Lavrnić, S., Daković, M. & Bačić, G. (2013). Brain iron MRI: a biomarker for amyotrophic lateral sclerosis. *Journal of magnetic resonance imaging*, *38*, 1472–1479. doi:10.1002/jmri.24121

Ingre, C., Roos, P. M., Piehl, F., Kamel, F. & Fang, F. (2015). Risk factors for amyotrophic lateral sclerosis. *Clinical epidemiology*, *7*, 181–193. doi:10.2147/CLEP.S37505

Ishikawa, K., Nagura, H., Yokota, T. & Yamanouchi, H. (1993). Signal loss in the motor cortex on magnetic resonance images in amyotrophic lateral sclerosis. *Annals of neurology*, *33*(2), 218–222

Iwata, N. K., Kwan, J. Y., Danielian, L. E., Butman, J. A., Tovar-Moll, F., Bayat, E. & Floeter, M. K. (2011). White matter alterations differ in primary lateral sclerosis and amyotrophic lateral sclerosis. *Brain*, *134*, 2642–2655. doi:10.1093/brain/awr178

Ivanhoe, C. B. & Reistetter, T. A. (2004). Spasticity: the misunderstood part of the upper motor neuron syndrome. *American journal of physical medicine & rehabilitation*, *83*(10), 3-9

Jin, J., Hu, F., Zhang, Q., Jia, R. & Dang, J. (2016). Hyperintensity of the corticospinal tract on FLAIR: A simple and sensitive objective upper motor neuron degeneration marker in clinically verified amyotrophic lateral sclerosis. *Journal of the neurological sciences*, *367*, 177–183. doi:10.1016/j.jns.2016.06.005

Karlsborg, M., Rosenbaum, S., Wiegell, M., Simonsen, H., Larsson, H., Werdelin, L. & Gredal, O. (2004). Corticospinal tract degeneration and possible pathogenesis in ALS evaluated by MR diffusion tensor imaging. *Amyotrophic lateral sclerosis and other motor neuron disorders*, *5*, 136–140. doi:10.1080/14660820410018982

Kassubek, J., Müller, H.-P., Del Tredici, K., Brettschneider, J., Pinkhardt, E. H., Lulé, D.,. . . Ludolph, A. C. (2014). Diffusion tensor imaging analysis of sequential spreading of disease in amyotrophic lateral sclerosis confirms patterns of TDP-43 pathology. *Brain*, *137*, 1733–1740. doi:10.1093/brain/awu090

Kassubek, J., Müller, H.-P., Del Tredici, K., Lulé, D., Gorges, M., Braak, H. & Ludolph, A. C. (2017). Imaging the pathoanatomy of amyotrophic lateral sclerosis in vivo: targeting a propagation-based biological marker. *Journal of neurology, neurosurgery, and psychiatry*, *89*, 374–381. doi:10.1136/jnnp-2017-316365

Keil, C., Prell, T., Peschel, T., Hartung, V., Dengler, R. & Grosskreutz, J. (2012). Longitudinal diffusion tensor imaging in amyotrophic lateral sclerosis. *BMC Neuroscience*, *13*, 141. doi:10.1186/1471-2202-13-141

Kiernan, M. C., Vucic, S., Cheah, B. C., Turner, M. R., Eisen, A., Hardiman, O.,. . . Zoing, M. C. (2011). Amyotrophic lateral sclerosis. *The Lancet*, *377*, 942–955. doi:10.1016/S0140-6736(10)61156-7

Klistorner, A., Wang, C., Yiannikas, C., Graham, S. L., Parratt, J. & Barnett, M. H. (2016). Progressive Injury in Chronic Multiple Sclerosis Lesions Is Gender-Specific: A DTI Study. *PloS one*, *11*, e0149245. doi:10.1371/journal.pone.0149245

Krupa, K. & Bekiesińska-Figatowska, M. (2015). Artifacts in Magnetic Resonance Imaging. *Polish journal of radiology*, *80*, 93–106. doi:10.12659/PJR.892628

Kuipers-Upmeijer, J., Jager, A. E. de, Hew, J. M., Snoek, J. W. & van Weerden, T. W. (2001). Primary lateral sclerosis: clinical, neurophysiological, and magnetic resonance findings. *Journal of neurology, neurosurgery, and psychiatry*, *71*(5), 615–620

Kwan, J. Y., Meoded, A., Danielian, L. E., Wu, T. & Floeter, M. K. (2012). Structural imaging differences and longitudinal changes in primary lateral sclerosis and amyotrophic lateral sclerosis. *NeuroImage Clinical*, *2*, 151–160. doi:10.1016/j.nicl.2012.12.003

Larson, T. C., Kaye, W., Mehta, P. & Horton, D. K. (2018). Amyotrophic Lateral Sclerosis Mortality in the United States, 2011-2014. *Neuroepidemiology*, *51*, 96-103

Lee, S. & Kim, H.-J. (2015). Prion-like Mechanism in Amyotrophic Lateral Sclerosis: are Protein Aggregates the Key? *Experimental neurobiology*, *24*, 1–7. doi:10.5607/en.2015.24.1.1

Lillo, P., Mioshi, E., Burrell, J. R., Kiernan, M. C., Hodges, J. R. & Hornberger, M. (2012). Grey and white matter changes across the amyotrophic lateral sclerosis-frontotemporal dementia continuum. *PloS one*, *7*, e43993. doi:10.1371/journal.pone.0043993

Lombardo, F., Frijia, F., Bongioanni, P., Canapicchi, R., Minichilli, F., Bianchi, F., Hlavata, H., Rossi, B. & Montanaro, D. (2009). Diffusion Tensor MRI and MR Spectroscopy in long lasting upper motor neuron involvement in Amyotrophic Lateral Sclerosis. *Achives Italiennes de Biologie*, *147*, 69-82

Ludolph, A. C. & Brettschneider, J. (2015). TDP-43 in amyotrophic lateral sclerosis - is it a prion disease? *European journal of neurology*, *22*, 753–761. doi:10.1111/ene.12706

Ludolph, A., Drory, V., Hardiman, O., Nakano, I., Ravits, J., Robberecht, W. & Shefner, J. (2015). A revision of the El Escorial criteria - 2015. *Amyotrophic lateral sclerosis & frontotemporal degeneration*, *16*, 291–292. doi:10.3109/21678421.2015.1049183

Lulé, D., Burkhardt, C., Abdulla, S., Böhm, S., Kollewe, K., Uttner, I.,. . . Ludolph, A. C. (2015). The Edinburgh Cognitive and Behavioural Amyotrophic Lateral Sclerosis Screen: a cross-sectional comparison of established screening tools in a German-Swiss population. *Amyotrophic lateral sclerosis & frontotemporal degeneration*, *16*, 16–23. doi:10.3109/21678421.2014.959451

Maniam, S. & Szklaruk, J. (2010). Magnetic resonance imaging: Review of imaging techniques and overview of liver imaging. *World journal of radiology*, *2*, 309–322. doi:10.4329/wjr.v2.i8.309

McMahon, K. L., Cowin, G. & Galloway, G. (2011). Magnetic resonance imaging: the underlying principles. *The Journal of orthopaedic and sports physical therapy*, *41*, 806–819. doi:10.2519/jospt.2011.3576

Meadowcroft, M. D., Mutic, N. J., Bigler, D. C., Wang, J.-L., Simmons, Z., Connor, J. R. & Yang, Q. X. (2015). Histological-MRI correlation in the primary motor cortex of patients with amyotrophic lateral sclerosis. *Journal of magnetic resonance imaging*, *41*, 665–675. doi:10.1002/jmri.24582

Menke, R. A. L., Abraham, I., Thiel, C. S., Filippini, N., Knight, S., Talbot, K. & Turner, M. R. (2012). Fractional anisotropy in the posterior limb of the internal capsule and prognosis in amyotrophic lateral sclerosis. *Archives of neurology*, *69*, 1493–1499. doi:10.1001/archneurol.2012.1122

Menke, R.A.L., Proudfoot, M., Talbot, K. & Turner, M. R. (2017). The two-year progression of structural and functional cerebral MRI in amyotrophic lateral sclerosis. *NeuroImage Clinical*, *17*, 953–961. doi:10.1016/j.nicl.2017.12.025

Metwalli, N. S., Benatar, M., Nair, G., Usher, S., Hu, X. & Carew, J. D. (2010). Utility of axial and radial diffusivity from diffusion tensor MRI as markers of neurodegeneration in amyotrophic lateral sclerosis. *Brain research*, *1348*, 156–164. doi:10.1016/j.brainres.2010.05.067

Meyer, J. R., Roychowdhury, S., Russell, E. J., Callahan, C., Gitelman, D. & Mesulam, M. M. (1996). Location of the central sulcus via cortical thickness of the precentral and postcentral gyri on MR. *American journal of neuroradiology*, *17*(9), 1699–1706

Mezzapesa, D. M., Ceccarelli, A., Dicuonzo, F., Carella, A., Caro, M. F. de, Lopez, M.,. . . Simone, I. L. (2007). Whole-brain and regional brain atrophy in amyotrophic lateral sclerosis. *American journal of neuroradiology*, *28*(2), 255–259

Mezzapesa, D. M., D'Errico, E., Tortelli, R., Distaso, E., Cortese, R., Tursi, M.,. . . Simone, I. L. (2013). Cortical thinning and clinical heterogeneity in amyotrophic lateral sclerosis. *PloS one*, *8*, e80748. doi:10.1371/journal.pone.0080748

Miller, R. G., Mitchell, J. D. & Moore, D. H. (2012). Riluzole for amyotrophic lateral sclerosis (ALS)/motor neuron disease (MND). *Cochrane Database Syst Rev*, *14*(3), 1465-1858

Mitchell, J. D. & Borasio, G. D. (2007). Amyotrophic lateral sclerosis. *The Lancet*, *369*, 2031–2041. doi:10.1016/S0140-6736(07)60944-1

Mitsumoto, H., Ulug, A. M., Pullman, S. L., Gooch, C. L., Chan, S., Tang, M.-X.,. . . Shungu, D. C. (2007). Quantitative objective markers for upper and lower motor neuron dysfunction in ALS. *Neurology*, *68*, 1402–1410. doi:10.1212/01.wnl.0000260065.57832.87

Mitsumoto, H., Brooks, B. R. & Silani, V. (2014). Clinical trials in amyotrophic lateral sclerosis: why so many negative trials and how can trials be improved? *The Lancet Neurology*, *13*, 1127–1138. doi:10.1016/S1474-4422(14)70129-2

Mohammadi, B., Kollewe, K., Samii, A., Dengler, R. & Münte, T. F. (2011). Functional neuroimaging at different disease stages reveals distinct phases of neuroplastic changes in amyotrophic lateral sclerosis. *Human brain mapping*, *32*, 750–758

Morgan, S. & Orrell, R. W. (2016). Pathogenesis of amyotrophic lateral sclerosis. *British medical bulletin*, *119*, 87–98. doi:10.1093/bmb/ldw026

Mori, S., Oishi, K., Jiang, H., Jiang, L., Li, X., Akhter, K.,. . . Mazziotta, J. (2008). Stereotaxic White Matter Atlas Based on Diffusion Tensor Imaging in an ICBM Template. *NeuroImage*, *40*, 570–582. doi:10.1016/j.neuroimage.2007.12.035

Muscolino, J. E. (2014). *Kinesiology: The Skeletal System and Muscle* Function (2nd ed.). NET Developers Series. London: Elsevier Health Sciences.

Nagel, G., Unal, H., Rosenbohm, A., Ludolph, A. C. & Rothenbacher, D. (2013). Implementation of a population-based epidemiological rare disease registry: study protocol of the amyotrophic lateral sclerosis (ALS)--registry Swabia. *BMC neurology*, *13*, 22. doi:10.1186/1471-2377-13-22

Nair, G., Carew, J. D., Usher, S., Lu, D., Hu, X. P. & Benatar, M. (2010). Diffusion tensor imaging reveals regional differences in the cervical spinal cord in amyotrophic lateral sclerosis. *NeuroImage*, *53*, 576–583. doi:10.1016/j.neuroimage.2010.06.060

Nasreddine, Z. S., Phillips, N. A., Bédirian, V., Charbonneau, S., Whitehead, V., Collin, I.,. . . Chertkow, H. (2005). The Montreal Cognitive Assessment, MoCA: a brief screening tool for mild cognitive impairment. *Journal of the American Geriatrics Society*, *53*, 695–699. doi:10.1111/j.1532-5415.2005.53221.x

Nefussy, B., Artamonov, I., Deutsch, V., Naparstek, E., Nagler, A. & Drory, V. E. (2010). Recombinant human granulocyte-colony stimulating factor administration for treating amyotrophic lateral sclerosis: A pilot study. *Amyotrophic lateral sclerosis : official publication of the World Federation of Neurology Research Group on Motor Neuron Diseases*, *11*, 187–193. doi:10.3109/17482960902933809

Neuwirth, C., Barkhaus, P. E., Burkhardt, C., Castro, J., Czell, D., Carvalho, M. de,. . . Weber, M. (2015). Tracking motor neuron loss in a set of six muscles in amyotrophic lateral sclerosis using the Motor Unit Number Index (MUNIX): a 15-month longitudinal multicentre trial. *Journal of neurology, neurosurgery, and psychiatry*, *86*, 1172–1179. doi:10.1136/jnnp-2015-310509

Neuwirth, C., Barkhaus, P. E., Burkhardt, C., Castro, J., Czell, D., Carvalho, M. de,. . . Weber, M. (2017). Motor Unit Number Index (MUNIX) detects motor neuron loss in pre-symptomatic muscles in Amyotrophic Lateral Sclerosis. *Clinical neurophysiology*, *128*, 495–500. doi:10.1016/j.clinph.2016.11.026

Ngai, S., Tang, Y. M., Du, L. & Stuckey, S. (2007). Hyperintensity of the precentral gyral subcortical white matter and hypointensity of the precentral gyrus on fluid-attenuated inversion recovery: variation with age and implications for the diagnosis of amyotrophic lateral sclerosis. *American journal of neuroradiology*, *28*(2), 250–254

Ohta, Y., Sato, K., Takemoto, M., Takahashi, Y., Morihara, R., Nakano, Y.,. . . Abe, K. (2017). Behavioral and affective features of amyotrophic lateral sclerosis patients. *Journal of the neurological sciences*, *381*, 119–125

Omer, T., Finegan, E., Hutchinson, S., Doherty, M., Vajda, A., McLaughlin, R. L., Pender, N., Hardiman, O., Bede, P. (2017). Neuroimaging patterns along the ALS-FTD spectrum: a multiparametric imaging study. *Amyotroph Lateral Scler Frontotemporal Degener*, *18*, 611-623

Orban, P., Devon, R. S., Hayden, M. R. & Leavitt, B. R. (2007). Chapter 15 Juvenile amyotrophic lateral sclerosis. *Handbook of clinical neurology*, *82*, 301–312. doi:10.1016/S0072-9752(07)80018-2

Parson, S. H. (2014). The singular qualities of motor neurones in health and disease. *Journal of anatomy*, *224*, 1–2. doi:10.1111/joa.12110

Paulukonis, S. T., Roberts, E. M., Valle, J. P., Collins, N. N., English, P. B. & Kaye, W. E. (2015). Survival and Cause of Death among a Cohort of Confirmed Amyotrophic Lateral Sclerosis Cases. *PLoS One*, *10*(7). doi:10.1371/journal.pone.0131965

Peretti-Viton, P., Azulay, J. P., Trefouret, S., Brunel, H., Daniel, C., Viton, J. M.,. . . Salamon, G. (1999). MRI of the intracranial corticospinal tracts in amyotrophic and primary lateral sclerosis. *Neuroradiology*, *41*(10), 744–749

Pfefferbaum, A., Adalsteinsson, E., Rohlfing, T. & Sullivan, E. V. (2008). Diffusion tensor imaging of deep gray matter brain structures: Effects of age and iron concentration. *Neurobiology of aging*, *31*, 482. doi:10.1016/j.neurobiolaging.2008.04.013

Pitzer, C., Krüger, C., Plaas, C., Kirsch, F., Dittgen, T., Müller, R.,. . . Schneider, A. (2008). Granulocyte-colony stimulating factor improves outcome in a mouse model of amyotrophic lateral sclerosis. *Brain*, *131*, 3335–3347. doi:10.1093/brain/awn243

Pizzimenti, A., Gori, M. C., Onesti, E., John, B. & Inghilleri, M. (2015). Communication of diagnosis in amyotrophic lateral sclerosis: stratification of patients for the estimation of the individual needs. *Frontiers in Psychology*, *6*. doi:10.3389/fpsyg.2015.00745

Plewes, D. B. & Kucharczyk, W. (2012). Physics of MRI: a primer. *Journal of magnetic resonance imaging*, *35*, 1038–1054. doi:10.1002/jmri.23642

Poujois, A., Schneider, F. C., Faillenot, I., Camdessanché, J.-P., Vandenberghe, N., Thomas-Antérion, C. & Antoine, J.-C. (2013). Brain plasticity in the motor network is correlated with disease progression in amyotrophic lateral sclerosis. *Human brain mapping*, *34*, 2391–2401. doi:10.1002/hbm.22070

Protogerou, G., Ralli, S., Tsougos, I., Patramani, I., Hadjigeorgiou, G., Fezoulidis, I. & Kapsalaki, E. Z. (2011). T2 FLAIR Increased Signal Intensity at the Posterior Limb of the Internal Capsule: Clinical Significance in ALS Patients. *The neuroradiology journal*, *24*, 226–234. doi:10.1177/197140091102400210

Prudlo, J., Bißbort, C., Glass, A., Grossmann, A., Hauenstein, K., Benecke, R. & Teipel, S. J. (2012). White matter pathology in ALS and lower motor neuron ALS variants: a diffusion tensor imaging study using tract-based spatial statistics. *Journal of neurology*, *259*, 1848–1859. doi:10.1007/s00415-012-6420-y

Pupillo, E., Messina, P., Logroscino, G. & Beghi, E. (2014). Long-term survival in amyotrophic lateral sclerosis: a population-based study. *Annals of neurology*, *75*, 287–297. doi:10.1002/ana.24096

Ravits, J., Appel, S., Baloh, R. H., Barohn, R., Brooks, B. R., Elman, L.,. . . Ringel, S. (2013). Deciphering amyotrophic lateral sclerosis: what phenotype, neuropathology and genetics are telling us about pathogenesis. *Amyotrophic lateral sclerosis & frontotemporal degeneration*, *14*, 5–18. doi:10.3109/21678421.2013.778548

Riva, N., Agosta, F., Lunetta, C., Filippi, M. & Quattrini, A. (2016). Recent advances in amyotrophic lateral sclerosis. *Journal of neurology*, *263*, 1241–1254. doi:10.1007/s00415-016-8091-6

Roccatagliata, L., Bonzano, L., Mancardi, G., Canepa, C. & Caponnetto, C. (2009). Detection of motor cortex thinning and corticospinal tract involvement by quantitative MRI in amyotrophic lateral sclerosis. *Amyotrophic lateral sclerosis : official publication of the World Federation of Neurology Research Group on Motor Neuron Diseases*, *10*, 47–52. doi:10.1080/17482960802267530

Rosenfeld, J. & Strong, M. J. (2015). Challenges in the Understanding and Treatment of Amyotrophic Lateral Sclerosis/Motor Neuron Disease. *Neurotherapeutics*, *12*, 317–325. doi:10.1007/s13311-014-0332-8

Rutkove, S. B. (2015). Clinical Measures of Disease Progression in Amyotrophic Lateral Sclerosis. *Neurotherapeutics*, *12*, 384–393. doi:10.1007/s13311-014-0331-9

Sach, M., Winkler, G., Glauche, V., Liepert, J., Heimbach, B., Koch, M. A.,. . . Weiller, C. (2004). Diffusion tensor MRI of early upper motor neuron involvement in amyotrophic lateral sclerosis. *Brain*, *127*, 340–350. doi:10.1093/brain/awh041

Sage, C. A., Peeters, R. R., Görner, A., Robberecht, W. & Sunaert, S. (2007). Quantitative diffusion tensor imaging in amyotrophic lateral sclerosis. *NeuroImage*, *34*, 486–499. doi:10.1016/j.neuroimage.2006.09.025

Sahin, N., Mohan, S., Maralani, P. J., Duddukuri, S., O'Rourke, D. M., Melhem, E. R. & Wolf, R. L. (2016). Assignment Confidence in Localization of the Hand Motor Cortex: Comparison of Structural Imaging With Functional MRI. *American journal of roentgenology*, *207*, 1263–1270. doi:10.2214/AJR.15.15119

Salat, D. H., Buckner, R. L., Snyder, A. Z., Greve, D. N., Desikan, R. S. R., Busa, E.,. . . Fischl, B. (2004). Thinning of the cerebral cortex in aging. *Cerebral cortex*, *14*, 721–730. doi:10.1093/cercor/bhh032

Sarica, A., Cerasa, A., Vasta, R., Perrotta, P., Valentino, P., Mangone, G.,. . . Quattrone, A. (2014). Tractography in amyotrophic lateral sclerosis using a novel probabilistic tool: a study with tract-based reconstruction compared to voxel-based approach. *Journal of neuroscience methods*, *224*, 79–87. doi:10.1016/j.jneumeth.2013.12.014

Sarikcioglu, L., Ozsoy, U. & Unver, G. (2007). Tapetum corporis callosi: carpet of the brain. *Journal of the history of the neurosciences*, *16*, 432–434. doi:10.1080/09647040600719013

Schäbitz, W.-R. & Schneider, A. (2007). New targets for established proteins: exploring G-CSF for the treatment of stroke. *Trends in pharmacological sciences*, *28*, 157–161. doi:10.1016/j.tips.2007.02.007

Schmidt, P., Gaser, C., Arsic, M., Buck, D., Förschler, A., Berthele, A.,. . . Mühlau, M. (2012). An automated tool for detection of FLAIR-hyperintense white-matter lesions in Multiple Sclerosis. *NeuroImage*, *59*, 3774–3783. doi:10.1016/j.neuroimage.2011.11.032

Schmidt, P. (2017). Bayesian inference for structured additive regression models for large-scale problems with applications to medical imaging. Dissertation, LMU München: Fakultät für Mathematik, Informatik und Statistik

Schneider, A., Krüger, C., Steigleder, T., Weber, D., Pitzer, C., Laage, R.,. . . Schäbitz, W.-R. (2005). The hematopoietic factor G-CSF is a neuronal ligand that counteracts programmed cell death and drives neurogenesis. *The Journal of clinical investigation*, *115*, 2083–2098. doi:10.1172/JCI23559

Schultz, J. (2018). Disease-modifying treatment of amyotrophic lateral sclerosis. *Am J Manag Care*, *24*, 327-335

Schuster, C., Kasper, E., Machts, J., Bittner, D., Kaufmann, J., Benecke, R.,. . . Prudlo, J. (2013). Focal thinning of the motor cortex mirrors clinical features of amyotrophic lateral sclerosis and their phenotypes: a neuroimaging study. *Journal of neurology*, *260*, 2856–2864. doi:10.1007/s00415-013-7083-z

Schuster, C., Kasper, E., Dyrba, M., Machts, J., Bittner, D., Kaufmann, J.,. . . Prudlo, J. (2014). Cortical thinning and its relation to cognition in amyotrophic lateral sclerosis. *Neurobiology of aging*, *35*, 240–246. doi:10.1016/j.neurobiolaging.2013.07.020

Schuster, C., Hardiman, O. & Bede, P. (2017). Survival prediction in Amyotrophic lateral sclerosis based on MRI measures and clinical characteristics. *BMC neurology*, *17*, 73. doi:10.1186/s12883-017-0854-x

Schweitzer, A. D., Liu, T., Gupta, A., Zheng, K., Seedial, S., Shtilbans, A.,. . . Tsiouris, A. J. (2015). Quantitative Susceptibility Mapping of the Motor Cortex in Amyotrophic Lateral Sclerosis and Primary Lateral Sclerosis. *American journal of roentgenology*, *204*, 1086–1092. doi:10.2214/AJR.14.13459

Simon, N. G., Turner, M. R., Vucic, S., Al-Chalabi, A., Shefner, J., Lomen-Hoerth, C. & Kiernan, M. C. (2014). Quantifying disease progression in amyotrophic lateral sclerosis. *Annals of neurology*, *76*, 643–657. doi:10.1002/ana.24273

Sorarù, G., D'Ascenzo, C., Nicolao, P., Volpe, M., Martignago, S., Palmieri, A.,. . . Angelini, C. (2008). Muscle histopathology in upper motor neuron-dominant amyotrophic lateral sclerosis. *Amyotrophic lateral sclerosis : official publication of the World Federation of Neurology Research Group on Motor Neuron Diseases*, *9*, 287–293. doi:10.1080/17482960802206801

Spinelli, E. G., Agosta, F., Ferraro, P. M., Riva, N., Lunetta, C., Falzone, Y. M.,. . . Filippi, M. (2016). Brain MR Imaging in Patients with Lower Motor Neuron-Predominant Disease. *Radiology*, *280*, 545–556. doi:10.1148/radiol.2016151846

Stein, F., Kobor, I., Bogdahn, U. & Schulte-Mattler, W. J. (2016). Toward the validation of a new method (MUNIX) for motor unit number assessment. *Journal of electromyography and kinesiology*, *27*, 73–77. doi:10.1016/j.jelekin.2016.02.001

Steinbach, R., Loewe, K., Kaufmann, J., Machts, J., Kollewe, K., Petri, S.,. . . Stoppel, C. M. (2015). Structural hallmarks of amyotrophic lateral sclerosis progression revealed by probabilistic fiber tractography. *Journal of neurology*, *262*, 2257–2270

Stifani, N. (2014). Motor neurons and the generation of spinal motor neuron diversity. *Frontiers in cellular neuroscience*, *8*, 293. doi:10.3389/fncel.2014.00293

Swinnen, B. & Robberecht, W. (2014). The phenotypic variability of amyotrophic lateral sclerosis. *Nature reviews Neurology*, *10*, 661–670. doi:10.1038/nrneurol.2014.184

Tang, M., Chen, X., Zhou, Q., Liu, B., Liu, Y., Liu, S. & Chen, Z. (2015). Quantitative assessment of amyotrophic lateral sclerosis with diffusion tensor imaging in 3.0T magnetic resonance. *Int J Clin Exp Med*, *8*(5), 8295-8303

Tao, Q.-Q. & Wu, Z.-Y. (2017). Amyotrophic Lateral Sclerosis: Precise Diagnosis and Individualized Treatment. *Chinese Medical Journal*, *130*, 2269–2272. doi:10.4103/0366-6999.215323

Tavazzi, E., Laganà, M. M., Bergsland, N., Tortorella, P., Pinardi, G., Lunetta, C.,. . . Rovaris, M. (2015). Grey matter damage in progressive multiple sclerosis versus amyotrophic lateral sclerosis: a voxel-based morphometry MRI study. *Neurological sciences*, *36*, 371–377. doi:10.1007/s10072-014-1954-7

Thivard, L., Pradat, P.-F., Lehéricy, S., Lacomblez, L., Dormont, D., Chiras, J.,. . . Meininger, V. (2007). Diffusion tensor imaging and voxel based morphometry study in amyotrophic lateral sclerosis: relationships with motor disability. *Journal of neurology, neurosurgery, and psychiatry*, *78*, 889–892. doi:10.1136/jnnp.2006.101758

Thorns, J., Jansma, H., Peschel, T., Grosskreutz, J., Mohammadi, B., Dengler, R. & Münte, T. F. (2013). Extent of cortical involvement in amyotrophic lateral sclerosis--an analysis based on cortical thickness. *BMC neurology*, *13*, 148. doi:10.1186/1471-2377-13-148

Thorpe, J. W., Moseley, I. F., Hawkes, C. H., MacManus, D. G., McDonald, W. I. & Miller, D. H. (1996). Brain and spinal cord MRI in motor neuron disease. *Journal of neurology, neurosurgery, and psychiatry*, *61*(3), 314–317

Tombaugh, T. N., McDowell, I., Kristjansson, B. & Hubley, A. M. (1996). Mini-Mental State Examination (MMSE) and the Modified MMSE (3MS): A psychometric comparison and normative data. *Psychological Assessment*, *8*, 48–59. doi:10.1037/1040-3590.8.1.48

Toosy, A., Werring, D., Orrell, R., Howard, R., King, M., Barker, G.,. . . Thompson, A. (2003). Diffusion tensor imaging detects corticospinal tract involvement at multiple levels in amyotrophic lateral sclerosis. *Journal of neurology, neurosurgery, and psychiatry*, *74*, 1250–1257. doi:10.1136/jnnp.74.9.1250

Turner, M. R., Barnwell, J., Al-Chalabi, A. & Eisen, A. (2012). Young-onset amyotrophic lateral sclerosis: historical and other observations. *Brain*, *135*, 2883–2891. doi:10.1093/brain/aws144

Turner, M. R., Bowser, R., Bruijn, L., Dupuis, L., Ludolph, A., McGrath, M.,. . . Fischbeck, K. H. (2013). Mechanisms, models and biomarkers in amyotrophic lateral sclerosis. *Amyotrophic lateral sclerosis & frontotemporal degeneration*, *14*, 19–32. doi:10.3109/21678421.2013.778554

Turner, M. R. & Verstraete, E. (2015). What does imaging reveal about the pathology of amyotrophic lateral sclerosis? *Current neurology and neuroscience reports*, *15*, 45. doi:10.1007/s11910-015-0569-6

Van Damme, P., Robberecht, W. & van den Bosch, L. (2017). Modelling amyotrophic lateral sclerosis: progress and possibilities. *Disease models & mechanisms*, *10*, 537–549. doi:10.1242/dmm.029058

Van der Graaff, M. M., Sage, C. A., Caan, M. W. A., Akkerman, E. M., Lavini, C., Majoie, C. B.,. . . Visser, M. de. (2011). Upper and extra-motoneuron involvement in early motoneuron disease: a diffusion tensor imaging study. *Brain*, *134*, 1211–1228. doi:10.1093/brain/awr016

Van Es, M. A., Hardiman, O., Chiò, A., Al-Chalabi, A., Pasterkamp, R. J., Veldink, J. H. & van den Berg, L. H. (2017). Amyotrophic lateral sclerosis. *The Lancet*, *390*, 2084–2098. doi:10.1016/S0140-6736(17)31287-4

Vázquez-Costa, J. F., Mazón, M., Carreres-Polo, J., Hervás, D., Pérez-Tur, J., Martí-Bonmatí, L. & Sevilla, T. (2018). Brain signal intensity changes as biomarkers in amyotrophic lateral sclerosis. *Acta neurologica Scandinavica*, *137*, 262–271. doi:10.1111/ane.12863

Verstraete, E., van den Heuvel, M. P., Veldink, J. H., Blanken, N., Mandl, R. C., Hulshoff Pol, H. E. & van den Berg, L. H. (2010). Motor network degeneration in amyotrophic lateral sclerosis: a structural and functional connectivity study. *PloS one*, *5*. doi:10.1371/journal.pone.0013664

Verstraete, E., Veldink, J. H., Mandl, R. C. W., van den Berg, L. H. & van den Heuvel, M. P. (2011). Impaired structural motor connectome in amyotrophic lateral sclerosis. *PloS one*, *6*. doi:10.1371/journal.pone.0024239

Verstraete, E., Veldink, J. H., Hendrikse, J., Schelhaas, H. J., van den Heuvel, M. P. & van den Berg, L. H. (2012). Structural MRI reveals cortical thinning in amyotrophic lateral sclerosis. *Journal of neurology, neurosurgery, and psychiatry*, *83*, 383–388. doi:10.1136/jnnp-2011-300909

Verstraete, E. & Foerster, B. R. (2015). Neuroimaging as a New Diagnostic Modality in Amyotrophic Lateral Sclerosis. *Neurotherapeutics*, *12*, 403–416. doi:10.1007/s13311-015-0347-9

Vijayalaxmi, Fatahi, M. & Speck, O. (2015). Magnetic resonance imaging (MRI): A review of genetic damage investigations. *Mutation research. Reviews in mutation research*, *764*, 51–63. doi:10.1016/j.mrrev.2015.02.002

Vu, L. T. & Bowser, R. (2017). Fluid-Based Biomarkers for Amyotrophic Lateral Sclerosis. *Neurotherapeutics*, *14*, 119–134. doi:10.1007/s13311-016-0503-x

Vucic, S., Ziemann, U., Eisen, A., Hallett, M. & Kiernan, M. C. (2012). Transcranial magnetic stimulation and amyotrophic lateral sclerosis: pathophysiological insights. *Journal of neurology, neurosurgery, and psychiatry*, *84*, 1161–1170. doi:10.1136/jnnp-2012-304019

Wagstyl, K., Ronan, L., Goodyer, I. M. & Fletcher, P. C. (2015). Cortical thickness gradients in structural hierarchies. *NeuroImage*, *111*, 241–250. doi:10.1016/j.neuroimage.2015.02.036

Walhout, R., Westeneng, H.-J., Verstraete, E., Hendrikse, J., Veldink, J. H., van den Heuvel, M. P. & van den Berg, L. H. (2015). Cortical thickness in ALS: towards a marker for upper motor neuron involvement. *Journal of neurology, neurosurgery, and psychiatry*, *86*, 288–294. doi:10.1136/jnnp-2013-306839

Wallner, S., Peters, S., Pitzer, C., Resch, H., Bogdahn, U. & Schneider, A. (2015). The Granulocyte-colony stimulating factor has a dual role in neuronal and vascular plasticity. *Frontiers in cell and developmental biology*, *3*, 48. doi:10.3389/fcell.2015.00048

Wang, J. Y., Abdi, H., Bakhadirov, K., Diaz-Arrastia, R. & Devous, M. D. (2011). A Comprehensive Reliability Assessment of Quantitative Diffusion Tensor Tractography. *NeuroImage*, *60*, 1127–1138. doi:10.1016/j.neuroimage.2011.12.062

Westeneng, H.-J., Walhout, R., Straathof, M., Schmidt, R., Hendrikse, J., Veldink, J. H.,. . . van den Berg, L. H. (2016). Widespread structural brain involvement in ALS is not limited to the C9orf72 repeat expansion. *Journal of neurology, neurosurgery, and psychiatry*, *87*, 1354–1360. doi:10.1136/jnnp-2016-313959

Wijesekera, L. C. & Leigh, P. N. (2009). Amyotrophic lateral sclerosis. *Orphanet journal of rare diseases*, *4*, 3. doi:10.1186/1750-1172-4-3

World Medical Association (2013). World Medical Association Declaration of Helsinki: Ethical Principles for Medical Research Involving Human Subjects. *JAMA*, *310*(20), 2191–2194. doi:10.1001/jama.2013.281053

Yeo, B. T. T., Krienen, F. M., Sepulcre, J., Sabuncu, M. R., Lashkari, D., Hollinshead, M.,. . . Buckner, R. L. (2011). The organization of the human cerebral cortex estimated by intrinsic functional connectivity. *Journal of neurophysiology*, *106*, 1125–1165. doi:10.1152/jn.00338.2011

Zago, S., Poletti, B., Morelli, C., Doretti, A. & Silani, V. (2011). Amyotrophic lateral sclerosis and frontotemporal dementia (ALS-FTD). *Archives italiennes de biologie*, *149*, 39–56. doi:10.4449/aib.v149i1.1263

Zhan, L., Zhou, J., Wang, Y., Jin, Y., Jahanshad, N., Prasad, G.,. . . For, T. A.'s. D. N. I. (2015). Comparison of nine tractography algorithms for detecting abnormal structural brain networks in Alzheimer's disease. *Frontiers in aging neuroscience*, *7*, 48. doi:10.3389/fnagi.2015.00048

Zhang, L., Ulug, A. M., Zimmerman, R. D., Lin, M. T., Rubin, M. & Beal, M. F. (2003). The diagnostic utility of FLAIR imaging in clinically verified amyotrophic lateral sclerosis. *Journal of magnetic resonance imaging*, *17*, 521–527. doi:10.1002/jmri.10293

Zhang, J., Yin, X., Zhao, L., Evans, A. C., Song, L., Xie, B.,. . . Wang, J. (2014). Regional alterations in cortical thickness and white matter integrity in amyotrophic lateral sclerosis. *Journal of neurology*, *261*, 412–421. doi:10.1007/s00415-013-7215-5

Zhang, F., Chen, G., He, M., Dai, J., Shang, H., Gong, Q. & Jia, Z. (2018). Altered white matter microarchitecture in amyotrophic lateral sclerosis: A voxel-based meta-analysis of diffusion tensor imaging. *NeuroImage : Clinical*, *19*, 122–129

Zugman, A., Sato, J. R. & Jackowski, A. P. (2016). Crisis in neuroimaging: is neuroimaging failing 15 years after the decade of the brain? *Revista brasileira de psiquiatria (Sao Paulo, Brazil : 1999)*, *38*, 267–269. doi:10.1590/1516-4446-2016-2071

APPENDIX 1

ALS Functional Rating Scale Revised (ALS-FRS-R)

Date:.....Name patient:.....Date of Birth:.....

Patient's number.....Right-/left-handed

Item 1: SPEECH

4 ☐ Normal speech process
3 ☐ Detectable speech disturbance
2 ☐ Intelligible with repeating
1 ☐ Speech combined with non-vocal communication
0 ☐ Loss of useful speech

Item 2: SALIVATION

4 ☐ Normal
3 ☐ Slight but definite excess of saliva in mouth; may have nighttime drooling
2 ☐ Moderately excessive saliva; may have minimal drooling (during the day)
1 ☐ Marked excess of saliva with some drooling
0 ☐ Marked drooling; requires constant tissue or handkerchief

Item 3: SWALLOWING

4 ☐ Normal eating habits
3 ☐ Early eating problems – occasional choking
2 ☐ Dietary consistency changes
1 ☐ Needs supplement tube feeding
0 ☐ NPO (exclusively parenteral or enteral feeding)

Item 4: HANDWRITING

4 ☐ Normal
3 ☐ Slow or sloppy: all words are legible
2 ☐ Not all words are legible
1 ☐ Able to grip pen, but unable to write
0 ☐ Unable to grip pen

Item 5a: CUTTING FOOD AND HANDLING UTENSILS
Patients without gastrostomy → Use 5b if >50% is through g-tube

4 ☐ Normal
3 ☐ Somewhat slow and clumsy, but no help needed
2 ☐ Can cut most foods (>50%), although slow and clumsy; some help needed
1 ☐ Food must be cut by someone, but can still feed slowly
0 ☐ Needs to be fed

Item 5b: CUTTING FOOD AND HANDLING UTENSILS
Patients with gastrostomy → 5b option is used if the patient has a gastrostomy and only if it is the primary method (more than 50%) of eating .

4 ☐ Normal
3 ☐ Clumsy, but able to perform all manipulations independently
2 ☐ Some help needed with closures and fasteners
1 ☐ Provides minimal assistance to caregiver
0 ☐ Unable to perform any aspect of task

Item 6: DRESSING AND HYGIENE

4☐ Normal function
3☐ Independent and complete self-care with effort or decreased efficiency
2☐ Intermittent assistance or substitute methods
1☐ Needs attendant for self-care
0☐ Total dependence

Item 7: TURNING IN BED AND ADJUSTING BED CLOTHES

4☐ Normal function
3☐ Somewhat slow and clumsy, but no help needed
2☐ Can turn alone, or adjust sheets, but with great difficulty
1☐ Can initiate, but not turn or adjust sheets alone
0☐ Helpless

Item 8: WALKING

4☐ Normal
3☐ Early ambulation difficulties
2☐ Walks with assistance
1☐ Non-ambulatory functional movement
0☐ No purposeful leg movement

Item 9: CLIMBING STAIRS

4☐ Normal
3☐ Slow
2☐ Mild unsteadiness or fatigue
1☐ Needs assistance
0☐ Cannot do

Item 10: DYSPNEA

4☐ None
3☐ Occurs when walking
2☐ Occurs with one or more of the following: eating, bathing, dressing (ADL)
1☐ Occurs at rest: difficulty breathing when either sitting or lying
0☐ Significant difficulty: considering using mechanical respiratory support

Item 11: ORTHOPNEA

4☐ None
3☐ Some difficulty sleeping at night due to shortness of breath, does not routinely use more than two pillows
2☐ Needs extra pillows in order to sleep (more than two)
1☐ Can only sleep sitting up
0☐ Unable to sleep without mechanical assistance

Item 12: RESPIRATORY INSUFFICIENCY

4☐ None
3☐ Intermittent use of BiPAP
2☐ Continuous use of BiPAP during the night
1☐ Continuous use of BiPAP during day & night
0☐ Invasive mechanical ventilation by intubation or tracheostomy

Interviewer's name.....

APPENDIX 2

EDINBURGH COGNITIVE and BEHAVIOURAL ALS SCREEN – ECAS revised German version

Demographie und Informationen zur ALS

Hintergrund

Geschlecht:

männlich ☐ weiblich ☐

Größe:

Gewicht:

BMI:

Aktuelle Medikation:

Klinischer Verlauf

Zeitpunkt der ersten Symptome:

Zeitpunkt der Diagnose: Alter bei Diagnose:

EL Escorial Klassifikation:

ALS (mögliche/wahrscheinliche/definitive):

Betroffene Regionen:

Bei Beginn:

Bulbär☐ Obere Extremitäten☐ Untere Extremitäten☐

Aktuell:

Bulbär☐ Obere Extremitäten☐ Untere Extremitäten☐

***Familiärer Hintergrund*:**

1sten Grades (Eltern, Kinder, Geschwister). Wenn "Ja", bitte spezifizieren

ALS/MND☐ Demenz☐ Parkinson☐

Zusatzdetails .....

Erweitert (Großeltern, Tante/Onkel/Cousine). Wenn "Ja", bitte spezifizieren

ALS/MND☐ Demenz☐ Parkinson☐

Zusatzdetails .....

Ernsthafte Psychiatrische Auffälligkeiten innerhalb der Familie? Wenn "Ja", bitte spezifizieren

.....

***Respiratorische Funktion*:**

SNIP(sniff nasal-inspiratory pressure): Puls-Oximetry:
Vorausgesagte FVC: %

Epworth Schläfrigkeitsscore (ESS):

Nicht-invasive Beatmung: Ja☐ Nein☐ Seit:

PEG: Ja☐ Nein☐ Seit:

ALS-FRS-r: /48

EDINBURGH COGNITIVE ALS – SCREEN (ECAS)

(Edinburgher ALS- Kognitionsscreeningverfahren)

revidierte Deutsche Version (2014)

Testdatum: .....

Alter am Ende der Ausbildung: .....

Beruf: .....

Schuljahre: .....

Studienjahre: .....

Ausbildungsjahre: .....

Patientencode:.....

Geburtsdatum: .....

Name des Krankenhauses mit Adresse:

.....

.....

.....

1. Sprache – Benennen

Sagen Sie: *„Sagen oder schreiben Sie die Namen dieser Bilder auf:“*

Punkte 0-8

.....

.....

.....

.....

.....

.....

.....

.....

2. Sprache – Sprachverständnis

Sagen Sie: *„Zeigen Sie auf das Bild, welches zu folgendem Satz passt:“*

Punkte 0-8 ☐

1. Etwas, worin man fliegen kann .....
2. Etwas, das Schwimmhäute besitzt .....
3. Ein Tier, das auf Bäume klettert .....
4. Etwas, das zum Holzhacken benutzt wird .....
5. Ein Transportmittel .....
6. Etwas mit einer scharfen Kante .....
7. Etwas, das einen Giftstachel besitzt .....
8. Etwas, das sich von Nüssen und Samen ernährt .....

3. Gedächtnis – Sofortige Erinnerung

Sagen Sie: *„Ich lese Ihnen eine kurze Geschichte vor. Bitte hören Sie aufmerksam zu. Wenn ich die Geschichte beendet habe, sagen Sie mir oder schreiben Sie alles auf, an was Sie sich erinnern können.“*

Vergeben sie 1 Punkt für jeden (vollständig oder teilweise) unterstrichenen Abschnitt im Text, der behalten wurde.

Punkte 0-10 ☐

Benutzen Sie diese Punktzahl um den prozentualen verzögerten Erinnerungs-Anteil weiter unten zu berechnen

Letzten Sonntag fand die alljährliche Müllsammelaktion im Primelwald statt. Zweiundvierzig Personen trafen sich, um alte Fahrräder oder Einkaufswagen zu entfernen. Herr Dieter Keller vom Waldprojekt erzählte den lokalen Journalisten, dass er sehr beeindruckt und besonders stolz auf die 17 Kinder sei, die kamen.

4. Sprache – Rechtschreibung/Buchstabieren

Sagen Sie: *„Buchstabieren Sie die folgenden Wörter, entweder schriftlich oder mündlich.“*

Falls die Person ein technisches Hilfsmittel benutzt, bitten Sie, jegliche Rechtschreibhilfe /Texthilfe auszuschalten.

Punkte 0-12 ☐

1. Briefumschlag .....
2. Trittbrett .....
3. Konstruktion .....
4. Partner .....
5. Plätzchen .....
6. Rasenmäher .....
7. Zustellen .....
8. Aufgenommen .....
9. Kleiderbügel .....
10. Orchester .....
11. Schraubenzieher .....
12. Brachte .....

5. Exekutive Funktion – Sprachflüssigkeit Buchstabe S (fluency letter S)

Sagen Sie: *„Ich werde Ihnen einen Buchstaben aus dem Alphabet nennen und möchte Sie bitten, mir so viele Wörter aufzuzählen oder aufzuschreiben, wie Sie können, die mit dem genannten Buchstaben beginnen. Bitte nennen Sie keine Eigennamen, Orte oder Zahlen."*

- Falls ***mündlich***, sagen Sie: *„Sie haben **eine** Minute. Der Buchstabe ist S."*
  Notieren Sie die generierten Wörter in gut leserlicher Schrift in dem folgenden grauen Feld.
- Falls **schriftlich**, sagen Sie: *„Sie haben **zwei** Minuten. Der Buchstabe ist S."*
  Der Teilnehmer soll das graue Feld oder ein separates Blatt zum Schreiben benutzen.

Als Nächstes soll die Person diese Worte abschreiben oder laut vorlesen.

- Falls ***mündlich***: *„Lesen Sie diese Wörter nun so schnell wie möglich laut vor. Bevor Sie anfangen, schauen Sie bitte, ob Sie alle Wörter lesen können. Ich werde die Zeit stoppen, die Sie zum Lesen brauchen. Fertig? Los."*
- Falls ***schriftlich***, sagen Sie: *„Schreiben Sie diese Wörter so schnell wie möglich ab. Ich werde die Zeit stoppen, die Sie dazu brauchen. Fertig? Los."*

Anzahl der richtigen Wörter

=

Zeit zum Abschreiben oder zum laut Lesen

=

Punkte 0-12

Berechnung der Sprachgewandtheit (Verbaler Fluenz Index, VFI)

Falls ***mündlich:***

VFI = 60 Sekunden –Anzahl der Sekunden zum lauten Vorlesen der Wörter / Anzahl der erzeugten richtigen Wörter

Falls ***schriftlich:***

VFI = 120 Sekunden –Anzahl der Sekunden zum Abschreiben der Wörter / Anzahl der erzeugten richtigen Wörter

	VFI-Umrechnungstabelle (S)	
Mündlicher VFI	Schriftlicher VFI	Punkte
≥19,63	≥23,52	**0**
16,20 – 19,62	19,37 – 23,51	**2**
12,76 – 16,19	15,22 – 19,36	**4**
9,33 – 12,75	11,07 – 15,21	**6**
5,90 – 9,32	6,92 – 11,06	**8**
2,48 – 5,89	2,79 – 6,91	**10**
≤2,47	≤2,78	**12**

6. Exekutive Funktion – Umgekehrte Zahlenspanne (Reverse Digit Span)

Punkte 0-12

Sagen Sie: *"Ich werde Ihnen einige Ziffernfolgen nennen und möchte, dass Sie diese in umgekehrter Reihenfolge wieder aufzählen. Zum Beispiel sage ich „2, 3, 4", dann sagen Sie „4, 3, 2". Lassen Sie uns eine Übung hierzu machen. Wenn ich sage „7, 1, 9", was würden Sie sagen?"*

Beenden Sie die Aufgabe, wenn die Person beide Versuche in einer Reihe falsch hat. Notieren Sie die Gesamtanzahl aller richtigen Versuche.

Versuch	Zahlenfolge	Kontrolle	Versuch	Zahlenfolge	Kontrolle
1	2 6		2	5 8	
3	9 3 5		4	4 1 6	
5	7 2 8 4		6	9 5 7 3	
7	6 9 4 2 1		8	8 3 2 5 6	
9	8 1 3 5 7 9		10	3 6 2 7 3 4	
11	1 6 9 3 5 8 6		12	2 3 6 8 4 9 2	

7. Exekutive Funktion – Alternation/Abwechslung

Punkte 0-12

Sagen Sie: *"Ich möchte, dass Sie Buchstaben des Alphabets mit der jeweiligen Nummer der Position im Alphabet verknüpfen. Beginnend mit 1-A, dann 2-B, 3-C und so weiter. Bitte machen Sie von hier an weiter. Ersetzen Sie die Zahl durch die nächste Zahl in der Zahlenfolge und den Buchstaben durch den nächsten Buchstaben in der Reihenfolge des Alphabets, ohne eine Nummer oder einen Buchstaben auszulassen. Fahren Sie fort bis ich stopp sage"*

Nr.		Kontr.	Nr.		Kontr.	Nr.		Kontr.	Nr.		Kontr.
1	4-D		2	5-E		3	6-F		4	7-G	
5	8-H		6	9-I		7	10-J		8	11-K	
9	12-L		10	13-M		11	14-N		12	15-O	

8. Exekutive Funktion – Sprachflüssigkeit Buchstabe G (fluency letter G)

Sagen Sie: *„Ich werde Ihnen einen Buchstaben aus dem Alphabet nennen und möchte Sie bitten, mir so viele Wörter aufzuzählen oder aufzuschreiben, wie Sie können, die mit dem genannten Buchstaben beginnen. Bitte nennen Sie keine Eigennamen, Orte oder Zahlen. Dieses Mal dürfen die Wörter aber nur 4 Buchstaben haben, nicht mehr und nicht weniger."*

- Falls ***mündlich***, sagen Sie: *„Sie haben **90 s** Zeit. Der Buchstabe ist G."*
  Notieren Sie die generierten Wörter in gut leserlicher Schrift in dem folgenden grauen Feld.
- Falls ***schriftlich***, sagen Sie: *„Sie haben **drei** Minuten Zeit. Der Buchstabe ist G."*

Anzahl der richtigen Wörter

=

Zeit zum Abschreiben oder zum laut Lesen

=

▪

Der Teilnehmer soll das graue Feld oder ein separates Blatt zum Schreiben benutzen.
Als Nächstes soll die Person diese Worte **abschreiben oder laut vorlesen**.

- Falls ***mündlich:*** *„Lesen Sie diese Wörter nun so schnell wie möglich laut vor. Bevor Sie anfangen, schauen Sie bitte, ob Sie alle Wörter lesen können. Ich werde die Zeit stoppen, die Sie dazu brauchen. Fertig? Los.“*
- Falls ***schriftlich***, sagen Sie: *„Schreiben Sie diese Wörter so schnell wie möglich ab. Ich werde die Zeit stoppen, die Sie dazu brauchen. Fertig? Los.“*

Punkte 0-12

☐

Berechnung der Sprachgewandtheit (Verbaler Fluenz Index, VFI)

Falls mündlich:

$$VFI = \frac{90 \text{ Sekunden} - \text{Anzahl der Sekunden zum laut Vorlesen der Wörter}}{\text{Anzahl der erzeugten richtigen Wörter}}$$

Falls schriftlich:

$$VFI = \frac{180 \text{ Sekunden} - \text{Anzahl der Sekunden zum Abschreiben der Wörter}}{\text{Anzahl der erzeugten richtigen Wörter}}$$

	VFI-Umrechnungstabelle (G)	
Mündlicher VFI	Schriftlicher VFI	Punkte
≥46,43	≥113,13	**0**
38,87 – 46,42	92,49 – 113,12	**2**
31,31 – 38,86	71,85 – 92,48	**4**
23,75 – 31,30	51,21 – 71,84	**6**
16,19 – 23,74	30,57 – 51,20	**8**
8,64 – 16,18	9,94 – 30,56	**10**
≤8,63	≤9,93	**12**

9. Räumlich-visuelle Vorstellung – Punkte Zählen (Dot counting)

Punkte 0- 4

Sagen Sie: *„Ich möchte, dass Sie zählen, wie viele Punkte in jedem Kasten sind, ohne mit dem Finger auf die Punkte zu zeigen."*

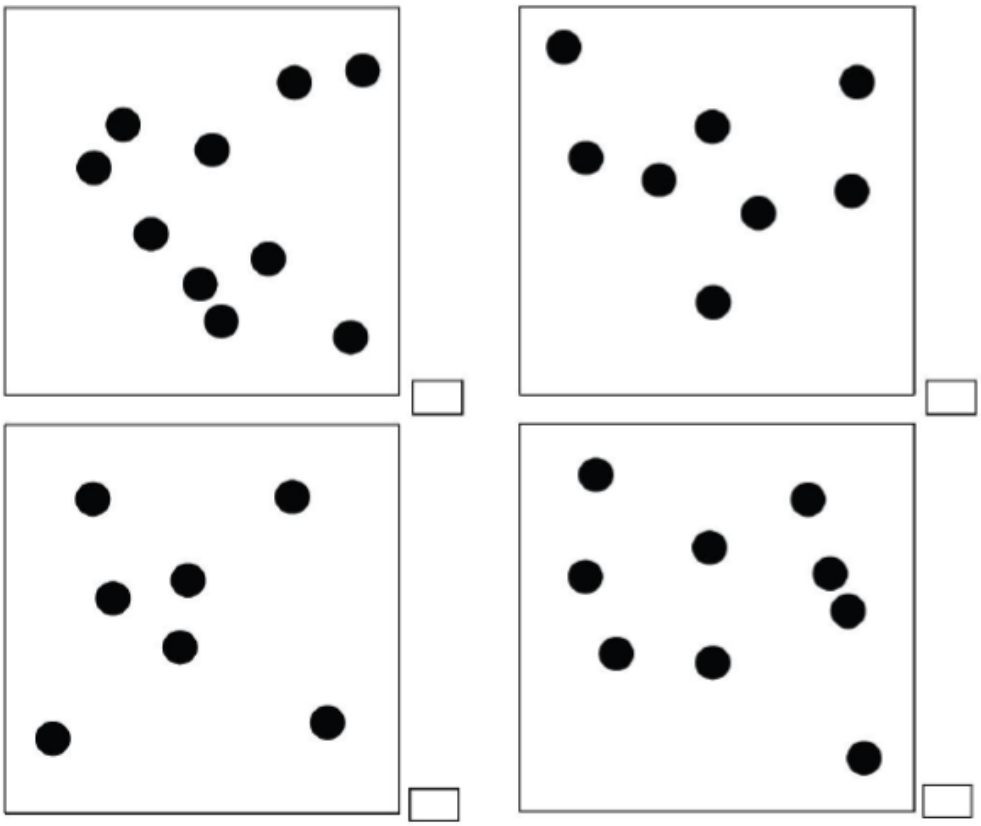

10. Räumlich-visuelle Vorstellung – Würfel Zählen (cube counting)

Sagen Sie: *„Wie viele Würfel bilden jeweils ein Objekt, einschließlich derjenigen Würfel, die man nicht sehen kann?“*

Punkte 0- 4

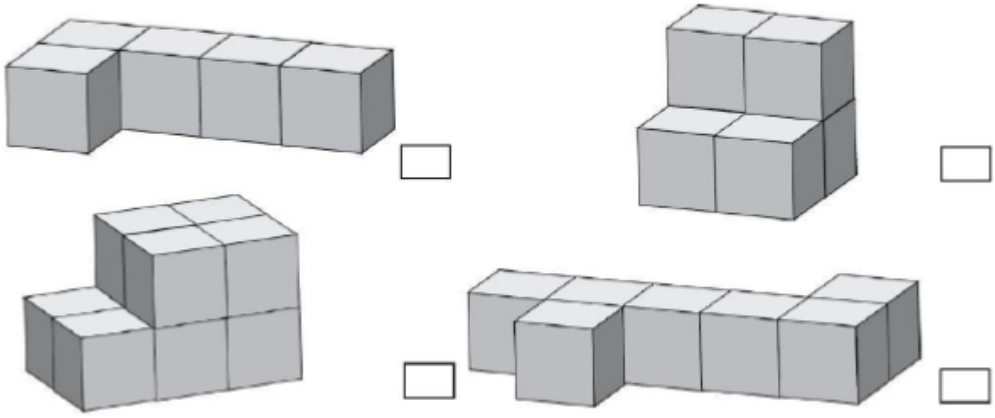

11. Räumlich-visuelle Vorstellung – Zahlen Lokalisieren (Number location)

Sagen Sie: *„Welche Zahl stimmt mit der Position des Punktes überein?“*

Punkte 0- 4

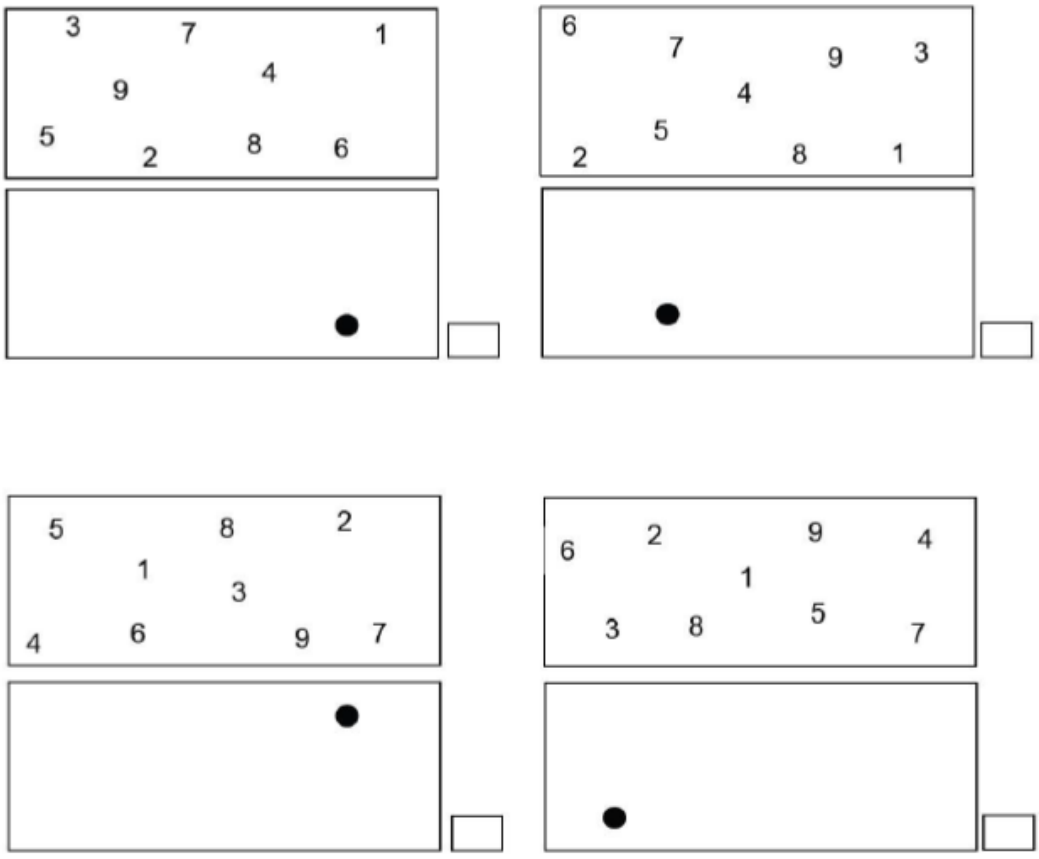

12. Exekutive Funktion – Sätze vervollständigen

Sagen Sie: *„Hören Sie aufmerksam auf die folgenden Sätzen und sobald ich einen Satz zu Ende gelesen habe, sagen Sie mir oder schreiben Sie ein Wort so schnell wie möglich auf, das den Satz sinnvoll beendet. Zum Beispiel: Sie war so müde, darum ging sie gleich zu … (Bett).“*

Werten Sie diese folgenden zwei Beispiele nicht.

1. Er rief im Restaurant an und reservierte …

2. Als sie am Morgen aufstand, hat die Sonne …

Sagen Sie: *„Nun möchte ich, dass Sie dieselbe Übung noch einmal machen, aber diesmal sollte das Wort, das Sie ergänzen, im Zusammenhang mit dem Satz absolut gar keinen Sinn ergeben. Es darf auch nichts mit dem Wort zu tun haben, welches den Satz tatsächlich beendet. Zum Beispiel, „Hans hat sich in die Hand geschnitten mit dem scharfen …. (Schnurrbart).“*

Wenn die Person nicht innerhalb von 20 Sekunden antwortet, gehen sie zur nächsten Frage über.

1. Der Briefträger klopfte an ……
2. Er brachte seinen Regenschirm mit, falls es……
3. Sara bestrich ihr Brötchen mit Butter und ……
4. Joseph ging zum Friseur und ließ sich die Haare ……...
5. Sie sprang in das Schwimm……
6. Sie gingen alle ins Restaurant, um dort etwas zu ……

Bewertung: Vergeben Sie 2 Punkte für jedes unabhängige Wort, 1 Punkt für ein verwandtes Wort (z. B. mit ähnlicher oder gegenteiliger Bedeutung) oder 0 Punkte für das genau richtige Wort.

Punkte 0- 12

13. Soziale Kognition (Soziale Kompetenz) – Teil A

Sagen Sie: *„Sie sehen nun ein paar Bilder, jedes in einer Ecke eines Kastens. Sie sollen sich das Bild aussuchen,* ***welches Ihnen am besten gefällt****. Entweder zeigen Sie auf das Bild oder Sie benennen das Bild, welches Ihnen am besten gefällt. Bitte antworten Sie so schnell wie möglich.“*

Kreisen Sie die Wahl des Teilnehmers ein.

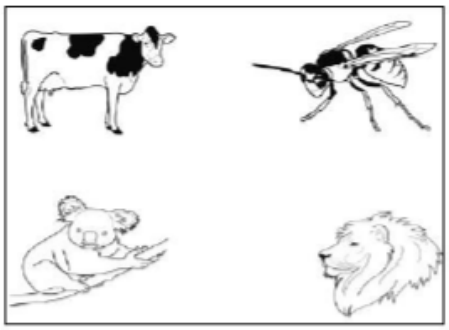

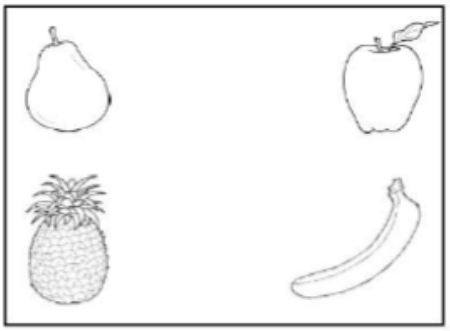

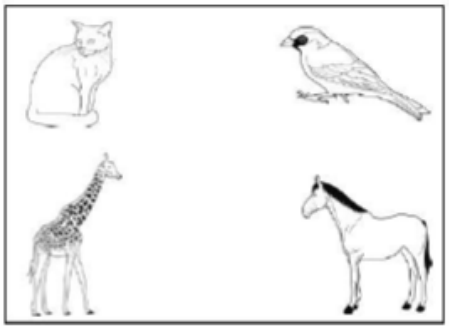

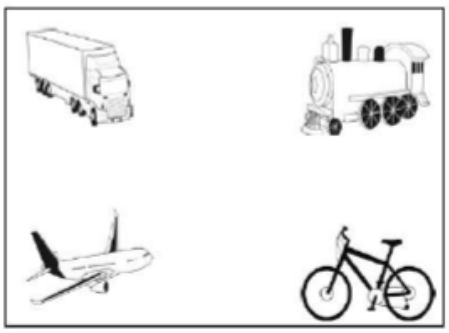

14. Soziale Kognition (Soziale Kompetenz) – Teil B

Punkte 0- 12

Sagen Sie: *„Sie sehen nun die selben Bilder in den Ecken der Kästen. Sie sollen sich nun entscheiden, welches Bild* ***das Gesicht in der Mitte am liebsten hat****. Entweder zeigen oder sagen Sie, welches* ***das Gesicht am liebsten hat****. Bitte antworten Sie wieder so schnell wie möglich.“*

Markieren Sie wieder die Teilnehmerwahl.

Korrekte Auswahl = 2 Punkte, fehlerhafte Auswahl = 1 Punkt, egozentrische Auswahl = 0 Punkte

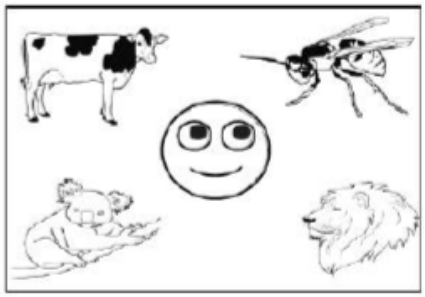
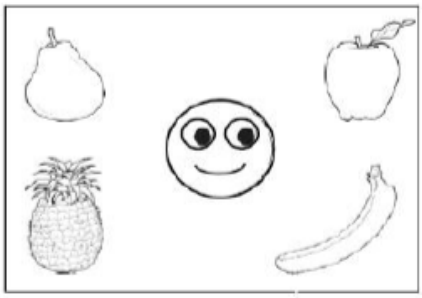
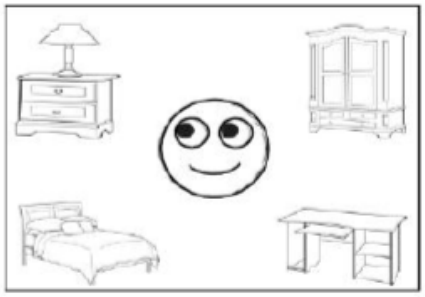
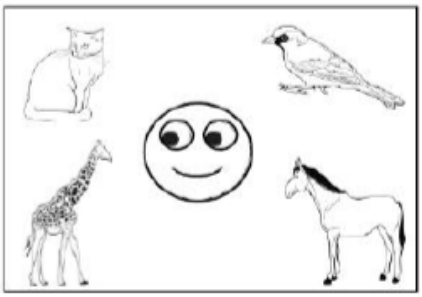
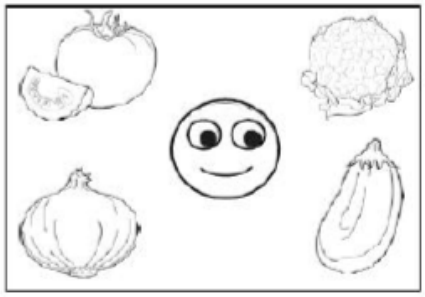
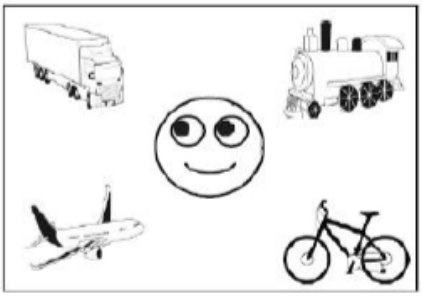

15. Gedächtnis – Verzögerte Erinnerung

Sagen Sie: *„Am Anfang dieser Befragung las ich Ihnen eine kurze Geschichte vor. Erzählen Sie mir bitte so viel Sie können, was Sie von dieser Geschichte noch behalten haben."*
Vergeben Sie je 1 Punkt für jeden (ganz oder teilweise) unterstrichenen Abschnitt im Text, der behalten wurde.

Letzen Sonntag fand die alljährliche Müllsammelaktion im Primelwald statt. Zweiundvierzig Personen trafen sich, um alte Fahrräder oder Einkaufswagen zu entfernen. Herr Dieter Keller vom Waldprojekt erzählte den lokalen Journalisten, dass er sehr beeindruckt und besonders stolz auf die 17 Kinder sei, die kamen.

Verzögerte Erinnerung Rohpunktzahl (0-10)

Bewertung der verzögerten Erinnerung:

Berechnen Sie den „Prozentsatz der korrekt erinnerten Wörter" aus der Geschichte, indem Sie die Punktzahl des „verzögert Erinnerten " durch die Punktzahl des „sofort Erinnerten" dividieren und mit 100 multiplizieren.
Aus der unten folgenden Tabelle lesen Sie die Punktzahl des Endergebnisses der verzögerten Erinnerung ab. Wenn der Prozentsatz = 0 ist, dann entspricht das umgerechnete Ergebnis = 0.

umgerechnete Erinnerungs-punktzahl (0-10)

Verzögerte Erinnerung zur Berechnung des Prozentsatzes des Erinnerten	Prozentsatz des Erinnerten
(verzögert Erinnertes) *X 100 = % erinnert* (sofort Erinnertes) (.....) *X 100 = % erinnert* (.....)	

erinnerter Prozentsatz	umgerech-neter Wert	erinnerter Prozentsatz	umgerech-neter Wert
1-10 %	1	51-60 %	6
11-20 %	2	61-70%	7
21-30 %	3	71-80 %	8
31-40 %	4	81-90 %	9
41-50 %	5	91-100 %	10

16. Gedächtnis – verzögerte Wiedererkennung

Punkte 0- 4

Wenn alle geforderten Begriffe erinnert wurden, überspringen Sie die folgenden Fragen und vergeben sofort 4 Punkte. Andernfalls stellen Sie folgende Fragen:
Sagen Sie: *„Schauen wir einmal, ob Sie sich an noch etwas mehr aus der Geschichte erinnern können. Ich werde Ihnen einige Fragen zur der Geschichte stellen. Bitte sagen Sie mir, ob die Aussagen wahr (W) oder falsch (F) sind."*
Kreisen Sie die Antwort (wahr (W) oder falsch (F)) ein und vergeben Sie einen Punkt für jedes Element, das erkannt wurde. Nutzen Sie die Tabelle darunter, um die Endbewertung zu berechnen.

War die Geschichte über ein Ereignis am letzten Samstag?	W	***F***	1
War das Ereignis die **alljährliche Müllsammelaktion**?	***W***	F	1
Fand diese im **Primelwald** statt?	***W***	F	1
Beseitigten sie alte Dosen und Verpackungen?	W	***F***	1
Hieß der Mann in der Geschichte **Herr Keller**?	***W***	F	1
War sein Vorname Thomas?	W	**F**	1
Sprach er mit lokalen Fotografen?	W	**F**	1
War er besonders **stolz**, dass die Kinder gekommen sind?	**W**	F	1

Wiedererkennungsbewertungs-Tabelle	
Anzahl der richtigen Antworten	Umgerechnetes Ergebnis
0-4	**0**
5	**1**
6	**2**
7	**3**
8	**4**

Gesamt-Bewertung		
Gedächtnis	Sofortige und verzögerte Erinnerung, verzögerte Wiedererkennung **(Test 3, 15, 16)**	/24
Räumliche Vorstellung	Punkte- und Würfelzählen, Zahlen Lokalisieren **(Test 9, 10, 11)**	/12
	NICHT-ALS-SPEZIFISCH	**/36**
Sprache	Benennen, Sprachverständnis, Buchstabieren/Rechtschreibung **(Test 1, 2, 4)**	/28
Sprachfluss	Sprachgewandtheit Buchstabe S und G **(Test 5, 8)**	/24
Exekutive Funktion	Umgekehrte Zahlenspanne, Alternation, Satzvervollständigung, Soziale Kognition **(Test 6, 7, 12, 14)**	/48
	ALS-SPEZIFISCH	**/100**
	GESAMTPUNKTZAHL	**/136**

APPENDIX 3

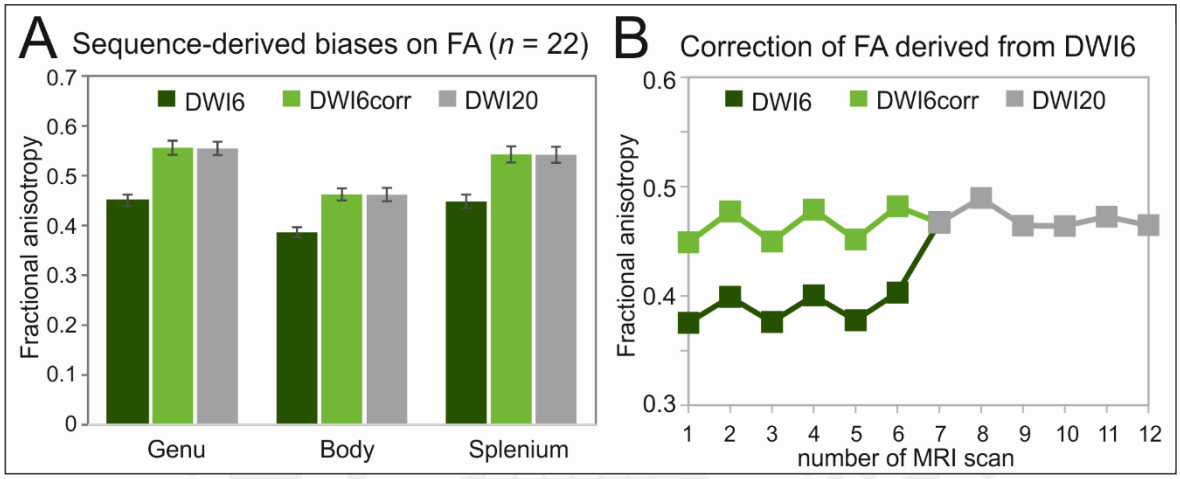

Supplementary figure 1. Correction of DWI sequence derived biases on fractional anisotropy. A) Control analysis on sequence derived biases on FA in 22 healthy controls. Excerpt of three out of 48 atlas-based WM regions (Mori et al. 2008) showing distinct deviations of FA of former DWI sequence (DWI6) from that of modified DWI sequence (DWI20). Calculation of multiplication factors enables the rise of FA levels of DWI6 to the level of DWI20. B) Effect of sequence derived biases on the evaluation of the longitudinal course of FA in the callosal body of an exemplary patient with 12 MRI scans. DWI sequence has been modified after six MRI scans. Without FA correction, the course may have been evaluated as an increase of FA. Correction of sequence derived biases on FA has helped to elucidate these erroneous interpretations.